IEEE Transactions on Quantum Engineering

Received 29 October 2024; revised 30 March 2025; accepted 8 April 2025; date of publication 15 April 2025; date of current version 16 May 2025.

Digital Object Identifier 10.1109/TQE.2025.3560403

Quantum Direct-Sequence Spread-Spectrum CDMA Communication Systems: Mathematical Foundations

MOHAMMAD AMIR DASTGHEIB[1,2], JAWAD A. SALEHI[1,2,3] (Fellow, IEEE), AND MOHAMMAD REZAI[2,3]

[1]Department of Electrical Engineering, Sharif University of Technology, Tehran 14588-89694, Iran
[2]Sharif Quantum Center, Sharif University of Technology, Tehran 14588-89694, Iran
[3]Institute for Convergence Science and Technology, Sharif University of Technology, Tehran 14588-89694, Iran

Corresponding author: Jawad A. Salehi (e-mail: jasalehi@sharif.edu).

An earlier version of this paper was presented in part at the 2024 IEEE Middle East Conference on Communications and Networking (MECOM) [DOI: 10.1109/MECOM61498.2024.10881055].

ABSTRACT This article describes the fundamental principles and mathematical foundations of quantum direct-sequence spread-spectrum code division multiple-access communication systems. The evolution of quantum signals through the quantum direct-sequence spread-spectrum multiple-access communication system is carefully characterized by a novel approach called the decomposition of creation operators. In this methodology, the creation operator of the transmitted quantum signal is decomposed into the chip-time interval creation operators, each of which is defined over the duration of a chip. These chip-time interval creation operators are the invariant building blocks of the spread-spectrum quantum communication systems. With the aid of the proposed chip-time decomposition approach, we can find closed-form relations for quantum signals at the receiver of such a quantum communication system. Furthermore, this article details the principles of narrowband filtering of quantum signals required at the receiver, a crucial step in designing and analyzing quantum communication systems. We show, that by employing coherent states as the transmitted quantum signals, the interuser interference appears as an additive term in the magnitude of the output coherent (Glauber) state, and the output of the quantum communication system is a pure quantum signal. On the other hand, if the transmitters utilize particle-like quantum signals (Fock states) such as single-photon states, the entanglement effect can arise at the receivers. The important techniques developed in this article are expected to have far-reaching implications for various applications in the exciting field of quantum communications and quantum signal processing.

INDEX TERMS Chip-time interval decomposition, direct sequence, quantum broadcasting channel, quantum code division multiple access (QCDMA), quantum communications, quantum filter, quantum interference, quantum multiple access, quantum networks, quantum signal processing, quantum spread-spectrum technology.

I. INTRODUCTION

Quantum information technologies are emerging due to the unique and fundamental features of the quantum phenomena such as superposition, entanglement, and quantum interference. Similar to the age of conventional information technologies, where classical communications was the key enabler, quantum communication plays a major role in the era of quantum-based information technologies [2], [3]. Compelling applications such as the transmission of quantum and classical information within the future quantum communication networks [4], [5], distributed quantum information processing networks [6], quantum signal processing [7], and the ultimate secure communications through quantum key distribution [8], [9] have made quantum communications a very active field of research.

Manipulating the shape of the quantum photon wavepackets is the central element of many quantum communication techniques. In this regard, the information can be encoded in quantum states of light, forming a quantum signal that can be transmitted through the quantum communication system [3].

High-speed electro-optical modulators can be utilized to arbitrarily modulate the amplitude and phase of temporal photon wavepackets [10], [11], [12].

The spread-spectrum technology is one of the most adopted techniques in classical communication systems due to multiple access and interference management capability and low probability of intercept [13]. The basic concept of spread-spectrum communication systems is to broaden the spectrum of the transmitted signals by the processing gain factor utilizing a spreading sequence. This process suppresses the signal and hides it below the noise. Decoding the transmitted signal with the same spreading sequence at the receiver increases the signal-to-noise ratio and reconstructs the signal for the intended user.

Direct-sequence spread-spectrum methods have been applied to single photons [14]. A quantum spread-spectrum multiple-access scheme based on optical circulators is described in [15]. Although the mentioned papers discuss the possibility of applying the spread-spectrum techniques to quantum signals, none has rigorously characterized the spread-spectrum communication systems in terms of the mathematical language of the quantum mechanics and technology. With this background, the essential steps toward describing the quantum mechanical principles of spectral domain quantum code division multiple-access (QCDMA) communication systems are taken in [16].

While Rezai and Salehi [16] present a spectral-domain framework for QCDMA that specifically targets coherent ultrashort quantum light pulses (also see [17]), our work explores a time-domain direct-sequence spread-spectrum QCDMA approach (see [13] for the classical counterpart). In the spectral-domain encoding of [16], the signal's sampling time plays a key role in retrieving transmitted information, whereas our time-domain method addresses distinct challenges involving signal reconstruction and filtering.

In this article, we introduce a novel method called the chip-time interval decomposition of creation operators, which serves as the quantum counterpart to "chips" in classical direct-sequence spread-spectrum code division multiple access (CDMA). This formulation unifies spread-spectrum encoding with quantum mechanical operators and provides a structured analysis of quantum signal evolution across the multiuser quantum communication network. Meanwhile, Rezai and Salehi [16] employ spectral-phase shifts for ultrashort pulses without requiring narrowband filtering, while our time-domain framework necessitates such filtering to recover transmitted signals effectively.

This new chip-time interval decomposition approach yields closed-form results for user interference, offers deeper insights into multiuser quantum signal processing, and highlights the role of entanglement in multiuser Fock state inputs. Moreover, the additional requirement of filtering in time-domain QCDMA—absent in the purely spectral encoding scheme of [16]—introduces another layer of complexity that our work explicitly addresses.

The rest of this article is organized as follows. Section II describes the operation of a quantum spread-spectrum transmitter, including the description of the quantum signals and the spreading operator. The quantum spread-spectrum communication receiver is described in Section III, where the signals are first decoded using the proper signature sequence. After applying the decoding operator, a narrowband filter (integrator) is used to reject the out-of-band interuser interference. This section develops a practical description of quantum filters for quantum communication systems from a novel perspective. A photon counting measurement is considered at the final state, giving the photon statistics of the received quantum signal. The overall quantum spread-spectrum communication system is described in Section IV. This section describes the effect of the quantum broadcasting channel, i.e., a star coupler, and derives the evolution of quantum signals in the considered multiple-access quantum communication system. In all of the mentioned sections, the system is carefully analyzed by the proposed chip-time interval decomposition approach that is introduced in Sections II-C and II-E. This approach gives closed-form expressions for the quantum signals that propagate through the system and leads to the chip-time decomposition methodology for the description of the quantum spread-spectrum CDMA communication systems in Section IV-C. Section V applies the proposed methods to a two-user spread-spectrum quantum communication system and presents the simulation results. Finally, Section VI concludes this article.

II. QUANTUM DIRECT-SEQUENCE SPREAD-SPECTRUM (QDSS) TRANSMITTER

In this section, we describe the application of spread-spectrum technology to quantum communication signals in terms of Dirac's formalism. A quantum communication signal is mathematically represented as a quantum state of light. At the transmitter, shown in Fig. 1, this quantum light goes through an electro-optical modulator that encodes a pseudo-random sequence onto the photon wavepacket of the transmitted quantum signal.

The sequence encoder (code multiplier) in our QDSS communication system can be physically realized by electro-optic modulation [18]. A variety of electro-optic modulator platforms can implement the phase shifts needed for direct-sequence spread-spectrum encoding (and decoding). In the following, we briefly highlight four major material-platform categories, drawing on recent progress in the technology [19].

1) *Lithium niobate:* Lithium niobate has traditionally been the utilized platform for high-speed electro-optics and is well known for enabling modulation of quantum signals [18]. Bulk lithium niobate modulators have already proven effective for notable proof-of-concept experimental demonstration of quantum spread-spectrum encoding and decoding at the single-photon level [14]. More recent thin-film and on-insulator lithium niobate

IEEE Transactions on Quantum Engineering

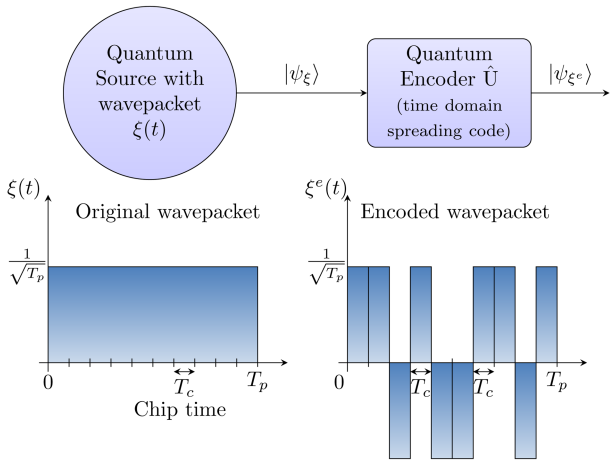

FIGURE 1. Effect of quantum encoder on the transmitted quantum communication signal with photon wavepacket $\xi(t)$ with processing gain (code length) of $N_c = \frac{T_p}{T_c}$.

devices allow compact Mach–Zehnder, ring-type, or topological modulators [20], [21] that can reach tens of gigahertz bandwidth [19].

2) *Indium phosphide:* Indium phosphide modulators can also deliver high bandwidth and relatively moderate drive voltages. Devices in this material have achieved bandwidths up to tens of gigahertz while maintaining small footprints [19].
3) *Silicon and hybrid-silicon approaches:* Silicon photonics technology naturally lends itself to tight integration with foundry-compatible processes. Also, silicon carbide on insulator modulators offer a different mechanism within a similar fabrication environment [22]. Although large-scale production is an advantage, pure-silicon modulators can be limited in speed or phase efficiency. To overcome these limitations, "hybrid-silicon" modulators incorporate additional electro-optic materials bonded or deposited onto silicon chips, taking advantage of silicon's existing infrastructure while improving bandwidth. Examples include polymer–silicon hybrids, lithium niobate–silicon systems, and plasmonic-organic slot waveguide designs [19].
4) *Two-dimensional materials:* Finally, 2-D materials, such as graphene, have also been considered for high-speed modulation at or near the single-photon level, due to their strong electro-absorption or refractive effects [19]. Although research remains at an early stage, the small footprints and potentially broad optical bandwidths of certain 2-D materials offer a future path for integrated QCDMA transmitters on a chip.

In the rest of this section, we show that analogous to the classical spread-spectrum communication signals, the temporal behavior of this photon wavepacket can be expressed based on the concept of chip-times. In this regard, we present a temporal decomposition for the creation operators of the transmitted quantum communication signals. The interested reader can find further details of quantum pulse shaping in [23].

A. QUANTUM SIGNAL DESCRIPTION

Quantum signals generated by a user's transmitter are in the form of quantum light pulses. The temporal shape of these quantum signals can be described by the so-called photon wavepacket $\xi(t)$. A pure quantum signal $|\psi_\xi\rangle$ with photon wavepacket $\xi(t)$ can thus be written as a superposition of number states with photon wavepacket $\xi(t)$, i.e., $|n_\xi\rangle$ [16]

$$|\psi_\xi\rangle = \sum_n c_n |n_\xi\rangle = f(\hat{a}_\xi^\dagger)|0\rangle \tag{1}$$

with $|0\rangle$ denoting the vacuum state and the creation operator of the quantum light pulse, i.e., $\hat{a}_\xi^\dagger$, is defined based on its corresponding photon wavepacket

$$\hat{a}_\xi^\dagger = \int_{-\infty}^{\infty} dt\, \xi(t)\hat{a}^\dagger(t) = \int_{-\infty}^{\infty} d\omega\, \bar{\xi}(\omega)\hat{a}^\dagger(\omega) \tag{2}$$

where $\hat{a}^\dagger(t)$ and $\hat{a}^\dagger(\omega)$ are the continuous mode creation operators in time t and frequency ω that are related to each other according to the Fourier transform relationship. It is more appealing to use the engineering convention[1] for imaginary numbers throughout this article. Thus, we may write [25]

$$\hat{a}(\omega) = \frac{1}{\sqrt{2\pi}} \int_{-\infty}^{\infty} dt \hat{a}(t) e^{-j\omega t}. \tag{3}$$

Based on the aforementioned definition, the spectral shape of the quantum signal, i.e., $\bar{\xi}(\omega)$ is the Fourier transform of the temporal wavepacket $\xi(t)$, i.e., $\bar{\xi}(\omega) = \mathcal{F}\{\xi(t)\}$.

Since $\xi(t)$ and $\bar{\xi}(\omega)$ represent the quantum probability amplitudes, they are normalized

$$\int_{-\infty}^{\infty} |\xi(t)|^2 dt = 1 \qquad \int_{-\infty}^{\infty} |\bar{\xi}(\omega)|^2 d\omega = 1. \tag{4}$$

Consider a quantum baseband rectangular signal of duration T_p. For such a quantum communication signal, we may obtain the corresponding creation operator as

$$\hat{a}_\xi^\dagger = \int_0^{T_p} dt \frac{1}{\sqrt{T_p}} \hat{a}^\dagger(t). \tag{5}$$

Any pure quantum communication signal with a particular wavepacket, such as $\xi(t)$, can be expressed in terms of the general equation in (1).

1) EXAMPLE 1

One choice for the transmitted quantum signals is photon number states $|n_\xi\rangle$ with wavepacket $\xi(t)$ and single-photon

[1] Since we deal with filters and signal processing throughout this article, it is more convenient to use the engineering convention for representing the imaginary numbers. The notions are thus consistent with the physics convention using $j = -i$ (see [24, p. 17]).

states $|1_\xi\rangle$ as a special case, defined as

$$|n_\xi\rangle := \frac{(\hat{a}_\xi^\dagger)^n}{\sqrt{n!}}|0\rangle \tag{6}$$

with $|1_\xi\rangle = \hat{a}_\xi^\dagger|0\rangle$ as a single-photon state.

2) EXAMPLE 2

As another example of quantum light, coherent (Glauber) states of the following form with the same wavepacket, $\xi(t)$, can be used for data transmission:

$$\begin{aligned}|\alpha_\xi\rangle &:= e^{-\frac{|\alpha|^2}{2}}\sum_{n=0}^{\infty}\frac{\alpha^n}{\sqrt{n!}}|n_\xi\rangle = e^{-\frac{|\alpha|^2}{2}}\sum_{n=0}^{\infty}\frac{\alpha^n(\hat{a}_\xi^\dagger)^n}{n!}|0\rangle \\ &= e^{-\frac{|\alpha|^2}{2}}e^{\alpha\hat{a}_\xi^\dagger}|0\rangle = e^{-\frac{|\alpha|^2}{2}}e^{\alpha\hat{a}_\xi^\dagger}e^{\alpha^*\hat{a}_\xi}|0\rangle \\ &= D(\alpha_\xi)|0\rangle \end{aligned} \tag{7}$$

where $D(\alpha_\xi) := e^{\alpha\hat{a}_\xi^\dagger - \alpha^*\hat{a}_\xi}$ is the displacement operator and the last equality is obtained using $\exp(\hat{A}+\hat{B}) = \exp(\hat{A})\exp(\hat{B})\exp(-\frac{1}{2}[\hat{A},\hat{B}])$. Also note that $e^{-\alpha^*\hat{a}_\xi}|0\rangle = |0\rangle$.

Although coherent states inherently possess quantum mechanical properties, including being described by a superposition of photon number states, their photon statistics follow a Poisson distribution. This statistical property makes them particularly interesting, as they demonstrate classical-like behavior, thus bridging quantum and classical regimes.

B. QUANTUM SPREADING OPERATOR

1) TEMPORAL MODULATION OF QUANTUM COMMUNICATION SIGNALS

In a quantum communication system, electro-optical modulators can be used to encode a user's spreading sequence on the temporal shape of the transmitted quantum signals [26]. Mathematically, this encoding corresponds to applying a unitary time-domain phase-shifting operator

$$\hat{\mathrm{U}} = \exp\left\{ j\int_0^{T_p}\theta(t)\,\hat{a}^\dagger(t)\,\hat{a}(t)\,dt\right\} \tag{8}$$

where $\theta(t)$ is a prescribed phase shift. When this operator acts on the Fock basis $|n_\xi\rangle$ (number states with photon wavepacket $\xi(t)$), it produces

$$\hat{\mathrm{U}}|n_\xi\rangle \;=\; |n_{\xi^e}\rangle \tag{9}$$

where $\xi^e(t) = e^{j\theta(t)}\xi(t)$. Hence, the original temporal wavepacket $\xi(t)$ is transformed into its encoded version $\xi^e(t)$. Acting on an arbitrary state $|\psi_\xi\rangle = \sum_n c_n|n_\xi\rangle$, we obtain

$$\hat{\mathrm{U}}|\psi_\xi\rangle = \sum_n c_n\hat{\mathrm{U}}|n_\xi\rangle = \sum_n c_n|n_{\xi^e}\rangle = |\psi_{\xi^e}\rangle \tag{10}$$

demonstrating that the phase-shifting operator converts the original wavepacket $\xi(t)$ into the modulated or encoded wavepacket $\xi^e(t)$.

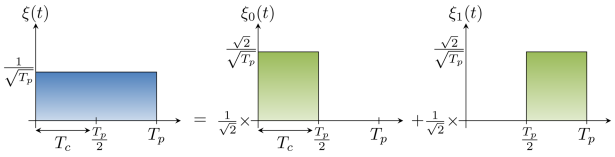

FIGURE 2. Temporal decomposition of photon wavepackets for $N_c = 2$. A photon wavepacket $\xi(t)$ can be viewed as a combination of chip-time wavepackets, $\xi_k(t)$.

2) DIRECT-SEQUENCE SPREAD-SPECTRUM ENCODING

In the rest of this article, we focus on a random binary spreading sequence whose phase-shift values are either 0 or π. Let the total pulse duration T_p be divided into N_c chips, as depicted in Fig. 1. Hence, the boundaries of the chips are $0 = t_0 < t_1 < \cdots < t_{N_c} = T_p$. Note that, over each chip time $[t_k, t_{k+1})$, the phase shift $\theta(t) = \theta_k$ remains constant at either 0 or π. Define

$$\lambda(t) := e^{j\theta(t)}. \tag{11}$$

Thus, for $t \in [t_k,\ t_{k+1})$

$$\theta(t) \equiv \theta_k \in \{0, \pi\} \qquad \lambda_k := e^{j\theta_k} \in \{-1, +1\}. \tag{12}$$

Hence

$$\lambda(t) \;=\; \sum_{k=0}^{N_c-1}\lambda_k\ \mathrm{rect}\left(\frac{t-t_k}{T_c}\right) \tag{13}$$

where $\mathrm{rect}(t)$ is a unity-amplitude rectangular function of unit duration. This random piecewise-constant $\lambda(t)$ encodes the user's spreading sequence on $\xi(t)$, producing the spread-spectrum wavepacket $\xi^e(t) = \lambda(t)\,\xi(t)$. Therefore, the code sequence can be denoted by $\Lambda = (\lambda_0, \lambda_1, \ldots, \lambda_{N_c-1})$.

C. CHIP-TIME CREATION OPERATORS

To analyze quantum spread-spectrum signals in the time domain, it is helpful to view the pulse as composed of chip-time subpulses. From a quantum-mechanical perspective, if each chip occupies $[t_k,\ t_{k+1})$ and satisfies

$$\int_{t_k}^{t_{k+1}}|\xi(t)|^2\,dt \;=\; \frac{1}{N_c} \tag{14}$$

then the probability of detecting a photon in each chip interval is $1/N_c$. Defining $\xi_k(t) := \sqrt{N_c}\,\xi(t)$ over $[t_k,\ t_{k+1})$ and 0 elsewhere, we see that $\xi_k(t)$ is a normalized photon wavepacket restricted to the kth chip (see Fig. 2 for an illustrative example). The corresponding chip-time creation operator is

$$\hat{a}_{\xi_k}^\dagger \;:=\; \int_{t_k}^{t_{k+1}}\xi_k(t)\,\hat{a}^\dagger(t)\,dt. \tag{15}$$

These $\hat{a}_{\xi_k}^\dagger$ operators serve as the natural building blocks for spread-spectrum signals, each representing photon creation

IEEE Transactions on Quantum Engineering

within a single chip. For instance, a rectangular $\xi(t)$ of duration T_p decomposes into N_c intervals of length T_c, with

$$\xi_k(t) = \begin{cases} \sqrt{\frac{N_c}{T_p}}, & t \in [t_k,\ t_{k+1}) \\ 0, & \text{otherwise.} \end{cases} \tag{16}$$

Because the chip-time intervals do not overlap, these creation operators commute for distinct k and l.

Proposition 1: The chip-time interval creation operators have the following properties.

1) The corresponding wavepacket satisfies the required normalization property of a photon wavepacket

$$\int_0^{T_p} |\xi_k(t)|^2 dt = 1. \tag{17}$$

2) Nonoverlapping chip-time interval creation operators commute

$$\left[\hat{a}_{\xi_l}, \hat{a}^\dagger_{\xi_k}\right] = \delta_{lk} \tag{18}$$

where δ_{lk} is the Kronecker delta, where $\hat{a}^\dagger_{\xi_k} = \int_{t_k}^{t_{k+1}} dt\ \xi_k(t)\hat{a}^\dagger(t)$.

Proof: See Appendix A. ■

Moreover, we show in the following theorem that any creation operator $\hat{a}^\dagger_\xi$ can be written as a linear combination of the chip-time interval creation operators, thereby simplifying the mathematical description of quantum spread-spectrum signals.

Theorem 1 (Chip-time Interval Creation Operators): A quantum field creation operator, $\hat{a}^\dagger_\xi$, with wavepacket $\xi(t)$ can be decomposed into chip-time interval creation operators according to the following relation:

$$\hat{a}^\dagger_\xi = \frac{1}{\sqrt{N_c}} \sum_{k=0}^{N_c-1} \hat{a}^\dagger_{\xi_k}. \tag{19}$$

Proof: See Appendix A. ■

The chip-time interval creation operators give us insight on how the spreading operator acts on different quantum states and how quantum signals evolve through a spread-spectrum communication system. This novel interpretation leads to the definition of chip-time number states

$$|n_{\xi_k}\rangle = \frac{(\hat{a}^\dagger_{\xi_k})^n}{\sqrt{n!}}|0\rangle \tag{20}$$

which indicates a quantum state with exactly n photons in interval $[t_k, t_{k+1})$ and wavepacket $\xi_k(t)$.

D. CHIP-TIME HILBERT SPACES

As discussed in the previous section, the chip-time interval creation operators are associated with chip-time number states. As we show throughout this article, these chip-time number states form an invariant basis for the quantum signals' evolution through the spread-spectrum communication system.

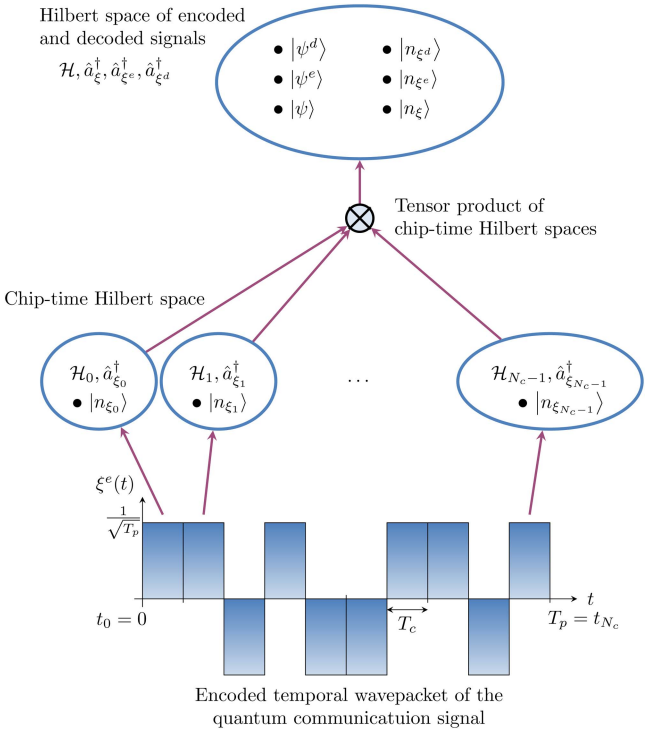

FIGURE 3. Hilbert space view of chip-time interval decomposition. A chip-time Hilbert space is associated with each chip-time interval of the quantum communication signal. The encoded and decoded quantum signals can be represented in the tensor product space of these chip-time Hilbert spaces.

The kth chip-time number states, $|n_{\xi_k}\rangle$, $n = 0, 1, \ldots$, naturally form a basis for a Hilbert space,[2] $\mathcal{H}_k$. We call this space a chip-time Hilbert space. Number states $|n_{\xi_k}\rangle$ associated with the creation operator $\hat{a}^\dagger_{\xi_k}$ form a basis for $\mathcal{H}_k$. Fig. 3 shows how the spread-spectrum quantum signals can be described in accordance with these chip-time Hilbert spaces. As seen in this figure, a Hilbert space is associated with each chip-time of the quantum spread-spectrum signal. The overall signal's wavepacket can always be decomposed into these chip-time building blocks. Each chip-time Hilbert space describes a single chip of the quantum signal. Since chip times are nonoverlapping, the overall Hilbert space representing the original, encoded, and decoded spread-spectrum quantum signals is the tensor product of the chip-time Hilbert spaces.

E. CHIP-TIME INTERVAL DECOMPOSITION OF QUANTUM SIGNALS

With the aid of the chip-time interval creation operators, we can decompose different quantum signals in time. Coherent states and number states are among the most important quantum signals. For coherent states, the decomposition has a tensor product form.

[2]The Hilbert space presented here corresponds to Fock space in the field of quantum many-particle systems [27].

Proposition 2: The coherent state $|\alpha_\xi\rangle$ can be written as the tensor product of coherent states on different intervals

$$D(\alpha_\xi) = \prod_{k=0}^{N_c-1} D\left(\frac{\alpha_{\xi_k}}{\sqrt{N_c}}\right) \tag{21}$$

$$|\alpha_\xi\rangle = \prod_{k=0}^{N_c-1} \left|\frac{\alpha_{\xi_k}}{\sqrt{N_c}}\right\rangle \tag{22}$$

where $|\frac{\alpha_{\xi_k}}{\sqrt{N_c}}\rangle = D(\frac{\alpha_{\xi_k}}{\sqrt{N_c}})|0\rangle = e^{-\frac{|\alpha|^2}{2N_c}} e^{\frac{\alpha}{\sqrt{N_c}}\hat{a}^\dagger_\xi}|0\rangle$.

Proof: See Appendix B. ■

For number states, the decomposition results in a superposition.

Proposition 3: The chip-time interval decomposition of number state $|n_\xi\rangle$ can be expressed in terms of the following superposition of different intervals:

$$\begin{aligned}|n_\xi\rangle &= \sum_{n_0+n_1+\cdots+n_{N_c-1}=n} \mathcal{C}_n(n_0, n_1, \ldots, n_{N_c-1}) \prod_{k=0}^{N_c-1} |n_{k,\xi_k}\rangle \\ &= \sum_{n_0+n_1+\cdots+n_{N_c-1}=n} \mathcal{C}_n(n_0, n_1, \ldots, n_{N_c-1}) \\ &\quad \times |n_{0,\xi_0}, n_{1,\xi_1}, \ldots, n_{N_c-1,\xi_{N_c-1}}\rangle \end{aligned} \tag{23}$$

where $|n_{0,\xi_0}, n_{1,\xi_1}, \ldots, n_{N_c-1,\xi_{N_c-1}}\rangle = |n_{0,\xi_0}\rangle|n_{1,\xi_1}\rangle \cdots |n_{N_c-1,\xi_{N_c-1}}\rangle$ and $|n_{k,\xi_k}\rangle$ means that the state has n_k photons with wavepacket $\xi_k(t)$ in interval $[t_k, t_{k+1})$ and its probability in the superposition is $|\mathcal{C}_n(n_0, n_1, \ldots, n_{N_c-1})|^2$, where

$$\mathcal{C}_n(n_0, n_1, \ldots, n_{N_c-1}) := \frac{1}{\sqrt{N_c^n}} \sqrt{\binom{n}{n_0, n_1, \ldots, n_{N_c-1}}} \tag{24}$$

and

$$\binom{n}{n_0, n_1, \ldots, n_{N_c-1}} = \frac{n!}{n_0! n_1! \cdots n_{N_c-1}!}. \tag{25}$$

Proof: See Appendix C. ■

For $n = 1$, i.e., the single-photon quantum signal, we have

$$|1_\xi\rangle = \frac{1}{\sqrt{N_c}} \sum_{k=0}^{N_c-1} |1_{\xi_k}\rangle \tag{26}$$

which means that a single photon with wavepacket $\xi(t)$ can be viewed as a superposition of single photons at different chips with probability $\frac{1}{N_c}$.

Since number states $|n_\xi\rangle$ form a basis for the Hilbert space of quantum signals with photon wavepacket $\xi(t)$, one can obtain the temporal decomposition of any arbitrary quantum signal by substituting Proposition 3 in $|\psi_\xi\rangle = \sum_n c_n |n_\xi\rangle$.

F. CHIP-TIME INTERVAL DECOMPOSITION OF THE SPREADING OPERATOR

In order to further investigate the effect of the spreading operator on the quantum signals, we decompose $\hat{\mathrm{U}}$ into its constructing chip-time interval operators. The following theorem shows that the spreading operator can be decomposed into operators that each act on an individual chip time.

Theorem 2: The chip-time interval decomposition of quantum spreading operator, $\hat{\mathrm{U}}$, results in the following expression:[3]

$$\hat{\mathrm{U}} = \prod_{k=0}^{N_c-1} \hat{\mathrm{U}}_k \tag{27}$$

where

$$\hat{\mathrm{U}}_k := \exp\left(j \int_{t_k}^{t_{k+1}} dt \theta_k \hat{a}^\dagger(t) \hat{a}(t)\right) \tag{28}$$

has the following property:

$$\left[\hat{\mathrm{U}}_k, f(\hat{a}^\dagger_{\xi_l})\right] = 0, \qquad l \neq k. \tag{29}$$

Proof: See Appendix D-A. ■

G. CHIP-TIME INTERVAL DECOMPOSITION OF SPREAD-SPECTRUM QUANTUM SIGNALS

In this section, we obtain the chip-time interval decomposition of the spread-spectrum quantum signals by applying the spreading operator to the transmitted quantum signals. As a result, we demonstrate that a spread-spectrum quantum signal can be characterized by chip-time interval creation operators.

Theorem 3: The effect of spreading operator on the creation operator of a quantum signal with wavepacket $\xi(t)$ is given by the following chip-time interval decomposition:

$$\hat{a}_{\xi^e} := \hat{\mathrm{U}} \hat{a}^\dagger_\xi \hat{\mathrm{U}}^\dagger = \frac{1}{\sqrt{N_c}} \sum_{k=0}^{N_c-1} \lambda_k \hat{a}^\dagger_{\xi_k}. \tag{30}$$

Proof: See Appendix D-B. ■

From Theorem 3, illustrated in Fig. 4, we obtain the chip-time interval decomposition of quantum signals in the following propositions.

Proposition 4: The spread-spectrum coherent state obtained by applying the spreading unitary transformation $\hat{\mathrm{U}}$ on $|\alpha_\xi\rangle$, i.e., $|\alpha_{\xi^e}\rangle$, can be written in the following tensor product form:

$$\hat{\mathrm{U}}|\alpha_\xi\rangle = |\alpha_{\xi^e}\rangle = \prod_{k=0}^{N_c-1} \left|\frac{\lambda_k \alpha_{\xi_k}}{\sqrt{N_c}}\right\rangle. \tag{31}$$

Proof: See Appendix E-A. ■

Proposition 5: The spread-spectrum number state obtained by applying the spreading unitary transformation $\hat{\mathrm{U}}$ on $|n_\xi\rangle$, i.e. $|n_{\xi^e}\rangle$, can be written in the following superposition form:

$$\hat{\mathrm{U}}|n_\xi\rangle = |n_{\xi^e}\rangle$$

[3]Some authors use $\otimes$ instead of $\prod$ to represent the tensor product. See Appendix M for related discussions.

IEEE Transactions on Quantum Engineering

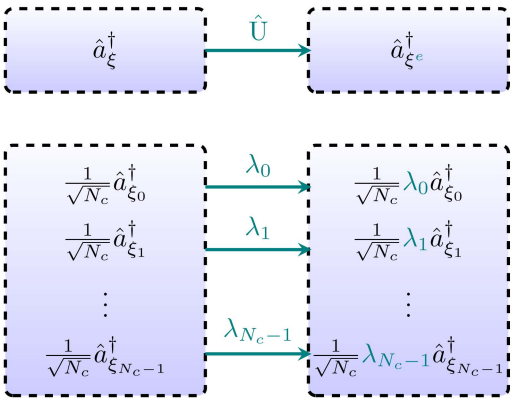

FIGURE 4. Effect of spreading operator on the creation operators. The spreading operator converts $\xi(t)$ to $\xi^e(t)$. According to Theorem 3, this evolution is equivalent to applying the code sequence on the individual chip-time interval creation operators.

$$= \sum_{n_0+n_1+\cdots+n_{N_c-1}=n} \mathcal{C}_n(n_0, n_1, \ldots, n_{N_c-1}) \prod_{k=0}^{N_c-1} (\lambda_k)^{n_k} |n_{\xi_k}\rangle. \tag{32}$$

Proof: See Appendix F-A. ■

As an example, we have simplified the results of Proposition 5 for $n = 1, 2, 3$ in Appendix F-A.

For $n = 1$, we have

$$\hat{U}|1_\xi\rangle = |1_{\xi^e}\rangle = \frac{1}{\sqrt{N_c}} \sum_{k=0}^{N_c-1} \lambda_k |1_{\xi_k}\rangle. \tag{33}$$

For $n = 2$, we obtain

$$\hat{U}|2_\xi\rangle = |2_{\xi^e}\rangle = \frac{1}{N_c} \sum_{k_0=0}^{N_c-1} |2_{\xi_{k_0}}\rangle + \frac{1}{N_c} \sum_{\substack{k_1=0 \\ \text{s.t. } k_1>k_0}}^{N_c-1} \sum_{k_0=0}^{N_c-1} \sqrt{2}\lambda_{k_0}\lambda_{k_1} |1_{\xi_{k_0}}\rangle |1_{\xi_{k_1}}\rangle. \tag{34}$$

For $n = 3$, we have

$$\begin{aligned}\hat{U}|3_\xi\rangle = |3_{\xi^e}\rangle = {} & \frac{1}{\sqrt{N_c^3}} \sum_{k_0=0}^{N_c-1} \lambda_{k_0} |3_{\xi_{k_0}}\rangle \\ & + \frac{1}{\sqrt{N_c^3}} \sum_{k_1=0}^{N_c-1} \sum_{k_0=0}^{N_c-1} \sqrt{3}\lambda_{k_0} |1_{\xi_{k_0}}\rangle |2_{\xi_{k_1}}\rangle \\ & + \frac{1}{\sqrt{N_c^3}} \sum_{\substack{k_2=0 \\ \text{s.t. } k_2>k_1>k_0}}^{N_c-1} \sum_{k_1=0}^{N_c-1} \sum_{k_0=0}^{N_c-1} \sqrt{3!}\lambda_{k_0}\lambda_{k_1}\lambda_{k_2} \\ & \times |1_{\xi_{k_0}}\rangle |1_{\xi_{k_1}}\rangle |1_{\xi_{k_2}}\rangle. \end{aligned} \tag{35}$$

We can observe that for number states, the spreading operator encodes the random sequence into the superposition coefficients of the chip-time interval number states. On the other hand, the same spreading operator results in separable chip-time encoded states for the coherent transmitted quantum signal.

III. QDSS RECEIVER

In order to investigate the basic operation of the quantum spread-spectrum receiver, consider a point-to-point communication scenario depicted in Fig. 5. The sequence Λ encodes the transmitted quantum signals in this scenario. Post encoding, the signals are decoded by another sequence $\tilde{\Lambda}$. Then, a narrowband filter is applied so that the correctly decoded signal arrives at the receiver end. The narrowband filter rejects the out-of-band incorrectly decoded signals, as they have higher bandwidth due to the use of spread-spectrum technology. Note that in our quantum optical setup, we treat multiuser interference as the primary source of noise. Hence, in the optical fiber point-to-point case, the channel is considered ideal. The star coupler serves as the shared quantum channel, as described in Section IV.

The typical point-to-point quantum spread-spectrum communication system of Fig. 5 comprises a quantum transmitter, a quantum spreading operator (encoder) with sequence Λ, a quantum despreading operator (decoder) with sequence $\tilde{\Lambda}$, a quantum filter, and a photodetector (quantum measurement). The quantum transmitter associates a pure quantum state to each transmitted data symbol. After that, the spreading operator $\hat{U}$ applies a unitary transformation to the transmitted quantum signal. This direct-sequence code multiplier may be realized using electro-optical modulators to apply the required random temporal phase shifts. The signal is then despread (decoded) at the receiver by applying the inverse of the quantum spreading operator $\hat{U}^\dagger$. The signal then passes through an optical narrowband filter. The desired output of the filter is possibly a mixed quantum signal and is denoted by ρ^T. In order to obtain the photon statistics of the received signal, we consider an ideal photodetector after the filter. The photon counting detector is described by the number operator $\hat{N}$. We show that decoding the quantum signal with a wrong code sequence results in noise due to unmatched spreading sequences at the receiver, while the original quantum signal can be recovered by decoding with the correct code.

A. DECODING THE DIRECT-SEQUENCE SPREAD-SPECTRUM QUANTUM SIGNALS

The description of decoded sequence can be obtained according to the proposed temporal decomposition framework.

Proposition 6: Decoding a spread-spectrum coherent state $|\alpha_{\xi^e}\rangle = \prod_{k=0}^{N_c-1} |\frac{\lambda_k\alpha_{\xi_k}}{\sqrt{N_c}}\rangle$ with spreading sequence Λ and despreading sequence $\tilde{\Lambda}$ gives the following state:

$$|\alpha_{\xi^d}\rangle = \prod_{k=0}^{N_c-1} \left|\frac{\tilde{\lambda}_k\lambda_k\alpha_{\xi_k}}{\sqrt{N_c}}\right\rangle. \tag{36}$$

Proof: See Appendix E-B. ■

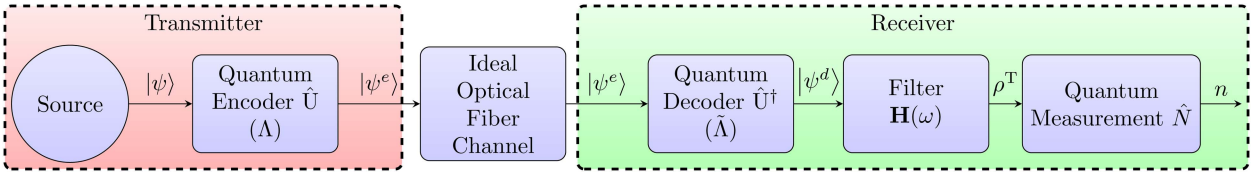

FIGURE 5. Point-to-point quantum spread-spectrum communication system.

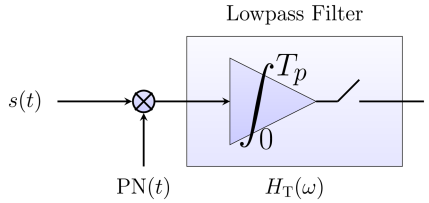

FIGURE 6. Typical receiver structure for classical baseband direct-sequence spread-spectrum communication systems. The received classical communication signal $s(t)$ is a pulse encoded with pseudorandom sequence PN(t). This signal is multiplied by the despreading code PN(t) at the receiver. The output passes through a low-pass filter (an integrator).

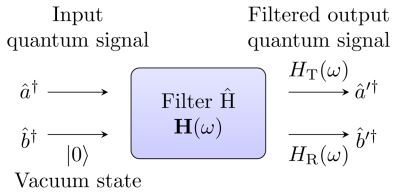

FIGURE 7. Filtering a quantum signal using a general structure with input two ports corresponding to $\hat{a}^\dagger$ and $\hat{b}^\dagger$ and two output ports corresponding to $\hat{a}'^\dagger$ and $\hat{b}'^\dagger$. At the receiver, the quantum signals are considered in the port corresponding to $\hat{a}^\dagger$, while the auxiliary mode $\hat{b}^\dagger$ is in vacuum state. The output of the filter corresponds to mode $\hat{a}'^\dagger$ with a narrowband response for $H_{\mathrm{T}}(\omega)$.

Proposition 7: Decoding a spread-spectrum number state $|n_{\xi^e}\rangle$ with spreading sequence Λ and decoding sequence $\tilde{\Lambda}$ gives the following state:

$$|n_{\xi^d}\rangle = \sum_{n_0+n_1+\cdots+n_{N_c-1}=n} \mathcal{C}_n(n_0, n_1, \ldots, n_{N_c-1}) \times \prod_{k=0}^{N_c-1} (\tilde{\lambda}_k \lambda_k)^{n_k} |n_{\xi_k}\rangle. \tag{37}$$

Proof: See Appendix F-B. ■

If the encoded quantum signal is decoded with the correct sequence, i.e., $\tilde{\Lambda} = \Lambda$, then the receiver will obtain the same signal as the transmitted one.

B. FILTERING QUANTUM SIGNALS AT THE RECEIVER

Fig. 6 shows a typical receiver structure for classical baseband direct-sequence spread-spectrum communication systems. In QCDMA, the decoding (despreading) operator plays the role of the classical multiplier in the quantum domain. After decoding the quantum signal, similar to classical spread-spectrum CDMA communication systems, a narrowband filter (low-pass filter for equivalent baseband signals) is required to reject the out-of-band signal.

In this article, we consider a general two-port passive time-invariant structure for the filter [28], [29], [30], as shown in Fig. 7. A time-independent quantum filter is a passive (energy-preserving) device that can be described by a unitary transformation on two sets of input modes described by creation operators $\hat{a}^\dagger(\omega)$ and $\hat{b}^\dagger(\omega)$. The input modes of interest $\hat{a}^\dagger(\omega)$ correspond to the quantum signal that is being filtered. In contrast, $\hat{b}^\dagger(\omega)$ belongs to auxiliary modes that are assumed initially to be in the vacuum state. Hence, a two-port quantum filter is a unitary operator $\mathbf{H}(\omega)$ that acts on two modes and generate new transmitted and reflected modes $\hat{a}'^\dagger(\omega)$ and $\hat{b}'^\dagger(\omega)$, respectively.

Conceptually, this filter, e.g., the narrowband Fabry–Pérot used in [14], generalizes a beam splitter model to include frequency-dependent (transmission/reflection) responses. Therefore, although it shares the fundamental unitary property of a beam splitter, this quantum filter incorporates a narrowband spectral shaping that discriminates between in-band and out-of-band frequency components. Assuming that the evolution operator of the filter is denoted by $\hat{\mathrm{H}}$, we may write [31]

$$\hat{\mathrm{H}} \begin{pmatrix} \hat{a}^\dagger(\omega) \\ \hat{b}^\dagger(\omega) \end{pmatrix} \hat{\mathrm{H}}^\dagger = \mathbf{H}(\omega) \begin{pmatrix} \hat{a}'^\dagger(\omega) \\ \hat{b}'^\dagger(\omega) \end{pmatrix} = \begin{pmatrix} H_{\mathrm{T}}(\omega) & H_{\mathrm{R}}(\omega) \\ H_{\mathrm{R}}(\omega) & H_{\mathrm{T}}(\omega) \end{pmatrix} \begin{pmatrix} \hat{a}'^\dagger(\omega) \\ \hat{b}'^\dagger(\omega) \end{pmatrix} \tag{38}$$

where $H_{\mathrm{T}}(\omega)$ and $H_{\mathrm{R}}(\omega)$ denote the complex frequency response of transmission (through the desired port of the filter) and reflection (of the other filter port) components, respectively. The unitary property of the transformation means that the filter coefficients must satisfy the following relationships [32]:

$$|H_{\mathrm{T}}(\omega)|^2 + |H_{\mathrm{R}}(\omega)|^2 = 1 \tag{39}$$

$$H_{\mathrm{T}}(\omega) H_{\mathrm{R}}^*(\omega) + H_{\mathrm{R}}(\omega) H_{\mathrm{T}}^*(\omega) = 0. \tag{40}$$

To obtain the filter's effect on the quantum signal, we write the evolution of the creation operator of the transmitted mode, which describes the received quantum signal

$$\hat{\mathrm{H}} \hat{a}_\xi^\dagger \hat{\mathrm{H}}^\dagger = \int_{-\infty}^{\infty} d\omega \bar{\xi}(\omega) \hat{\mathrm{H}} \hat{a}^\dagger(\omega) \hat{\mathrm{H}}^\dagger \tag{41}$$

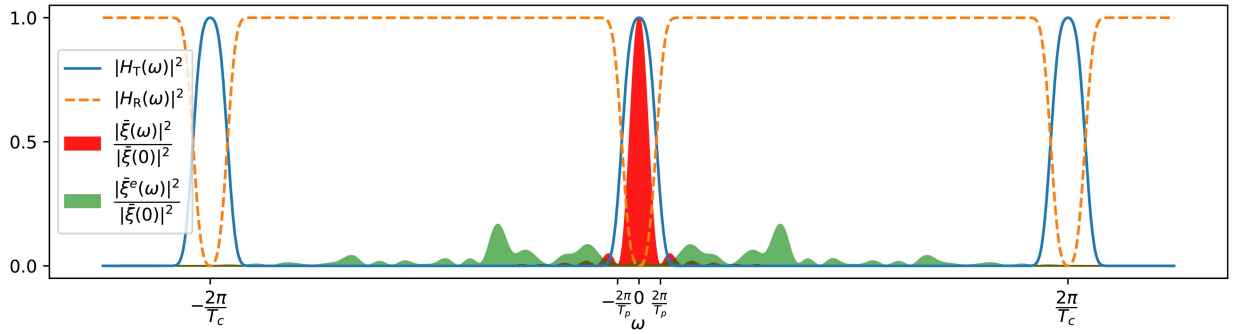

FIGURE 8. Frequency response of a typical low-pass baseband filter. The 3-dB bandwidth of the transmission filter $H_T(\omega)$ is equal to the bandwidth of the original quantum signal and $N_c = 20$. The quantum spread-spectrum signal has a higher bandwidth and does not significantly pass through $H_T(\omega)$ but significantly passes through $H_R(\omega)$. Also note that $|H_T(\omega)|^2 + |H_R(\omega)|^2 = 1$ (all-pass filter).

$$= \int_{-\infty}^{\infty} d\omega H_T(\omega)\bar{\xi}(\omega)\hat{a}'^{\dagger}(\omega) + \int_{-\infty}^{\infty} d\omega H_R(\omega)\bar{\xi}(\omega)\hat{b}'^{\dagger}(\omega) \tag{42}$$

$$= \int_{-\infty}^{\infty} dt(h_T(t) * \xi(t))\hat{a}'^{\dagger}(t) + \int_{-\infty}^{\infty} dt(h_R(t) * \xi(t))b'^{\dagger}(t) \tag{43}$$

$$:= w_T\hat{a}'^{\dagger}_{\xi_T} + w_R\hat{b}'^{\dagger}_{\xi_R} \tag{44}$$

where $*$ stands for convolution, $h_T(t) = \mathcal{F}^{-1}\{H_T(\omega)\}$, $h_R(t) = \mathcal{F}^{-1}\{H_R(\omega)\}$, $H_T(\omega)\bar{\xi}(\omega) = \mathcal{F}\{h_T(t) * \xi(t)\}$, and $H_R(\omega)\bar{\xi}(\omega) = \mathcal{F}\{h_R(t) * \xi(t)\}$. Also

$$\hat{a}'^{\dagger}_{\xi_T} := \frac{1}{w_T}\int_{-\infty}^{\infty} dt(h_T(t) * \xi(t))\hat{a}'^{\dagger}(t) \tag{45}$$

$$\hat{b}'^{\dagger}_{\xi_R} := \frac{1}{w_R}\int_{-\infty}^{\infty} dt(h_R(t) * \xi(t))\hat{b}'^{\dagger}(t). \tag{46}$$

Note that for the quantum filter, transmission probability is

$$w_T^2 := \int_{-\infty}^{\infty} dt|h_T(t) * \xi(t)|^2 \tag{47}$$

and the reflection probability

$$w_R^2 := \int_{-\infty}^{\infty} dt|h_R(t) * \xi(t)|^2. \tag{48}$$

Indeed (using Parseval's theorem), we have $w_T^2 + w_R^2 = 1$, that is, the probabilities of reflection and transmission should sum to one.

C. CHIP-TIME INTERVAL DECOMPOSITION OF THE QUANTUM FILTER

1) GENERAL TWO-PORT FILTER

We can represent a general optical filter [33] by the Fourier series of its transfer function. Thus, for a causal optical filter [34, Sect. 10.7.1], we may write

$$H_T(\omega) = \sum_{l=0}^{\infty} d_l e^{-jl\omega\tau} \tag{49}$$

$$H_R(\omega) = \sum_{l=0}^{\infty} f_l e^{-jl\omega\tau}. \tag{50}$$

The case of $\tau = T_c$ is of special interest for the quantum spread-spectrum communication system, where T_c is the chip time. For this case, we obtain the temporal decomposition of the creation operators for rectangular wavepackets.

As shown in Fig. 8, in a spread-spectrum communication system, $H_T(\omega)$ has effectively a low-pass baseband frequency response. The transmission response of the filter should have a bandwidth equal to the signal bandwidth, i.e., $\frac{2\pi}{T_p}$. The response of the filter is periodic with period $\frac{2\pi}{T_c}$, which is larger than the bandwidth of the spread-spectrum quantum signal.

Proposition 8: The chip-time interval creation operators of the input mode to a quantum filter with a rectangular wavepacket can be expressed in terms of the chip-time interval creation operators as follows:

$$\hat{H}\hat{a}^{\dagger}_{\xi_k}\hat{H}^{\dagger} = \sum_{l=0}^{\infty}(d_l\hat{a}'^{\dagger}_{\xi_{k+l}} + f_l\hat{b}'^{\dagger}_{\xi_{k+l}}). \tag{51}$$

Proof: See Appendix G. ■

We further track the filter's effect on a creation operator with wavepacket $\xi(t)$ utilizing the temporal decomposition of creation operators.

Theorem 4: The creation operator of the input mode to a quantum filter with a rectangular wavepacket can be expressed in terms of the chip-time interval creation operators as follows:

$$\hat{H}\hat{a}^{\dagger}_{\xi}\hat{H}^{\dagger} = \sum_{q=0}^{\infty}(D_q\hat{a}'^{\dagger}_{\xi_q} + F_q\hat{b}'^{\dagger}_{\xi_q}) \tag{52}$$

where the transmitted and reflected probability amplitude coefficients at time interval q are, respectively

$$D_q := \sum_{l=\max(0,q-N_c+1)}^{q} \frac{1}{\sqrt{N_c}} d_l \tag{53}$$

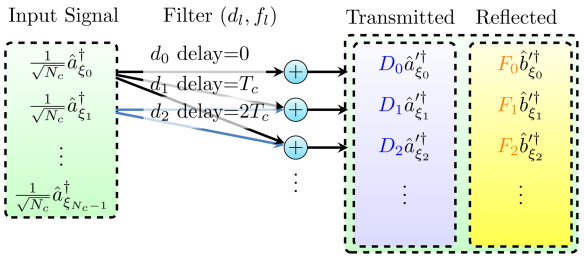

FIGURE 9. Filter interleaves the chip-time interval creation operators. Only transmission coefficients d_l are illustrated. Note that the time-interval creation operators do not backtrack due to the causality of the filter.

$$F_q := \sum_{l=\max(0,q-N_c+1)}^{q} \frac{1}{\sqrt{N_c}} f_l. \tag{54}$$

Proof: See Appendix G. ■

Note that the unitary condition implies that

$$\sum_{q=0}^{\infty} \left(|D_q|^2 + |F_q|^2 \right) = 1. \tag{55}$$

Fig. 9 illustrates the results of Theorem 4.

2) FINITE IMPULSE RESPONSE (FIR) FILTER

The filtering coefficients reduce to the following expression for FIR filters with a maximum delay of LT_c, where L is the number of FIR filter coefficients:

$$D_q = \sum_{l=\max(0,q-N_c+1)}^{\min(q,L)} \frac{1}{\sqrt{N_c}} d_l \tag{56}$$

$$F_q = \sum_{l=\max(0,q-N_c+1)}^{\min(q,L)} \frac{1}{\sqrt{N_c}} f_l. \tag{57}$$

Fig. 10(a) depicts typical asymptotic behavior of values D_q and F_q for near ideal filters.

D. SPREAD-SPECTRUM SIGNAL AFTER FILTER

To further investigate the effect of filter on the encoded (spreaded) and decoded (despreaded) spread-spectrum quantum signals, we first define the corresponding filter coefficients as follows:

$$\tilde{D}_q := \sum_{l=\max(0,q-N_c+1)}^{q} \frac{1}{\sqrt{N_c}} d_l \tilde{\lambda}_{q-l} \lambda_{q-l} \tag{58}$$

$$\tilde{F}_q := \sum_{l=\max(0,q-N_c+1)}^{q} \frac{1}{\sqrt{N_c}} f_l \tilde{\lambda}_{q-l} \lambda_{q-l}. \tag{59}$$

From a signal processing point of view, we can also describe the aforementioned coefficients as the result of a discrete-time convolution [35, Sect. 2.9.6], i.e.,

$$\tilde{D}_q := d_q * \Pi_q^{\tilde{\Lambda}\Lambda} \tag{60}$$

$$\tilde{F}_q := f_q * \Pi_q^{\tilde{\Lambda}\Lambda} \tag{61}$$

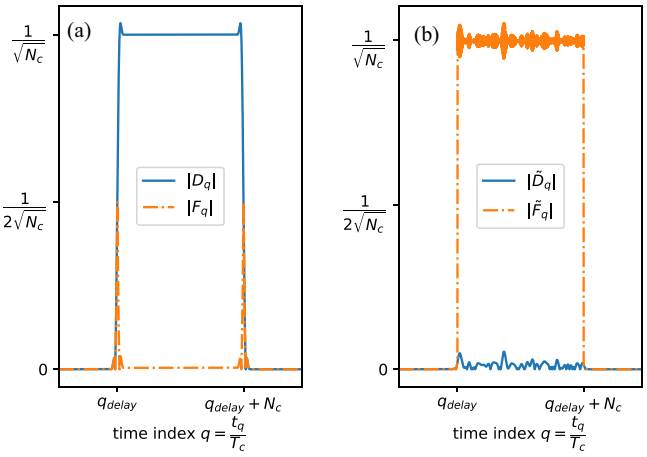

FIGURE 10. (a) and (b) Asymptotic behavior of the discrete coefficients of the filter's output, where the filter's bandwidth is sufficiently greater than the quantum signal's bandwidth and a high processing gain is used, i.e., $T_c \ll T$. To investigate the asymptotic behavior, we choose $N_c = 100000$ and the bandwidth of filter is $20 \times \frac{2\pi}{T_p}$. Both filters, $H_T(\omega)$ and $H_R(\omega)$, are approximated with type I FIR filters with odd number of taps $L = 10001$ and designed using the windowing method [35].

where

$$\Pi_q^{\tilde{\Lambda}\Lambda} := \begin{cases} \frac{1}{\sqrt{N_c}} \tilde{\lambda}_q \lambda_q, & 0 \le q \le N_c - 1 \\ 0, & \text{o.w.} \end{cases} \tag{62}$$

The following proposition describes the evolution of creation operators through the filter using the proposed chip-time interval decomposition methodology.

Proposition 9: The creation operator of a quantum signal encoded with Λ and decoded with $\tilde{\Lambda}$ can be expressed in terms of the chip-time interval creation operators as follows:

$$\hat{\mathrm{H}} \hat{a}_{\xi^d}^{\dagger} \hat{\mathrm{H}}^{\dagger} = \sum_{q=0}^{\infty} (\tilde{D}_q \hat{a}_{\xi_q}^{\prime\dagger} + \tilde{F}_q \hat{b}_{\xi_q}^{\prime\dagger}). \tag{63}$$

Proof: See Appendix G. ■

Fig. 10(b) depicts typical asymptotic behavior of values $\tilde{D}_q$ and $\tilde{F}_q$ when the random codes Λ and $\tilde{\Lambda}$ does not match, i.e., $\Lambda \neq \tilde{\Lambda}$.

If the decoding sequence is different from the encoding sequence, the output of the decoder is wideband and thus is rejected by the filter. In other words, the values of $\tilde{F}_q$ and D_q are large over the duration of the transmitted quantum signal, while the values of F_q and $\tilde{D}_q$ are small.

As discussed in Appendix G-A, the shape of the transmitted wavepacket $\xi(t)$ is asymptotically preserved after correct decoding of the quantum signals. Therefore, the transmitted wavepacket is almost equal to the signal wavepacket, i.e., $\langle \xi(t) | \xi_{\mathrm{T}}(t - T_{\mathrm{delay}}) \rangle \approx 1$, where $T_{\mathrm{delay}} = q_{\mathrm{delay}} \times T_c$ is the delay imposed by the causal filter and q_{delay} is the number of chip times corresponding to T_{delay}.

The evolution of specific quantum signals can also be expressed in terms of chip-time intervals as follows.

Proposition 10: The coherent quantum signal encoded with sequence Λ and decoded with sequence $\tilde{\Lambda}$ results in the following pure quantum signal after the filter:

$$|\alpha_{\xi_T}\rangle = \prod_{q=0}^{\infty} |\tilde{D}_q \alpha_{\xi_q}\rangle \tag{64}$$

where T in $|\alpha_{\xi_T}\rangle$ means that the output state is in the transmitted mode of the filter, and $|\alpha_{\xi_q}\rangle$ corresponds to the related chip-time interval coherent state.

Proof: See Appendix H. ■

At the receiver, a photodetector can be used to perform a measurement on the signal after filtering. Each term in the tensor product results in a Poisson distribution for the number of photons in that specific chip-time, i.e., n_{q,ξ_q}. Therefore, the output statistics can be obtained by noticing that the sum of independent Poisson random variables is also a Poisson random variable. We obtain the total photon number distribution

$$\mathbb{P}(n) = \sum_{n_0+n_1+\cdots=n} \left|\langle n_{0,\xi_0}, n_{1,\xi_1}, \cdots |\alpha_{\xi_T}\rangle\right|^2 \tag{65}$$

$$= e^{-\mu} \frac{\mu^n}{n!} \tag{66}$$

where $\mu = |\alpha|^2 \sum_{q=0}^{\infty} |\tilde{D}_q|^2$ is the mean photon number of the received coherent (Glauber) quantum signal.

Proposition 11: A single-photon quantum signal encoded with sequence Λ and decoded with sequence $\tilde{\Lambda}$ results in a mixed quantum signal after filter with a density operator as follows:

$$\rho^T = \left(\sum_{q=0}^{\infty} |\tilde{F}_q|^2\right) |0\rangle\langle 0| + \left(\sum_{q=0}^{\infty} |\tilde{D}_q|^2\right) |1_{\xi_T}\rangle\langle 1_{\xi_T}| \tag{67}$$

where

$$|1_{\xi_T}\rangle := \frac{1}{\sqrt{\sum_{q=0}^{\infty} |\tilde{D}_q|^2}} \sum_{q=0}^{\infty} \tilde{D}_q |1_{T,\xi_q}\rangle. \tag{68}$$

Proof: See Appendix H. ■

The term $\sum_{q=0}^{\infty} |\tilde{F}_q|^2$ shows the probability of reflection from the filter. On the other hand, the term $\sum_{q=0}^{\infty} |\tilde{D}_q|^2$ implies that the properly decoded quantum signal is recovered at the receiver. From the discussion of Appendix G-A, we observe that when the codes match, i.e., $\Lambda = \tilde{\Lambda}$, we have $\rho^{\mathrm{T}} \approx |1_{\xi_T}\rangle\langle 1_{\xi_T}|$ asymptotically. Also, for random codes $\Lambda \neq \tilde{\Lambda}$, the asymptotic behavior of ρ^{T} is $\rho^{\mathrm{T}} \approx |0\rangle\langle 0|$.

IV. QUANTUM DIRECT-SEQUENCE SPREAD-SPECTRUM CDMA

The quantum spread-spectrum CDMA communication system utilizes the quantum spread-spectrum transmitter and receiver described in the previous sections to transmit the classical or quantum information over a quantum broadcasting interference channel. Similar to QCDMA systems with spectral encoding [16], the quantum broadcasting channel can be modeled as a passive star coupler. In this model, the encoded spread-spectrum quantum signals are broadcasted by an $M \times M$ star coupler. The broadcasting channel performs a unitary transformation on the transmitted signals according to a unitary matrix B.

A. SCHRODINGER'S PICTURE OF QUANTUM SPREAD-SPECTRUM CDMA

Fig. 11 depicts the Schrodinger's picture of the quantum spread-spectrum CDMA communication system. From this viewpoint, quantum signals evolve as they propagate through the quantum communication system. The transmitted pure quantum signals from M different users, i.e., $|\psi_0\rangle, |\psi_1\rangle, \ldots, |\psi_{M-1}\rangle$ form a general tensor product state

$$|\Psi\rangle = \prod_{s=0}^{M-1} |\psi_s\rangle. \tag{69}$$

Each transmitter s utilizes an electro-optical modulator to construct the spread-spectrum signal, $|\psi_s^e\rangle$. The encoder acts as a unitary operator $\hat{\mathrm{U}}_s$ to modulate the wavepacket of the transmitted quantum signal with pseudorandom code sequence $\Lambda_s = (\lambda_{s,0}, \lambda_{s,1}, \ldots, \lambda_{s,N_c-1})$. The resulting quantum state of the system before the broadcasting channel is thus

$$|\Psi^e\rangle = \hat{\mathrm{U}}|\Psi\rangle = \prod_{s=0}^{M-1} |\psi_s^e\rangle \tag{70}$$

where $\hat{\mathrm{U}} = \prod_{s=0}^{M-1} \hat{\mathrm{U}}_s$ considers the effect of all encoders of all users.

The tensor product state $|\Psi^e\rangle$ passes through the broadcasting channel evolving into pure state $|\Phi^e\rangle$. The received signal at each receiver can be obtained by taking the partial trace of $|\Phi^e\rangle$ with respect to all other receivers. As we show, the received quantum signal includes interference from other users and can potentially be an entangled quantum state. The entanglement results in a mixed quantum signal after taking the partial trace with respect to other users. The receivers then apply the decoding operation utilizing an electro-optical modulator to recover their intended signals. An optical narrowband filter is then used to discard the interference. At this point, we show that for a typical optical filter, the system's overall state can be a mixed state. The quantum signal representing the output of all receivers is denoted by the density ρ^{T} (T stands for transmission of the filter) and is obtained by taking the partial trace of the filter expression with respect to the reflected portion of the incoming quantum signal.

In the following section, we describe the evolution of quantum signals through the quantum spread-spectrum multiple access communication system utilizing our proposed chip-time interval decomposition approach.

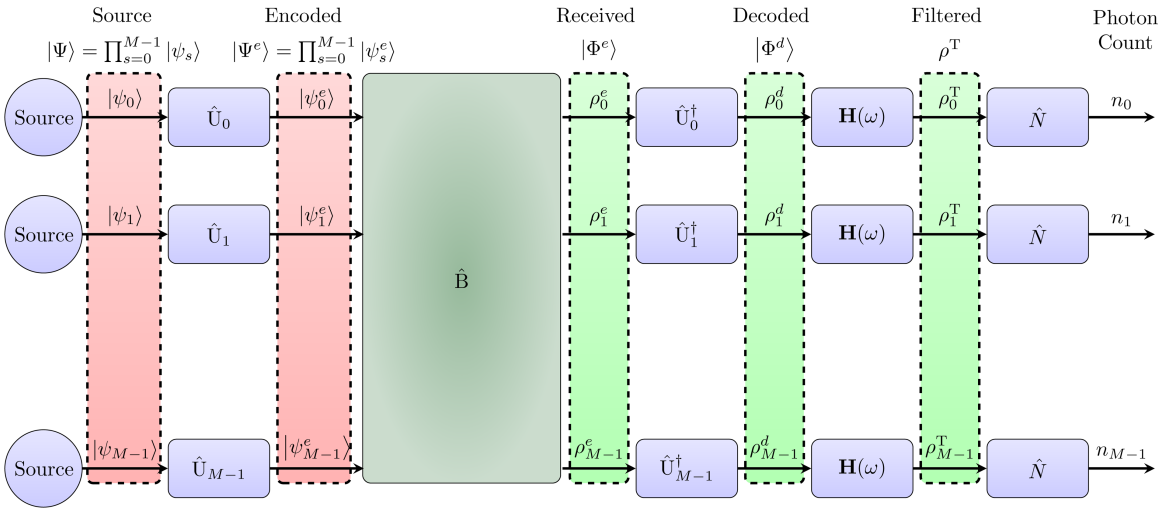

FIGURE 11. Multiple-access quantum spread-spectrum CDMA communication system in Schrodinger's picture. In this picture, the quantum communication signals evolve through the quantum communication system. A transmitted pure quantum signal may mix with other transmitters and is expressed generally by a density matrix on the receivers' end. In this figure, we assume that receiver r is using the decoding (despreading) sequence corresponding to user $s = r$.

B. QUANTUM BROADCASTING CHANNEL

The broadcasting star-coupler channel is described by a single global unitary operator, $\hat{\mathrm{B}}$. The action of $\hat{\mathrm{B}}$ on the input-mode creation operator, $\hat{a}^\dagger_{s,\xi}$, can be expressed in matrix form via [16]

$$\hat{\mathrm{B}}\,\hat{a}^\dagger_{s,\xi}\,\hat{\mathrm{B}}^\dagger \;=\; \sum_{r=0}^{M-1} B_{rs}\,\hat{a}^\dagger_{r,\xi} \tag{71}$$

where $\hat{\mathrm{B}}$ is a single unitary acting on the entire set of modes, while the coefficients B_{rs} form the numerical representation of that operator when mapping each input mode s to each output mode r. Fig. 12 illustrates this broadcasting process. Throughout this article, we assume that all transmitters are synchronized and employ the same wavepacket $\xi(t)$.

In the context of the proposed temporal decomposition approach, we may write

$$\hat{\mathrm{B}}\hat{a}^\dagger_{s,\xi}\hat{\mathrm{B}}^\dagger = \frac{1}{\sqrt{N_c}} \sum_{k=0}^{N_c-1} \sum_{r=0}^{M-1} B_{rs}\hat{a}^\dagger_{r,\xi_k}. \tag{72}$$

Hence

$$|\Phi\rangle = \hat{\mathrm{B}}|\Psi\rangle = \prod_{s=0}^{M-1} f_s(\hat{\mathrm{B}}\hat{a}^\dagger_{s,\xi}\hat{\mathrm{B}}^\dagger)|0\rangle \tag{73}$$

$$= \prod_{s=0}^{M-1} f_s\left(\frac{1}{\sqrt{N_c}} \sum_{k=0}^{N_c-1} \hat{\mathrm{B}}\hat{a}^\dagger_{s,\xi_k}\hat{\mathrm{B}}^\dagger\right)|0\rangle \tag{74}$$

$$= \prod_{s=0}^{M-1} f_s\left(\frac{1}{\sqrt{N_c}} \sum_{k=0}^{N_c-1} \sum_{s=0}^{M-1} B_{rs}\hat{a}^\dagger_{r,\xi_k}\right)|0\rangle. \tag{75}$$

The aforementioned relation is the general form of the decomposed quantum signals after the broadcasting channel.

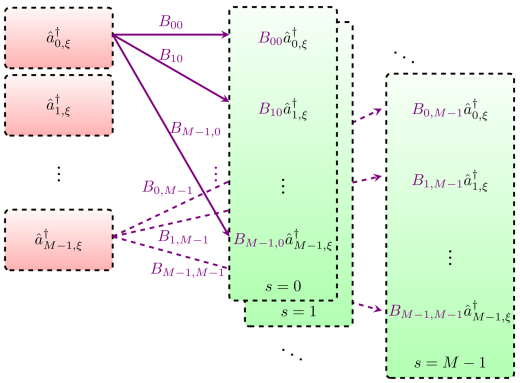

FIGURE 12. Effect of quantum broadcasting channel on the creation operators. The creation operator corresponding to each transmitter s is broadcasted toward all receivers resulting in possible entanglement between them. For simplicity, only the connections regarding transmitter $s = 0$ and $s = M-1$ are illustrated. The effect of other transmitters given by (73) is in terms of a tensor product, which is demonstrated using indices $s = 0$, $s = 1, \ldots,$ $s = M-1$. Inspired by the representation of tensor networks from classical and quantum machine learning [36], the tensor product is shown as a stack of blocks.

In the rest of this section, we derive the exact relations for coherent and number states.

1) COHERENT STATE

Proposition 12: The effect of the quantum broadcasting channel (star coupler) on the coherent state inputs turns to the tensor product of each chip of receivers' decomposed states

$$|\Phi\rangle = \hat{\mathrm{B}}|\Psi\rangle = \hat{\mathrm{B}}\prod_{s=0}^{M-1}|\alpha_{s,\xi}\rangle = \prod_{r=0}^{M-1}\prod_{k=0}^{N_c-1}\left|\sum_{s=0}^{M-1}\frac{B_{rs}}{\sqrt{N_c}}\alpha_{s,\xi_k}\right\rangle. \tag{76}$$

Proof: See Appendix I. ■

From the aforementioned proposition, we obtain the received quantum state at a particular receiver, r, by taking the partial trace of the density operator $|\Phi\rangle\langle\Phi|$ with respect to the other receivers, which gives

$$|\phi_r\rangle = \prod_{k=0}^{N_c-1} \left| \sum_{s=0}^{M-1} \frac{B_{rs}}{\sqrt{N_c}} \alpha_{s,\xi_k} \right\rangle. \tag{77}$$

Let us consider the effect of encoding and decoding. The encoding operator at transmitter s, $\hat{\mathrm{U}}_s$, converts the original wavepacket, $\xi(t)$, into the encoded (spreaded) wavepacket, $\xi^{e_s}(t)$. Receiver r applies its decoding operator $\hat{\mathrm{U}}_r^\dagger$, which turns the wavepacket $\xi^{e_s}(t)$ to the decoded (despreaded) wavepacket $\xi^{e_s d_r}(t)$. Since we assume that receiver $r = s$ is decoding the data from transmitter s, we have $\xi^{e_s d_{r=s}}(t) = \xi(t)$.

Proposition 13: The output of the spread-spectrum QCDMA communication system utilizing coherent states at receiver r after decoding the data of transmitter $s = r$ is

$$|\phi_r^d\rangle = \prod_{k=0}^{N_c-1} \left| \frac{B_{rr}}{\sqrt{N_c}} \alpha_{s=r,\xi_k} + \frac{1}{\sqrt{N_c}} \sum_{s\neq r} \lambda_{r,k}\lambda_{s,k} B_{rs} \alpha_{s,\xi_k} \right\rangle \tag{78}$$

$$= \left| B_{rr}\alpha_{s=r,\xi} + \sum_{s\neq r} B_{rs}\alpha_{s,\xi^{e_s d_r}} \right\rangle. \tag{79}$$

Proof: See Appendix I. ■

Similar to point-to-point communication, (58) and (59), we define the following coefficients that track the effect of encoding and decoding operators and quantum filter

$$D_q^{s,r} := \sum_{l=\max(0,q-N_c+1)}^{q} \frac{1}{\sqrt{N_c}} d_l \lambda_{s,q-l}\lambda_{r,q-l} \tag{80}$$

$$F_q^{s,r} := \sum_{l=\max(0,q-N_c+1)}^{q} \frac{1}{\sqrt{N_c}} f_l \lambda_{s,q-l}\lambda_{r,q-l}. \tag{81}$$

For multiple-access communication systems, this article uses superscript $\{s, r\}$ for D and F coefficients to specify the corresponding sender and receiver and their encoding and decoding code sequences.

Proposition 14: The coherent quantum signal decoded at the receiver r from transmitter $s = r$ results in the following pure quantum signal after the filter:

$$|\alpha_{r,\xi_\mathrm{T}}\rangle = \prod_{q=0}^{\infty} \left| B_{rr} D_q \alpha_{s=r,\xi_q} + \sum_{s\neq r} B_{rs} D_q^{s,r} \alpha_{s,\xi_q} \right\rangle. \tag{82}$$

2) NUMBER STATE

Unlike the spread-spectrum system with coherent quantum signals, the system with continuous mode Fock states does not result in a separable state at each receiver. For this case, we write the overall state of encoded transmitted signals as

$$|\Psi^e\rangle = \prod_{s=0}^{M-1} |\psi^e\rangle = \prod_{s=0}^{M-1} |n_{s,\xi^e}\rangle \tag{83}$$

$$= \prod_{s=0}^{M-1} \frac{1}{\sqrt{n_s!}} (\hat{a}_{s,\xi^e}^\dagger)^{n_s} |0\rangle \tag{84}$$

$$= \prod_{s=0}^{M-1} \frac{1}{\sqrt{n_s!}} \left(\frac{1}{\sqrt{N_c}} \sum_{k=0}^{N_c-1} \hat{a}_{s,\xi_k^e}^\dagger \right)^{n_s} |0\rangle \tag{85}$$

$$= \prod_{s=0}^{M-1} \frac{1}{\sqrt{n_s!}} \left(\frac{1}{\sqrt{N_c}} \sum_{k=0}^{N_c-1} \lambda_{s,k} \hat{a}_{s,\xi_k}^\dagger \right)^{n_s} |0\rangle. \tag{86}$$

Proposition 15: The output of a quantum spread-spectrum CDMA communication system with Fock state transmitted quantum signals after the broadcasting channel is

$$|\Phi^e\rangle = \hat{\mathrm{B}}|\Psi^e\rangle = \prod_{s=0}^{M-1} \frac{1}{\sqrt{n_s!}} \left(\frac{1}{\sqrt{N_c}} \sum_{k=0}^{N_c-1} \sum_{r=0}^{M-1} B_{rs}\lambda_{s,k} \hat{a}_{r,\xi_k}^\dagger \right)^{n_s} |0\rangle. \tag{87}$$

After applying the decoding operators by each user, the overall received quantum signal is

$$|\Phi^d\rangle = \hat{\mathrm{U}}^\dagger |\Phi^e\rangle = \prod_{s=0}^{M-1} \frac{1}{\sqrt{n_s!}} \left(\frac{1}{\sqrt{N_c}} \sum_{k=0}^{N_c-1} \left(B_{ss} \hat{a}_{r=s,\xi_k}^\dagger + \sum_{r\neq s} B_{rs}\lambda_{s,k}\lambda_{r,k} \hat{a}_{r,\xi_k}^\dagger \right) \right)^{n_s} |0\rangle$$

$$= \prod_{s=0}^{M-1} \frac{1}{\sqrt{n_s!}} \left(B_{ss} \hat{a}_{r=s,\xi}^\dagger + \sum_{r\neq s} B_{rs} \hat{a}_{r,\xi^{e_s d_r}}^\dagger \right)^{n_s} |0\rangle. \tag{88}$$

Proof: See Appendix I. ■

To consider the effect of the filter, we note that

$$\hat{\mathrm{H}} \hat{a}_{\xi^{e_s d_r}}^\dagger \hat{\mathrm{H}}^\dagger = \sum_{q=0}^{\infty} (D_q^{s,r} \hat{a}_{r,\xi_q}^{\prime\dagger} + F_q^{s,r} \hat{b}_{r,\xi_q}^{\prime\dagger}). \tag{89}$$

Thus, the quantum signal has the following form as the result of the filter:

$$|\Phi^F\rangle = \hat{\mathrm{H}}|\Phi^d\rangle = \prod_{s=0}^{M-1} \frac{1}{\sqrt{n_s!}} \left(\sum_{q=0}^{\infty} \sum_{r=0}^{M-1} B_{rs} (D_q^{s,r} \hat{a}_{r,\xi_q}^{\prime\dagger} + F_q^{s,r} \hat{b}_{r,\xi_q}^{\prime\dagger}) \right)^{n_s} |0\rangle$$

$$= \prod_{s=0}^{M-1} \frac{1}{\sqrt{n_s!}} \left(\sum_{q=0}^{\infty} \left(B_{ss} (D_q \hat{a}_{r=s,\xi_q}^{\prime\dagger} + F_q \hat{b}_{r=s,\xi_q}^{\prime\dagger} \right) \right.$$

$$+\sum_{r\neq s}^{M-1} B_{rs}(D_q^{s,r}\hat{a}_{r,\xi_q}^{\prime\dagger}+F_q^{s,r}\hat{b}_{r,\xi_q}^{\prime\dagger})\Bigg)\Bigg)^{n_s}|0\rangle. \tag{90}$$

The transmitted part of the aforementioned quantum signal can be obtained using a partial trace with respect to the reflected modes

$$\rho^{\mathrm{T}}=\mathrm{Tr}_R\left(|\Phi^F\rangle\langle\Phi^F|\right). \tag{91}$$

C. CHIP-TIME DECOMPOSITION METHODOLOGY IN A NUTSHELL

As a corollary of the propositions regarding the use of the proposed chip-time interval decomposition method, we can give a complete picture of the quantum spread-spectrum CDMA communication systems according to the evolution of the creation operators. The following corollary summarizes the proposed chip-time decomposition methodology for description of the quantum communication system.

Corollary 1 (Chip-time Decomposition Methodology): The chip-time interval decomposition results in the following evolution for creation operators:

$$\hat{a}_{s,\xi}^{\dagger}=\frac{1}{\sqrt{N_c}}\sum_{k=0}^{N_c-1}\hat{a}_{s,\xi_k}^{\dagger} \tag{92}$$

$$\hat{\mathrm{U}}\hat{a}_{s,\xi}^{\dagger}\hat{\mathrm{U}}^{\dagger}=\frac{1}{\sqrt{N_c}}\sum_{k=0}^{N_c-1}\lambda_{s,k}\hat{a}_{s,\xi_k}^{\dagger}=\hat{a}_{s,\xi^{es}}^{\dagger} \tag{93}$$

$$\hat{\mathrm{B}}\hat{a}_{s,\xi^{es}}^{\dagger}\hat{\mathrm{B}}^{\dagger}=\frac{1}{\sqrt{N_c}}\sum_{r=0}^{M-1}\sum_{k=0}^{N_c-1}B_{rs}\lambda_{s,k}\hat{a}_{r,\xi_k}^{\dagger}=\sum_{r=0}^{M-1}B_{rs}\hat{a}_{r,\xi^{es}}^{\dagger} \tag{94}$$

$$\hat{\mathrm{U}}^{\dagger}\hat{a}_{r,\xi^{es}}^{\dagger}\hat{\mathrm{U}}=\frac{1}{\sqrt{N_c}}\sum_{k=0}^{N_c-1}\lambda_{s,k}\lambda_{r,k}\hat{a}_{r,\xi_k}^{\dagger}=\hat{a}_{r,\xi^{es,dr}}^{\dagger}. \tag{95}$$

For rectangular $\xi(t)$, we further have

$$\hat{\mathrm{H}}\hat{a}_{r,\xi^{es,dr}}^{\dagger}\hat{\mathrm{H}}^{\dagger}=\sum_{q=0}^{\infty}\left(D_q^{s,r}\hat{a}_{r,\xi_q}^{\prime\dagger}+F_q^{s,r}\hat{b}_{r,\xi_q}^{\prime\dagger}\right). \tag{96}$$

According to Corollary 1, the chip-time interval creation operators, $\hat{a}_{\xi_k}^{\dagger}$ are invariant building blocks of the quantum spread-spectrum CDMA communication systems. The evolution of the field creation operators mixes these basic elements.

According to the proposed chip-time interval decomposition methodology, the transmitted signal described as a mixture of chip-time interval creation operators is modulated using the spread-spectrum encoder. The coefficients of the spreading sequence act as a multiplier for the corresponding chip-time interval creation operators. The signals then pass through a quantum broadcasting channel, which transforms each individual chip-time interval creation operator. The star coupler mixes the chip-time interval creation operators from different users resulting in interuser interference.

At the receiver, the creation operators admit another multiplicative factor due to the decoder. Then, the optical narrowband filter breaks this decoded signal into two parts. The reflected part is due to the rejected interuser interference. In contrast, the transmitted part is due to the intended signal that is correctly decoded along with inevitable interuser interference that passes through the narrowband filter. The duration of the output quantum signal at the receiver depends on the impulse response of the optical filter.

Corollary 2 summarizes the overall behavior of the considered quantum communication system.

Corollary 2 (Overall Evolution): The overall evolution of the creation operators in a quantum spread-spectrum CDMA communication system, where receiver r is decoding the signal from transmitter $s=r$, is given by

$$\begin{aligned}\hat{\mathrm{H}}\hat{\mathrm{U}}^{\dagger}\hat{\mathrm{B}}\hat{\mathrm{U}}\hat{a}_{s,\xi}^{\dagger}\hat{\mathrm{U}}^{\dagger}\hat{\mathrm{B}}^{\dagger}\hat{\mathrm{U}}\hat{\mathrm{H}}^{\dagger}&=\underbrace{B_{ss}\sum_{q=0}^{\infty}D_q\hat{a}_{r=s,\xi_q}^{\prime\dagger}}_{\text{Desired quantum signal}}+\underbrace{\sum_{r\neq s}B_{rs}\sum_{q=0}^{\infty}D_q^{s,r}\hat{a}_{r,\xi_q}^{\prime\dagger}}_{\text{Multiaccess interference}}\\&+\underbrace{B_{ss}\sum_{q=0}^{\infty}F_q\hat{b}_{r=s,\xi_q}^{\prime\dagger}}_{\text{Filter's frequency mismatch}}+\underbrace{\sum_{r\neq s}B_{rs}\sum_{q=0}^{\infty}F_q^{s,r}\hat{b}_{r,\xi_q}^{\prime\dagger}}_{\text{Filtered interference}}.\end{aligned} \tag{97}$$

From Corollary 2, we observe that the term $\sum_{q=0}^{\infty}D_q\hat{a}_{r=s,\xi_q}^{\prime\dagger}$ corresponds to the recovered quantum signal that is transmitted through the filter, $\sum_{q=0}^{\infty}F_q\hat{b}_{r=s,\xi_q}^{\prime\dagger}$ denotes the reflected portion of the desired quantum signal due to loss induced by the frequency mismatch between the bandwidth of filter and wavepacket of the desired quantum signal, $\sum_{r\neq s}B_{rs}\sum_{q=0}^{\infty}(D_q^{s,r}\hat{a}_{r,\xi_q}^{\prime\dagger})$ denotes the interference caused by transmitter s at other receivers $r\neq s$, and $\sum_{r\neq s}B_{rs}\sum_{q=0}^{\infty}(F_q^{s,r}\hat{b}_{r,\xi_q}^{\prime\dagger})$ corresponds to the part of the signal of transmitter s, reached receiver $r\neq s$ and filtered out.

From the discussion of Appendix G-A on the asymptotic behavior of the quantum spread-spectrum communication systems, the values of the output transmission coefficients of the filter $D_q^{s,r}$ are negligible for interfering quantum signals. On the other hand, for the correctly decoded signal of the transmitter s at receiver $r=s$, the values of $F_q^{s,r=s}=F_q$ are negligible (see Fig. 10). Thus, we may argue that the results of Corollary 2 can be further simplified asymptotically as

$$\hat{\mathrm{H}}\hat{\mathrm{U}}^{\dagger}\hat{\mathrm{B}}\hat{\mathrm{U}}\hat{a}_{s,\xi}^{\dagger}\hat{\mathrm{U}}^{\dagger}\hat{\mathrm{B}}^{\dagger}\hat{\mathrm{U}}\hat{\mathrm{H}}^{\dagger} \tag{98}$$

$$\approx B_{ss}\sum_{q=q_{\mathrm{delay}}}^{q_{\mathrm{delay}}+N_c}D_q\hat{a}_{r=s,\xi_q}^{\prime\dagger}+\sum_{r\neq s}B_{rs}\sum_{q=q_{\mathrm{delay}}}^{q_{\mathrm{delay}}+N_c}F_q^{s,r}\hat{b}_{r,\xi_q}^{\prime\dagger}$$

$$\approx B_{ss}\hat{a}_{r=s,\xi(t-T_{\mathrm{delay}})}^{\prime\dagger}+\sum_{r\neq s}B_{rs}\hat{b}_{r,\xi^{es}dr}^{\prime\dagger} \tag{99}$$

which shows that the creation operator of the transmitted signal from user s is approximately completely recovered at receiver $r = s$ after the filter and rejected (reflected toward the other port of the filter) at receivers $r \neq s$.

D. SIGNAL INTENSITY

In this section, we calculate the intensity of the received quantum signals. The instantaneous intensity of the quantum signal at receiver r_0 at time t is obtained as

$$I_{r_0}(t) = \langle \Phi^d | \hat{a}'^{\dagger}_{r_0}(t) \hat{a}'_{r_0}(t) | \Phi^d \rangle. \tag{100}$$

Also, the total intensity of the chip time k can be defined as follows:

$$I_{r_0,k} = \int_{t_k}^{t_{k+1}} I_{r_0}(t) dt. \tag{101}$$

The following lemma would be useful in our calculations.

Lemma 1: The filter coefficients have the following property:

$$\sum_{q=0}^{\infty} (D_q^{s,r*} D_q^{s',r} + F_q^{s,r*} F_q^{s',r}) = \frac{1}{N_c} \sum_{k=0}^{N_c-1} \lambda_{s,k} \lambda_{s',k} = \langle \Lambda_s | \Lambda_{s'} \rangle \tag{102}$$

where $\langle \Lambda_s | \Lambda_{s'} \rangle$ corresponds to the normalized correlation between code sequences Λ_s and $\Lambda_{s'}$.

Proof: See Appendix J. ■

Proposition 16: The intensity of the received quantum signal of a spread-spectrum CDMA communication system incorporating either number states or coherent states at the transmitters at receiver r_0 is given as follows.

1) For number state transmitted quantum signals

$$I_{r_0}(t) = \frac{N_c}{T_p} \sum_{s=0}^{M-1} n_s |B_{r_0 s} D_q^{s,r_0}|^2, \quad t \in [t_q, t_{q+1}) \tag{103}$$

and the total intensity of the time interval q is

$$I_{r_0,q} = \sum_{s=0}^{M-1} n_s |B_{r_0 s} D_q^{s,r_0}|^2. \tag{104}$$

2) For coherent state transmitted quantum signals

$$I_{r_0}(t) = \frac{N_c}{T_p} \left| \sum_{s=0}^{M-1} B_{r_0 s} D_q^{s,r_0} \alpha_s \right|^2, \quad t \in [t_q, t_{q+1}) \tag{105}$$

and the total intensity of the chip time q is

$$I_{r_0,q} = \left| \sum_{s=0}^{M-1} B_{r_0 s} D_q^{s,r_0} \alpha_s \right|^2. \tag{106}$$

Proof: See Appendix J. ■

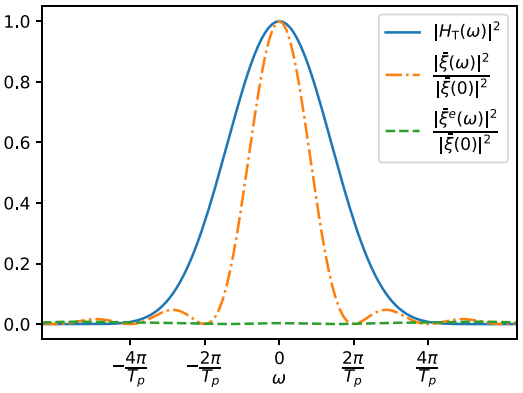

FIGURE 13. Frequency response of the filter compared to $|\tilde{\xi}(\omega)|^2$ and $|\tilde{\xi}^e(\omega)|^2$. The frequency-domain wavepackets are divided by $|\tilde{\xi}(0)|^2$ for better illustration. Note that the original signal's temporal wavepacket is $\xi(t)$ and spread-spectrum signal has the temporal wavepacket of $\xi^e(t)$.

For a balanced star coupler $|B_{rs}|^2 = \frac{1}{M}$ and $r_0 = 0$, for number state transmission

$$I_0(t) = \frac{1}{M} \frac{N_c}{T_p} \left(n_0 |D_q|^2 + \sum_{s \neq 0} n_s |D_q^{s,0}|^2 \right), \quad t \in [t_q, t_{q+1}). \tag{107}$$

As can be seen, the intensity is the sum of the weakened decoded signal $\frac{1}{M} \frac{N_c}{T_p} n_0 |D_q|^2$ and the multiaccess interfering signal, $\frac{1}{M} \frac{N_c}{T_p} \sum_{s \neq 0} n_s |D_q^{s,0}|^2$.

For coherent states, the corresponding intensity is

$$I_0(t) = \frac{1}{M} \frac{N_c}{T_p} \left| D_q \alpha_0 + \sum_{s \neq 0} D_q^{s,0} \alpha_s \right|^2, \quad t \in [t_q, t_{q+1}) \tag{108}$$

where the signal, $D_q \alpha_0$, and interference, $\sum_{s \neq 0} D_q^{s,0} \alpha_s$, are being added coherently.

The difference between these two detection schemes, namely the coherent detection scheme for Glauber states and the incoherent detection scheme for number states, arises from the Heisenberg uncertainty principle. Similar to the spectral QCDMA, in the context of quantum spread-spectrum CDMA communication systems, the uncertainty principle leads to the unpredictability of the quantum phase angles of number states at the time of measurement, which fundamentally changes the expression of the received intensity as discussed in [16]. For further details, including a detailed analysis of a two-user single-photon QDSS-CDMA communication system demonstrating the spread-spectrum Hong–Ou–Mandel effect, entanglement, and how the output can become a mixed state (see Appendix K).

V. SIMULATION RESULTS

In this section, a two-user spread-spectrum QCDMA system with $N_c = 100$ is simulated. As an example, we study a two-user multiple-access communication system utilizing

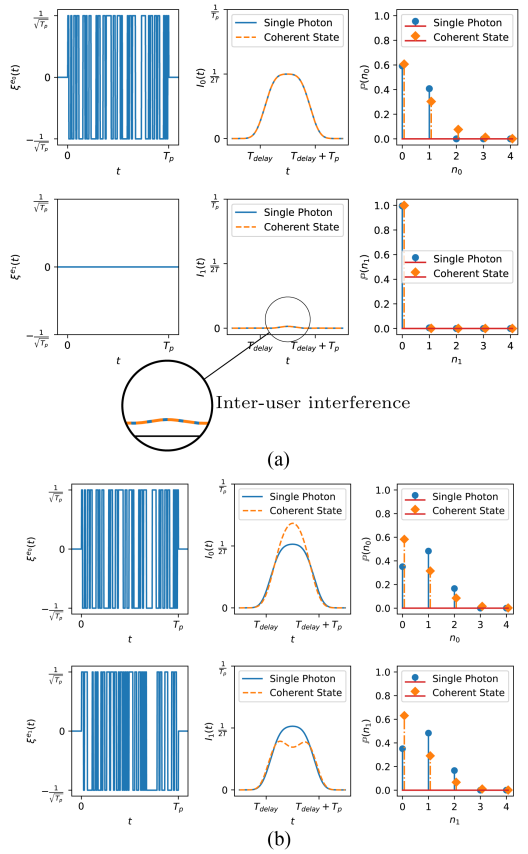

FIGURE 14. Comparison of signal reconstructions for a two-user system. (a) Signals for a two-user system when only the first transmitter is ON. The signal is reconstructed when the correct code is used at receiver $r = 0$, while a small amount of interuser interference from the first user is observed at $r = 1$. (b) Signals for a two-user system when both transmitters are ON. The signals are reconstructed at the intended users.

ON–OFF keying (OOK) modulation for the transmission of one bit. Assume that the receiver with index 0 is decoding the signal from transmitter 0. We consider a balanced star coupler, i.e.,

$$\begin{pmatrix} B_{00} & B_{01} \\ B_{10} & B_{11} \end{pmatrix} = \frac{1}{\sqrt{2}} \begin{pmatrix} 1 & 1 \\ -1 & 1 \end{pmatrix}. \tag{109}$$

The simulations are done using Python 3 and the filters are designed using the windowing method [35] available in scipy's signal processing package.[4] The transmitters are either transmitting single photons, $|1\rangle$, or coherent states $|\alpha\rangle$ with $\alpha = 1$ and the signal duration is T_p. As can be seen in Fig. 13, the encoding operator spreads the spectrum of the original signal into $\tilde{\xi}^e(\omega)$. The transmission response of the narrowband filter is shown in Fig. 13. The considered casual narrowband filter is an FIR filter with $L = 101$.

Fig. 14(a) shows the signals when only the first user, $s = 0$, is transmitting and the second user, $s = 1$, is in vacuum state. According to the received signal intensity, the signal is reconstructed when the correct code is used at receiver $r = 0$. On the other hand, at receiver $r = 1$, the interuser interference from the first user is observed, which is negligible due to the use of the spread-spectrum technique. This negligible interference can also be observed from the photon statistics, where almost all of the probability is concentrated around $n_1 = 0$. We also observe that while the average intensity of the signals for both coherent state and single-photon sources are the same, their photon statistics are different.

Fig. 14(b) depicts the system's behavior when both users are transmitting simultaneously. In this scenario, when single-photon sources are used, the average intensity of the received signal is similar for both users. In contrast, when coherent quantum signals are used, the average intensity of user $r = 0$ is higher compared to receiver $r = 1$ due to the positive sign of the interference term in (105). The photon statistics are also shifted to higher photon counts compared to when only one user was transmitting data.

[4]Accessed: 3 January 2025. [Online]. Available: https://docs.scipy.org/doc/scipy/reference/signal.html

VI. CONCLUSION

This article presents a comprehensive unified mathematical approach to QDSS-CDMA communication systems. By introducing the chip-time interval decomposition of creation operators, we establish a quantum analogue to classical CDMA "chips," revealing that these chip-time operators form the building blocks of QDSS-CDMA. In particular, we analyze two limiting cases for transmitter signals—Fock (number) states and Glauber (coherent) states—and show that entanglement in multiuser Fock states leads to mixed outputs at each receiver, whereas multiuser coherent-state inputs produce pure outputs. Using the chip-time interval decomposition, we interpret narrowband filtering in quantum systems through a novel perspective: creation operators evolve as weighted sums of chip-time operators across the system. This framework not only simplifies understanding of multiuser interference but also highlights how quantum signals can be processed and filtered effectively. The mathematical models and techniques presented in this article, with respect to filtering quantum signals and the application of quantum spread-spectrum technology, provides a solid foundation for future research and development in the fields of quantum communications and signal processing.

APPENDIX A
COMMUTATION OF CHIP-TIME INTERVAL CREATION OPERATORS

It is evident that the function $\xi_k(t)$ has the required normalization property of a photon wavepacket

$$\int_0^{T_p} |\xi_k(t)|^2 dt = \int_{t_k}^{t_{k+1}} |\sqrt{N_c}\xi(t)|^2 dt = \int_{t_k}^{t_{k+1}} N_c |\xi(t)|^2 dt = 1. \tag{A.1}$$

IEEE Transactions on Quantum Engineering

Hence, we may define the creation operator of each chip time by letting $\hat{a}^\dagger_{\xi_k}$ be the creation operator for chip-time $[t_k, t_{k+1})$. Based on the wavepacket of (16), we may write

$$\hat{a}^\dagger_{\xi_k} := \int_{t_k}^{t_{k+1}} dt \xi_k(t)\hat{a}^\dagger(t) = \int_{t_k}^{t_{k+1}} dt \sqrt{N_c}\xi(t)\hat{a}^\dagger(t). \quad \text{(A.2)}$$

We first show that according to the definition of the chip-time interval creation operators, $[\hat{a}_{\xi_l}, \hat{a}^\dagger_{\xi_k}] = \delta_{lk}$. For $l = k$, the relation $[\hat{a}_{\xi_k}, \hat{a}^\dagger_{\xi_k}] = 1$ is trivial. For $l \neq k$, we may write

$$\hat{a}_{\xi_l}\hat{a}^\dagger_{\xi_k}$$

$$= \int_{t_l}^{t_{l+1}} dt \xi_l^*(t)\hat{a}(t) \int_{t_k}^{t_{k+1}} dt' \xi_k(t')\hat{a}^\dagger(t') \quad \text{(A.3)}$$

$$= \int_{t_l}^{t_{l+1}} \int_{t_k}^{t_{k+1}} dt dt' \xi_l^*(t)\xi_k(t')\hat{a}(t)\hat{a}^\dagger(t') \quad \text{(A.4)}$$

$$= \int_{t_l}^{t_{l+1}} \int_{t_k}^{t_{k+1}} dt dt' \xi_l^*(t)\xi_k(t') \left(\delta(t-t') + \hat{a}^\dagger(t')\hat{a}(t)\right) \quad \text{(A.5)}$$

$$= \int_{t_l}^{t_{l+1}} \int_{t_k}^{t_{k+1}} dt dt' \xi_l^*(t)\xi_k(t')\hat{a}^\dagger(t')\hat{a}(t), \text{ since } t \neq t' \quad \text{(A.6)}$$

$$= \int_{t_k}^{t_{k+1}} dt' \xi_k(t')\hat{a}^\dagger(t') \int_{t_l}^{t_{l+1}} dt \xi_l^*(t)\hat{a}(t) = \hat{a}^\dagger_{\xi_k}\hat{a}_{\xi_l} \quad \text{(A.7)}$$

$$\Rightarrow \left[\hat{a}_{\xi_l}, \hat{a}^\dagger_{\xi_k}\right] = 0. \quad \text{(A.8)}$$

Note that since $\xi_l(t)$ and $\xi_k(t)$ are disjoint, we may write

$$\int_{t_l}^{t_{l+1}} \int_{t_k}^{t_{k+1}} dt dt' \xi_l^*(t)\xi_k(t')\delta(t-t') \quad \text{(A.9)}$$

$$= \int_{t_l}^{t_{l+1}} dt \xi_l^*(t) \int_{t_k}^{t_{k+1}} dt' \xi_k(t')\delta(t-t') \quad \text{(A.10)}$$

$$= \int_{t_l}^{t_{l+1}} dt \xi_l^*(t)\xi_k(t) = 0. \quad \text{(A.11)}$$

Next, we prove the chip-time interval decomposition theorem

$$\hat{a}^\dagger_\xi = \int_0^{T_p} dt \xi(t)\hat{a}^\dagger(t) = \sum_{k=0}^{N_c-1} \int_{t_k}^{t_{k+1}} dt \xi(t)\hat{a}^\dagger(t)$$

$$= \frac{1}{\sqrt{N_c}} \sum_{k=0}^{N_c-1} \int_{t_k}^{t_{k+1}} dt \sqrt{N_c}\xi(t)\hat{a}^\dagger(t)$$

$$= \frac{1}{\sqrt{N_c}} \sum_{k=0}^{N_c-1} \int_{t_k}^{t_{k+1}} dt \xi_k(t)\hat{a}^\dagger(t)$$

$$= \frac{1}{\sqrt{N_c}} \sum_{k=0}^{N_c-1} \hat{a}^\dagger_{\xi_k}. \quad \text{(A.12)}$$

APPENDIX B
COHERENT STATE DECOMPOSITION

We start by the displacement operator

$$D(\alpha_\xi) = \exp(\alpha\hat{a}^\dagger_\xi - \alpha^*\hat{a}_\xi) \quad \text{(B.1)}$$

$$= \exp\left(\frac{\alpha}{\sqrt{N_c}} \sum_{k=0}^{N_c-1} \hat{a}^\dagger_{\xi_k} - \frac{\alpha^*}{\sqrt{N_c}} \sum_{k=0}^{N_c-1} \hat{a}_{\xi_k}\right) \quad \text{(B.2)}$$

$$= \exp\left(\sum_{k=0}^{N_c-1} \left[\frac{\alpha}{\sqrt{N_c}}\hat{a}^\dagger_{\xi_k} - \frac{\alpha^*}{\sqrt{N_c}}\hat{a}_{\xi_k}\right]\right) \quad \text{(B.3)}$$

$$= \prod_{k=0}^{N_c-1} \exp\left(\frac{\alpha}{\sqrt{N_c}}\hat{a}^\dagger_{\xi_k} - \frac{\alpha^*}{\sqrt{N_c}}\hat{a}_{\xi_k}\right) \quad \text{(B.4)}$$

$$= \prod_{k=0}^{N_c-1} D\left(\frac{\alpha_{\xi_k}}{\sqrt{N_c}}\right) \quad \text{(B.5)}$$

where we have used the fact that for $l \neq k$ [see (A.8)]

$$\left[\frac{\alpha}{\sqrt{N_c}}\hat{a}^\dagger_{\xi_l} - \frac{\alpha^*}{\sqrt{N_c}}\hat{a}_{\xi_l}, \frac{\alpha}{\sqrt{N_c}}\hat{a}^\dagger_{\xi_k} - \frac{\alpha^*}{\sqrt{N_c}}\hat{a}_{\xi_k}\right] = 0 \quad \text{(B.6)}$$

and

$$\exp(\hat{A}+\hat{B}) = \exp(\hat{A})\exp(\hat{B})\exp\left(-\frac{1}{2}[\hat{A},\hat{B}]\right). \quad \text{(B.7)}$$

The decomposition of coherent state can be obtained utilizing the displacement operator

$$|\alpha_\xi\rangle = D(\alpha_\xi)|0\rangle = \left(\prod_{k=0}^{N_c-1} D\left(\frac{\alpha_{\xi_k}}{\sqrt{N_c}}\right)\right)|0\rangle$$

$$= \prod_{k=0}^{N_c-1} D\left(\frac{\alpha_{\xi_k}}{\sqrt{N_c}}\right)\Big|0\rangle = \prod_{k=0}^{N_c-1} |\frac{\alpha_{\xi_k}}{\sqrt{N_c}}\rangle. \quad \text{(B.8)}$$

APPENDIX C
NUMBER STATE DECOMPOSITION

For the number states, we may write

$$|n_\xi\rangle = \frac{(\hat{a}^\dagger_\xi)^n}{\sqrt{n!}}|0\rangle \quad \text{(C.1)}$$

$$= \frac{1}{\sqrt{n!}}\left(\frac{1}{\sqrt{N_c}} \sum_{k=0}^{N_c-1} \hat{a}^\dagger_{\xi_k}\right)^n |0\rangle \quad \text{(C.2)}$$

$$= \frac{1}{\sqrt{n!}\sqrt{N_c^n}}\left(\sum_{k=0}^{N_c-1} \hat{a}^\dagger_{\xi_k}\right)^n |0\rangle \quad \text{(C.3)}$$

$$= \frac{1}{\sqrt{n!N_c^n}} \sum_{n_0+n_1+\cdots+n_{N_c-1}=n} \binom{n}{n_0, n_1, \ldots, n_{N_c-1}}$$

$$\times \prod_{k=0}^{N_c-1} (\hat{a}^\dagger_{\xi_k})^{n_k}|0\rangle \quad \text{(C.4)}$$

$$= \frac{1}{\sqrt{n!N_c^n}} \sum_{n_0+n_1+\cdots+n_{N_c-1}=n} \binom{n}{n_0, n_1, \ldots, n_{N_c-1}} \times \prod_{k=0}^{N_c-1} \sqrt{n_k!} \frac{(\hat{a}^\dagger_{\xi_k})^{n_k}}{\sqrt{n_k!}} |0\rangle \tag{C.5}$$

$$= \frac{1}{\sqrt{n!N_c^n}} \sum_{n_0+n_1+\cdots+n_{N_c-1}=n} \binom{n}{n_0, n_1, \ldots, n_{N_c-1}} \times \prod_{k=0}^{N_c-1} \sqrt{n_k!} |n_{k,\xi_k}\rangle \tag{C.6}$$

$$= \sum_{n_0+n_1+\cdots+n_{N_c-1}=n} \mathcal{C}_n(n_0, n_1, \ldots, n_{N_c-1}) \times \prod_{k=0}^{N_c-1} |n_{k,\xi_k}\rangle \tag{C.7}$$

$$= \sum_{n_0+n_1+\cdots+n_{N_c-1}=n} \mathcal{C}_n(n_0, n_1, \ldots, n_{N_c-1}) \times |n_{0,\xi_0}, n_{1,\xi_1}, \ldots, n_{N_c-1,\xi_{N_c-1}}\rangle \tag{C.8}$$

where $|n_{k,\xi_k}\rangle$ denotes that the state has n_k photons with wavepacket $\xi_k(t)$ in interval $[t_k, t_{k+1})$. And, $\prod_{k=0}^{N_c-1} |n_{k,\xi_k}\rangle = |n_{0,\xi_0}, n_{1,\xi_1}, \ldots, n_{N_c-1,\xi_{N_c-1}}\rangle$ denotes a quantum state with n_0 photons in $[t_0, t_1)$, n_{N_c-1} photons in $[t_{N_c-1}, t_{N_c})$. This state occurs with probability $|\mathcal{C}_n(n_0, n_1, \ldots, n_{N_c-1})|^2$, where

$$\mathcal{C}_n(n_0, n_1, \ldots, n_{N_c-1}) := \frac{1}{\sqrt{n!N_c^n}} \binom{n}{n_0, n_1, \ldots, n_{N_c-1}} \times \prod_{k=0}^{N_c-1} \sqrt{n_k!} = \frac{1}{\sqrt{N_c^n}} \sqrt{\binom{n}{n_0, n_1, \ldots, n_{N_c-1}}}$$

and

$$\binom{n}{n_0, n_1, \ldots, n_{N_c-1}} = \frac{n!}{n_0! n_1! \cdots n_{N_c-1}!}. \tag{C.9}$$

In the aforementioned derivation, we have used the multinomial theorem (for commuting operators)

$$\left(\sum_{k=0}^{N_c-1} \hat{x}_k\right)^n = \sum_{n_0+n_1+\cdots+n_{N_c-1}=n} \binom{n}{n_0, n_1, \ldots, n_{N_c-1}} \times \prod_{k=0}^{N_c-1} (\hat{x}_k)^{n_k}. \tag{C.10}$$

APPENDIX D
DECOMPOSITION OF THE UNITARY SPREADING OPERATOR

A. COMMUTATION RELATION

The decomposition is obtained from the definition

$$\hat{\mathrm{U}} = \exp\left(j \sum_{k=0}^{N_c-1} \int_{t_k}^{t_{k+1}} dt\theta(t)\hat{a}^\dagger(t)\hat{a}(t)\right) \tag{D.1}$$

$$= \prod_{k=0}^{N_c-1} \exp\left(j \int_{t_k}^{t_{k+1}} dt\theta(t)\hat{a}^\dagger(t)\hat{a}(t)\right) \tag{D.2}$$

$$= \prod_{k=0}^{N_c-1} \exp\left(j \int_{t_k}^{t_{k+1}} dt\theta_k\hat{a}^\dagger(t)\hat{a}(t)\right) \tag{D.3}$$

$$= \prod_{k=0}^{N_c-1} \hat{\mathrm{U}}_k \tag{D.4}$$

where

$$\hat{\mathrm{U}}_k := \exp\left(j \int_{t_k}^{t_{k+1}} dt\theta_k\hat{a}^\dagger(t)\hat{a}(t)\right) \tag{D.5}$$

and we have used the fact that for $l \neq k$,

$$\left[\int_{t_k}^{t_{k+1}} dt\theta(t)\hat{a}^\dagger(t)\hat{a}(t), \int_{t_l}^{t_{l+1}} dt\theta(t')\hat{a}^\dagger(t')\hat{a}(t')\right] = 0. \tag{D.6}$$

Continuing our discussion regarding the spreading operator, we show that $[\hat{\mathrm{U}}_k, \hat{a}^\dagger_{\xi_l}] = 0$, $l \neq k$. It is sufficient to prove that

$$\left[\hat{\mathrm{U}}_k, \hat{a}^\dagger(t)\right] = 0, \qquad t \notin [t_k, t_{k+1}). \tag{D.7}$$

Again, we begin by the definition

$$\hat{\mathrm{U}}_k\hat{a}^\dagger(t) = \exp\left(j \int_{t_k}^{t_{k+1}} dt'\theta_k\hat{a}^\dagger(t')\hat{a}(t')\right)\hat{a}^\dagger(t) \tag{D.8}$$

$$= \sum_{l=0}^{\infty} \frac{(j)^l}{l!} \left(\int_{t_k}^{t_{k+1}} dt'\theta_k\hat{a}^\dagger(t')\hat{a}(t')\right)^l \hat{a}^\dagger(t) \tag{D.9}$$

$$= \left[I + j \int_{t_k}^{t_{k+1}} dt'\theta_k\hat{a}^\dagger(t')\hat{a}(t') + \frac{(j)^2}{2!} \int_{t_k}^{t_{k+1}} dt'\theta_k\hat{a}^\dagger(t')\hat{a}(t') \times \int_{t_k}^{t_{k+1}} dt''\theta_k\hat{a}^\dagger(t'')\hat{a}(t'') + \cdots\right]\hat{a}^\dagger(t) \tag{D.10}$$

$$= \hat{a}^\dagger(t) \sum_{l=0}^{\infty} \frac{(j)^l}{l!} \left(j \int_{t_k}^{t_{k+1}} dt'\theta_k\hat{a}^\dagger(t')\hat{a}(t')\right)^l \tag{D.11}$$

$$= \hat{a}^\dagger(t)\hat{\mathrm{U}}_k. \tag{D.12}$$

The first term is trivial

$$I\hat{a}^\dagger(t) = \hat{a}^\dagger(t)I. \tag{D.13}$$

Note that we always have $[\hat{a}^\dagger(t), \hat{a}^\dagger(t')] = 0$; therefore, $\hat{a}^\dagger(t)\hat{a}^\dagger(t') = \hat{a}^\dagger(t')\hat{a}^\dagger(t)$. Also since $t' \in [t_k, t_{k+1})$ and $t \notin [t_k, t_{k+1})$, we have $\hat{a}(t')\hat{a}^\dagger(t) = \delta(t'-t) + \hat{a}^\dagger(t)\hat{a}(t') = \hat{a}^\dagger(t)\hat{a}(t')$. Hence, the second term will be

$$\begin{aligned}
&\int_{t_k}^{t_{k+1}} dt'\theta_k \hat{a}^\dagger(t')\hat{a}(t')\hat{a}^\dagger(t) \\
&= \int_{t_k}^{t_{k+1}} dt'\theta_k \hat{a}^\dagger(t')\hat{a}^\dagger(t)\hat{a}(t') \\
&= \int_{t_k}^{t_{k+1}} dt'\theta_k \hat{a}^\dagger(t)\hat{a}^\dagger(t')\hat{a}(t') \\
&= \hat{a}^\dagger(t)\int_{t_k}^{t_{k+1}} dt'\theta_k \hat{a}^\dagger(t')\hat{a}(t'). \qquad \text{(D.14)}
\end{aligned}$$

With the same procedure, we can prove that

$$\begin{aligned}
&\left(\int_{t_k}^{t_{k+1}} dt'\theta_k \hat{a}^\dagger(t')\hat{a}(t')\right)^l \hat{a}^\dagger(t) \\
&= \hat{a}^\dagger(t)\left(\int_{t_k}^{t_{k+1}} dt'\theta_k \hat{a}^\dagger(t')\hat{a}(t')\right)^l. \qquad \text{(D.15)}
\end{aligned}$$

Thus, we have shown that

$$\left[\hat{\mathrm{U}}_k, \hat{a}^\dagger_{\xi_l}\right] = 0, \qquad l \neq k. \qquad \text{(D.16)}$$

Hence, utilizing Taylor expansion of the function $f(\cdot)$, we obtain

$$\left[\hat{\mathrm{U}}_k, f(\hat{a}^\dagger_{\xi_l})\right] = 0, \qquad l \neq k. \qquad \text{(D.17)}$$

B. EFFECT OF SPREADING UNITARY OPERATOR ON THE CREATION OPERATOR OF QUANTUM SIGNALS

Applying $\hat{\mathrm{U}}_k$ changes the photon wavepacket $\xi_k(t)$ to $\xi^e_k(t) = e^{j\theta_k}\xi_k(t) = \lambda_k\xi_k(t)$. Hence

$$\begin{aligned}
\hat{a}^\dagger_{\xi^e_k} &= \int_{t_k}^{t_{k+1}} dt\xi^e_k(t)\hat{a}^\dagger(t) = \int_{t_k}^{t_{k+1}} dt\lambda_k\xi_k(t)\hat{a}^\dagger(t) \\
&= \lambda_k\int_{t_k}^{t_{k+1}} dt\xi_k(t)\hat{a}^\dagger(t) = \lambda_k\hat{a}^\dagger_{\xi_k}. \qquad \text{(D.18)}
\end{aligned}$$

Thus, we conclude that

$$\hat{\mathrm{U}}\hat{a}^\dagger_{\xi_k}\hat{\mathrm{U}}^\dagger = \hat{\mathrm{U}}_k\hat{a}^\dagger_{\xi_k}\hat{\mathrm{U}}^\dagger_k = \lambda_k\hat{a}^\dagger_{\xi_k}. \qquad \text{(D.19)}$$

Therefore, we may write

$$\hat{\mathrm{U}}\hat{a}^\dagger_\xi\hat{\mathrm{U}}^\dagger = \frac{1}{\sqrt{N_c}}\sum_{k=0}^{N_c-1}\hat{\mathrm{U}}\hat{a}^\dagger_{\xi_k}\hat{\mathrm{U}}^\dagger = \frac{1}{\sqrt{N_c}}\sum_{k=0}^{N_c-1}\lambda_k\hat{a}^\dagger_{\xi_k}. \qquad \text{(D.20)}$$

APPENDIX E
SPREAD-SPECTRUM COHERENT STATE

A. ENCODING

The effect of encoding operator on the coherent state

$$\begin{aligned}
|\alpha_{\xi^e}\rangle = \hat{\mathrm{U}}|\alpha_\xi\rangle &= \left(\prod_{k=0}^{N_c-1}\hat{\mathrm{U}}_k\right)\left(\prod_{k=0}^{N_c-1}\left|\frac{\alpha_{\xi_k}}{\sqrt{N_c}}\right\rangle\right) \qquad \text{(E.1)} \\
&= \left(\hat{\mathrm{U}}_0\hat{\mathrm{U}}_1\cdots\hat{\mathrm{U}}_{N_c-1}\right)\left(\left|\frac{\alpha_{\xi_1}}{\sqrt{N_c}}\right\rangle\cdots\left|\frac{\alpha_{\xi_{N_c-1}}}{\sqrt{N_c}}\right\rangle\right) \qquad \text{(E.2)} \\
&= \left(\hat{\mathrm{U}}_0\hat{\mathrm{U}}_1\cdots\hat{\mathrm{U}}_{N_c-1}\right)\left(f(\hat{a}^\dagger_{\xi_0})f(\hat{a}^\dagger_{\xi_1})\cdots f(\hat{a}^\dagger_{\xi_{N_c-1}})\right)|0\rangle \qquad \text{(E.3)} \\
&= \hat{\mathrm{U}}_0 f(\hat{a}^\dagger_{\xi_0})\hat{\mathrm{U}}_1 f(\hat{a}^\dagger_{\xi_1})\cdots\hat{\mathrm{U}}_{N_c-1}f(\hat{a}^\dagger_{\xi_{N_c-1}})|0\rangle \qquad \text{(E.4)} \\
&= \prod_{k=0}^{N_c-1}\hat{\mathrm{U}}_k f(\hat{a}^\dagger_{\xi_k})|0\rangle = \prod_{k=0}^{N_c-1}\hat{\mathrm{U}}_k\left|\frac{\alpha_{\xi_k}}{\sqrt{N_c}}\right\rangle \qquad \text{(E.5)}
\end{aligned}$$

where we have used $[\hat{\mathrm{U}}_k, f(\hat{a}^\dagger_{\xi_l})] = 0, l \neq k$.

Example for $N_c = 2$:

$$\begin{aligned}
\hat{\mathrm{U}}_0\hat{\mathrm{U}}_1|\alpha_\xi\rangle &= \hat{\mathrm{U}}_0\hat{\mathrm{U}}_1 f(\hat{a}^\dagger_{\xi_0})f(\hat{a}^\dagger_{\xi_1})|0\rangle \\
&= \hat{\mathrm{U}}_0 f(\hat{a}^\dagger_{\xi_0})\hat{\mathrm{U}}_1 f(\hat{a}^\dagger_{\xi_1})|0\rangle \qquad \text{(E.6)} \\
\hat{\mathrm{U}}_k\left|\frac{\alpha_{\xi_k}}{\sqrt{N_c}}\right\rangle &= \left|\frac{\alpha_{\xi^e_k}}{\sqrt{N_c}}\right\rangle \qquad \text{(E.7)} \\
&= e^{-\frac{1}{2}\left|\frac{\alpha}{\sqrt{N_c}}\right|^2} e^{\frac{\alpha}{\sqrt{N_c}}\hat{a}^\dagger_{\xi^e_k}}|0\rangle \qquad \text{(E.8)} \\
&= e^{-\frac{1}{2}\left|\frac{\alpha}{\sqrt{N_c}}\right|^2} e^{\frac{\alpha}{\sqrt{N_c}}\lambda_k\hat{a}^\dagger_{\xi_k}}|0\rangle \qquad \text{(E.9)} \\
&= e^{-\frac{1}{2}\left|\frac{\lambda_k\alpha}{\sqrt{N_c}}\right|^2} e^{\frac{\alpha}{\sqrt{N_c}}\lambda_k\hat{a}^\dagger_{\xi_k}}|0\rangle = \left|\frac{\lambda_k\alpha_{\xi_k}}{\sqrt{N_c}}\right\rangle. \qquad \text{(E.10)}
\end{aligned}$$

B. DECODING

The effect of decoding operator with decoding sequence $\tilde{\Lambda}$ on the coherent states encoded with sequence Λ is derived as follows:

$$\begin{aligned}
|\alpha_{\xi^d}\rangle = \hat{\mathrm{U}}^\dagger|\alpha_{\xi^e}\rangle &= \left(\prod_{k=0}^{N_c-1}\hat{\mathrm{U}}^\dagger_k\right)\left(\prod_{k=0}^{N_c-1}|\frac{\lambda_k\alpha_{\xi_k}}{\sqrt{N_c}}\rangle\right) \qquad \text{(E.11)} \\
&= \left(\prod_{k=0}^{N_c-1}\hat{\mathrm{U}}^\dagger_k\right)\left(\prod_{k=0}^{N_c-1}f(\lambda_k\hat{a}^\dagger_{\xi_k})\right)|0\rangle \qquad \text{(E.12)} \\
&= \prod_{k=0}^{N_c-1}\hat{\mathrm{U}}^\dagger_k f(\lambda_k\hat{a}^\dagger_{\xi_k})|0\rangle = \prod_{k=0}^{N_c-1}\hat{\mathrm{U}}^\dagger_k\left|\frac{\lambda_k\alpha_{\xi_k}}{\sqrt{N_c}}\right\rangle. \qquad \text{(E.13)}
\end{aligned}$$

Applying $\hat{\mathrm{U}}^\dagger_k$ changes the photon wavepacket $\xi^e_k(t)$ to $\xi^d_k(t) = e^{-j\tilde{\theta}_k}\xi^e_k(t) = \tilde{\lambda}_k\xi^e_k(t) = \tilde{\lambda}_k\lambda_k\xi_k(t)$, where $\tilde{\lambda}_k$ is the value of despreading code at chip time k. Hence

$$\begin{aligned}
\hat{a}^\dagger_{\xi^d_k} &= \int_{t_k}^{t_{k+1}} dt\xi^d_k(t)\hat{a}^\dagger(t) = \int_{t_k}^{t_{k+1}} dt\tilde{\lambda}_k\xi^e_k(t)\hat{a}^\dagger(t) \\
&= \tilde{\lambda}_k\lambda_k\int_{t_k}^{t_{k+1}} dt\xi_k(t)\hat{a}^\dagger(t) = \tilde{\lambda}_k\lambda_k\hat{a}^\dagger_{\xi_k}. \qquad \text{(E.14)}
\end{aligned}$$

The rest of the proof is similar to the previous part.

APPENDIX F
SPREAD-SPECTRUM NUMBER STATE

A. ENCODING

The effect of encoding (spreading) operator on the number states is derived as follows:

$$\hat{\mathrm{U}}|n_\xi\rangle = \hat{\mathrm{U}}\frac{1}{\sqrt{n!N_c^n}}\sum_{n_0+\cdots+n_{N_c-1}=n}\binom{n}{n_0,n_1,\ldots,n_{N_c-1}} \times\prod_{k=0}^{N_c-1}(\hat{a}^\dagger_{\xi_k})^{n_k}|0\rangle \tag{F.1}$$

$$=\frac{1}{\sqrt{n!N_c^n}}\sum_{n_0+\cdots+n_{N_c-1}=n}\binom{n}{n_0,n_1,\ldots,n_{N_c-1}}\hat{\mathrm{U}} \times\prod_{k=0}^{N_c-1}(\hat{a}^\dagger_{\xi_k})^{n_k}|0\rangle \tag{F.2}$$

$$=\frac{1}{\sqrt{n!N_c^n}}\sum_{n_0+\cdots+n_{N_c-1}=n}\binom{n}{n_0,n_1,\ldots,n_{N_c-1}} \times\left(\prod_{k=0}^{N_c-1}\hat{\mathrm{U}}_k\right)\left(\prod_{k=0}^{N_c-1}(\hat{a}^\dagger_{\xi_k})^{n_k}\right)|0\rangle \tag{F.3}$$

$$=\frac{1}{\sqrt{n!N_c^n}}\sum_{n_0+\cdots+n_{N_c-1}=n}\binom{n}{n_0,n_1,\ldots,n_{N_c-1}} \times\prod_{k=0}^{N_c-1}\hat{\mathrm{U}}_k(\hat{a}^\dagger_{\xi_k})^{n_k}|0\rangle \tag{F.4}$$

$$=\frac{1}{\sqrt{n!N_c^n}}\sum_{n_0+\cdots+n_{N_c-1}=n}\binom{n}{n_0,n_1,\ldots,n_{N_c-1}} \times\prod_{k=0}^{N_c-1}\sqrt{n_k!}\hat{\mathrm{U}}_k|n_{\xi_k}\rangle \tag{F.5}$$

$$=\frac{1}{\sqrt{n!N_c^n}}\sum_{n_0+\cdots+n_{N_c-1}=n}\binom{n}{n_0,n_1,\ldots,n_{N_c-1}} \times\prod_{k=0}^{N_c-1}\sqrt{n_k!}|n_{\xi_k^e}\rangle \tag{F.6}$$

$$=\sum_{n_0+\cdots+n_{N_c-1}=n}\mathcal{C}_n(n_0,n_1,\ldots,n_{N_c-1})\prod_{k=0}^{N_c-1}|n_{\xi_k^e}\rangle \tag{F.7}$$

where

$$|n_{\xi_k^e}\rangle=\hat{\mathrm{U}}_k|n_{\xi_k}\rangle=\frac{(\hat{a}^\dagger_{\xi_k^e})^{n_k}}{\sqrt{n_k!}}|0\rangle \tag{F.8}$$

$$=\frac{1}{\sqrt{n_k!}}\left(\int_{t_k}^{t_{k+1}}dt\lambda_k\xi_k(t)\hat{a}^\dagger(t)\right)^{n_k}|0\rangle \tag{F.9}$$

$$=\frac{1}{\sqrt{n_k!}}(\lambda_k)^{n_k}\left(\int_{t_k}^{t_{k+1}}dt\xi_k(t)\hat{a}^\dagger(t)\right)^{n_k}|0\rangle \tag{F.10}$$

$$=(\lambda_k)^{n_k}\frac{(\hat{a}^\dagger_{\xi_k})^{n_k}}{\sqrt{n_k!}}|0\rangle=(\lambda_k)^{n_k}|n_{\xi_k}\rangle. \tag{F.11}$$

This means that the chip-time number states are eigenstates of the operator $\hat{\mathrm{U}}_k$ with eigenvalue $(\lambda_k)^{n_k}$.

Hence

$$\hat{\mathrm{U}}|n_\xi\rangle=|n_{\xi^e}\rangle=\sum_{n_0+\cdots+n_{N_c-1}=n}\mathcal{C}_n(n_0,n_1,\ldots,n_{N_c-1}) \times\prod_{k=0}^{N_c-1}(\lambda_k)^{n_k}|n_{\xi_k}\rangle. \tag{F.12}$$

1) EXAMPLE, $n = 1$

For this case, the constraint $n_0+\cdots+n_{N_c-1}=n=1$ implies that only one chip time should contain the single photon, while other chip times are in vacuum state. Therefore, for some k_0, we have $n_{k_0}=1$ and $n_l=0, l\neq k_0$. The overall encoded state is thus the superposition that can be expressed as a summation over $k_0=0,1,\ldots,N_c-1$

$$|1_{\xi^e}\rangle=\sum_{n_0+\cdots+n_{N_c-1}=1}\mathcal{C}_n(n_0,n_1,\ldots,n_{N_c-1}) \times\prod_{k=0}^{N_c-1}(\lambda_k)^{n_k}|n_{\xi_k}\rangle \tag{F.13}$$

$$=\sum_{k_0=0}^{N_c-1}\frac{1}{\sqrt{N_c}}\sqrt{\frac{1!}{\underbrace{0!\cdots0!}_{k_0}1!\underbrace{0!\cdots0!}_{N_c-k_0-1}}} \times(\lambda_{k_0})^1|1_{\xi_{k_0}}\rangle\prod_{k\neq k_0}^{N_c-1}(\lambda_k)^0|0_{\xi_k}\rangle \tag{F.14}$$

$$=\frac{1}{\sqrt{N_c}}\sum_{k_0=0}^{N_c-1}\lambda_{k_0}|1_{\xi_{k_0}}\rangle. \tag{F.15}$$

2) EXAMPLE, $n = 2$

For this case, the constraint $n_0+\cdots+n_{N_c-1}=n=2$ means that either for some k_0, the corresponding chip time contains two photons, or for some k_0 and $k_1>k_0$, the two chip times k_0 and k_1 contain a single photon simultaneously. Therefore

$$|2_{\xi^e}\rangle=\sum_{n_0+\cdots+n_{N_c-1}=2}\mathcal{C}_n(n_0,n_1,\ldots,n_{N_c-1}) \times\prod_{k=0}^{N_c-1}(\lambda_k)^{n_k}|n_{\xi_k}\rangle \tag{F.16}$$

$$= \sum_{k_0=0}^{N_c-1} \frac{1}{\sqrt{N_c^2}} \sqrt{\frac{2!}{\underbrace{0!\cdots 0!}_{k_0} 2! \underbrace{0!\cdots 0!}_{N_c-k_0-1}}} \times (\lambda_{k_0})^2 |2_{\xi_{k_0}}\rangle \prod_{k\neq k_0}^{N_c-1} (\lambda_k)^0 |0_{\xi_k}\rangle + \sum_{\substack{k_1=0 \\ \text{s.t. } k_1>k_0}}^{N_c-1} \sum_{k_0=0}^{N_c-1} \frac{1}{\sqrt{N_c^2}} \sqrt{\frac{2!}{1!1!}} (\lambda_{k_0})^1 (\lambda_{k_1})^1 |1_{\xi_{k_0}}\rangle |1_{\xi_{k_1}}\rangle \times \prod_{k\neq k_0,k_1} (\lambda_k)^0 |0_{\xi_k}\rangle \tag{F.17}$$

$$= \frac{1}{N_c} \sum_{k_0=0}^{N_c-1} |2_{\xi_{k_0}}\rangle + \frac{1}{N_c} \sum_{\substack{k_1=0 \\ \text{s.t. } k_1>k_0}}^{N_c-1} \sum_{k_0=0}^{N_c-1} \sqrt{2} \lambda_{k_0} \lambda_{k_1} |1_{\xi_{k_0}}\rangle |1_{\xi_{k_1}}\rangle. \tag{F.18}$$

3) EXAMPLE, $n = 3$

For this case, from constraint $n_0 + \cdots + n_{N_c-1} = n = 3$, we have three possible cases.

1) For some k_0, the corresponding chip time contains three photons $|3_{\xi_{k_0}}\rangle$.
2) For some k_0 and k_1, there is a single photon at chip time k_0 and two photons at chip time k_1, $|1_{\xi_{k_0}}\rangle |2_{\xi_{k_1}}\rangle$.
3) For some $k_2 > k_1 > k_0$, there is a single photon at chip times k_0, k_1, and k_2, $|1_{\xi_{k_0}}\rangle |1_{\xi_{k_1}}\rangle |1_{\xi_{k_2}}\rangle$.

We may obtain the corresponding coefficient of each case using Proposition 5 as follows:

$$|3_{\xi^e}\rangle = \sum_{n_0+\cdots+n_{N_c-1}=3} \mathcal{C}_n(n_0, n_1, \ldots, n_{N_c-1}) \times \prod_{k=0}^{N_c-1} (\lambda_k)^{n_k} |n_{\xi_k}\rangle \tag{F.19}$$

$$= \sum_{k_0=0}^{N_c-1} \frac{1}{\sqrt{N_c^3}} \sqrt{\frac{3!}{\underbrace{0!\cdots 0!}_{k_0} 3! \underbrace{0!\cdots 0!}_{N_c-k_0-1}}} \times (\lambda_{k_0})^3 |3_{\xi_{k_0}}\rangle \prod_{k\neq k_0}^{N_c-1} (\lambda_k)^0 |0_{\xi_k}\rangle + \sum_{k_1=0}^{N_c-1} \sum_{k_0=0}^{N_c-1} \frac{1}{\sqrt{N_c^3}} \sqrt{\frac{3!}{1!2!}} (\lambda_{k_0})^1 (\lambda_{k_1})^2 |1_{\xi_{k_0}}\rangle |2_{\xi_{k_1}}\rangle \times \prod_{k\neq k_0,k_1} (\lambda_k)^0 |0_{\xi_k}\rangle \tag{F.20}$$

$$+ \sum_{\substack{k_2=0 \\ \text{s.t. } k_2>k_1>k_0}}^{N_c-1} \sum_{k_1=0}^{N_c-1} \sum_{k_0=0}^{N_c-1} \frac{1}{\sqrt{N_c^3}} \sqrt{\frac{3!}{1!1!1!}} (\lambda_{k_0})^1 (\lambda_{k_1})^1 (\lambda_{k_2})^1 \times |1_{\xi_{k_0}}\rangle |1_{\xi_{k_1}}\rangle |1_{\xi_{k_2}}\rangle \prod_{k\neq k_0,k_1,k_2} (\lambda_k)^0 |0_{\xi_k}\rangle \tag{F.21}$$

$$= \frac{1}{\sqrt{N_c^3}} \sum_{k_0=0}^{N_c-1} \lambda_{k_0} |3_{\xi_{k_0}}\rangle + \frac{1}{\sqrt{N_c^3}} \sum_{k_1=0}^{N_c-1} \sum_{k_0=0}^{N_c-1} \sqrt{3} \lambda_{k_0} |1_{\xi_{k_0}}\rangle |2_{\xi_{k_1}}\rangle + \frac{1}{\sqrt{N_c^3}} \sum_{\substack{k_2=0 \\ \text{s.t. } k_2>k_1>k_0}}^{N_c-1} \sum_{k_1=0}^{N_c-1} \sum_{k_0=0}^{N_c-1} \sqrt{3!} \lambda_{k_0} \lambda_{k_1} \lambda_{k_2} |1_{\xi_{k_0}}\rangle |1_{\xi_{k_1}}\rangle |1_{\xi_{k_2}}\rangle. \tag{F.22}$$

B. DECODING

Let $\hat{\mathrm{U}}_{\tilde{\Lambda}}^\dagger$ be the despreading operator associated with decoding sequence $\tilde{\Lambda}$. Denote the chip-time decomposition of $\hat{\mathrm{U}}_{\tilde{\Lambda}}^\dagger$ by $\prod_{k=0}^{N_c-1} \hat{\mathrm{U}}_{k,\tilde{\Lambda}}^\dagger$. The effect of decoding operator with decoding sequence $\tilde{\Lambda}$ on the number states encoded with sequence Λ is derived as follows:

$$\hat{\mathrm{U}}_{\tilde{\Lambda}}^\dagger |n_{\xi^e}\rangle = \hat{\mathrm{U}}_{\tilde{\Lambda}}^\dagger \sum_{n_0+\cdots+n_{N_c-1}=n} \mathcal{C}_n(n_0, n_1, \ldots, n_{N_c-1}) \times \prod_{k=0}^{N_c-1} (\lambda_k)^{n_k} |n_{\xi_k}\rangle \tag{F.23}$$

$$= \sum_{n_0+\cdots+n_{N_c-1}=n} \mathcal{C}_n(n_0, n_1, \ldots, n_{N_c-1}) \hat{\mathrm{U}}_{\tilde{\Lambda}}^\dagger \times \prod_{k=0}^{N_c-1} (\lambda_k)^{n_k} |n_{\xi_k}\rangle \tag{F.24}$$

$$= \sum_{n_0+\cdots+n_{N_c-1}=n} \mathcal{C}_n(n_0, n_1, \ldots, n_{N_c-1}) \times \left(\prod_{k=0}^{N_c-1} \hat{\mathrm{U}}_{k,\tilde{\Lambda}}^\dagger\right) \left(\prod_{k=0}^{N_c-1} (\lambda_k)^{n_k} |n_{\xi_k}\rangle\right) \tag{F.25}$$

$$= \sum_{n_0+\cdots+n_{N_c-1}=n} \mathcal{C}_n(n_0, n_1, \ldots, n_{N_c-1}) \times \prod_{k=0}^{N_c-1} (\lambda_k)^{n_k} \hat{\mathrm{U}}_{k,\tilde{\Lambda}}^\dagger |n_{\xi_k}\rangle \tag{F.26}$$

$$= \sum_{n_0+\cdots+n_{N_c-1}=n} \mathcal{C}_n(n_0, n_1, \ldots, n_{N_c-1}) \times \prod_{k=0}^{N_c-1} (\lambda_k)^{n_k} (\tilde{\lambda}_k)^{n_k} |n_{\xi_k}\rangle \tag{F.27}$$

$$= \sum_{n_0+\cdots+n_{N_c-1}=n} \mathcal{C}_n(n_0, n_1, \ldots, n_{N_c-1}) \times \prod_{k=0}^{N_c-1} (\tilde{\lambda}_k \lambda_k)^{n_k} |n_{\xi_k}\rangle \quad \text{(F.28)}$$

where the last two steps are obtained similar to (F.11).

APPENDIX G
GENERAL FILTER

Now, assume a general filter [33] with the Fourier series of their transfer function given by

$$H_{\mathrm{T}}(\omega) = \sum_{l=0}^{\infty} d_l e^{-jl\omega\tau} \qquad H_{\mathrm{R}}(\omega) = \sum_{l=0}^{\infty} f_l e^{-jl\omega\tau} \quad \text{(G.1)}$$

where $H_{\mathrm{T}}(\omega)$ and $H_{\mathrm{R}}(\omega)$ are the transmission response and reflection response of the filter, respectively.

Applying the filter to an input with frequency-domain wavepacket $\bar{\xi}(\omega)$ results in the following transmitted wavepacket:

$$H_{\mathrm{T}}(\omega)\bar{\xi}(\omega) = \sum_{l=0}^{\infty} d_l e^{-jl\omega\tau} \bar{\xi}(\omega). \quad \text{(G.2)}$$

Therefore

$$h_{\mathrm{T}}(t) * \xi(t) = \sum_{l=0}^{\infty} d_l \xi(t - l\tau). \quad \text{(G.3)}$$

From (38), we have

$$\hat{\mathrm{H}}\hat{a}^{\dagger}(\omega)\hat{\mathrm{H}}^{\dagger} = H_{\mathrm{T}}(\omega)\hat{a}'^{\dagger}(\omega) + H_{\mathrm{R}}(\omega)\hat{b}'^{\dagger}(\omega). \quad \text{(G.4)}$$

Therefore

$$\hat{\mathrm{H}}\hat{a}^{\dagger}_{\bar{\xi}}\hat{\mathrm{H}}^{\dagger} = \int d\omega \bar{\xi}(\omega)\hat{\mathrm{H}}\hat{a}^{\dagger}(\omega)\hat{\mathrm{H}}^{\dagger} \quad \text{(G.5)}$$

$$= \int d\omega \bar{\xi}(\omega)\left[H_{\mathrm{T}}(\omega)\hat{a}'^{\dagger}(\omega) + H_{\mathrm{R}}(\omega)\hat{b}'^{\dagger}(\omega)\right] \quad \text{(G.6)}$$

$$= \int d\omega H_{\mathrm{T}}(\omega)\bar{\xi}(\omega)\hat{a}'^{\dagger}(\omega) + \int d\omega H_{\mathrm{R}}(\omega)\bar{\xi}(\omega)\hat{b}'^{\dagger}(\omega) \quad \text{(G.7)}$$

$$= \int dt (h_{\mathrm{T}}(t) * \xi(t))\hat{a}'^{\dagger}(t) + \int dt (h_{\mathrm{R}}(t) * \xi(t))b'^{\dagger}(t) \quad \text{(G.8)}$$

$$= \int dt \sum_{l=0}^{\infty} d_l \xi(t - l\tau)\hat{a}'^{\dagger}(t) + \int dt \sum_{l=0}^{\infty} f_l \xi(t - l\tau)\hat{b}'^{\dagger}(t) \quad \text{(G.9)}$$

$$= \sum_{l=0}^{\infty}\left(d_l \int dt \xi(t - l\tau)\hat{a}'^{\dagger}(t) + f_l \int dt \xi(t - l\tau)\hat{b}'^{\dagger}(t)\right). \quad \text{(G.10)}$$

The case of $\tau = T_c$ with rectangular wavepacket is of particular interest. First, we derive the evolution of chip-time creation operators $\hat{a}^{\dagger}_{\xi_k}$ through a filter

$$\hat{\mathrm{H}}\hat{a}^{\dagger}_{\xi_k}\hat{\mathrm{H}}^{\dagger} = \sum_{l=0}^{\infty}\left(d_l \int dt \xi_k(t - lT_c)\hat{a}'^{\dagger}(t) + f_l \int dt \xi_k(t - lT_c)\hat{b}'^{\dagger}(t)\right) \quad \text{(G.11)}$$

$$= \sum_{l=0}^{\infty}\left(d_l \int_{(l+k)T_c}^{(l+k+1)T_c} dt \xi_k(t - lT_c)\hat{a}'^{\dagger}(t) + f_l \int_{(l+k)T_c}^{(l+k+1)T_c} dt \xi_k(t - lT_c)\hat{b}'^{\dagger}(t)\right) \quad \text{(G.12)}$$

$$= \sum_{l=0}^{\infty}\left(d_l \int_{(l+k)T_c}^{(l+k+1)T_c} dt \xi_0(t - (l+k)T_c)\hat{a}'^{\dagger}(t) + f_l \int_{(l+k)T_c}^{(l+k+1)T_c} dt \xi_0(t - (l+k)T_c)\hat{b}'^{\dagger}(t)\right) \quad \text{(G.13)}$$

$$= \sum_{l=0}^{\infty}\left(d_l \hat{a}'^{\dagger}_{\xi_{k+l}} + f_l \hat{b}'^{\dagger}_{\xi_{k+l}}\right). \quad \text{(G.14)}$$

At the next step, the effect of the filter on the creation operator of the quantum signal with wavepacket $\xi(t)$ is

$$\hat{\mathrm{H}}\hat{a}^{\dagger}_{\xi}\hat{\mathrm{H}}^{\dagger} = \sum_{l=0}^{\infty}\left(d_l \int_{lT_c}^{T_p+lT_c} dt \xi(t - lT_c)\hat{a}'^{\dagger}(t) + f_l \int_{lT_c}^{T_p+lT_c} dt \xi(t - lT_c)\hat{b}'^{\dagger}(t)\right) \quad \text{(G.15)}$$

$$= \sum_{l=0}^{\infty}\left(d_l \sum_{k=0}^{N_c-1} \int_{t_{l+k}}^{t_{l+k+1}} dt \xi(t - lT_c)\hat{a}'^{\dagger}(t) + f_l \sum_{k=0}^{N_c-1} \int_{t_{l+k}}^{t_{l+k+1}} dt \xi(t - lT_c)\hat{b}'^{\dagger}(t)\right) \quad \text{(G.16)}$$

$$= \sum_{l=0}^{\infty}\left(d_l \frac{1}{\sqrt{N_c}} \sum_{k=0}^{N_c-1} \int_{t_{l+k}}^{t_{l+k+1}} dt \sqrt{N_c}\xi(t - lT_c)\hat{a}'^{\dagger}(t) + f_l \frac{1}{\sqrt{N_c}} \sum_{k=0}^{N_c-1} \int_{t_{l+k}}^{t_{l+k+1}} dt \sqrt{N_c}\xi(t - lT_c)\hat{b}'^{\dagger}(t)\right). \quad \text{(G.17)}$$

Assuming that $\xi(t)$ has a rectangular wavepacket, we can further simplify the results as follows:

$$\hat{\mathrm{H}}\hat{a}^{\dagger}_{\xi}\hat{\mathrm{H}}^{\dagger} = \sum_{l=0}^{\infty}\left(d_l \frac{1}{\sqrt{N_c}} \sum_{k=0}^{N_c-1} \int_{t_{l+k}}^{t_{l+k+1}} dt \sqrt{\frac{N_c}{T_p}}\hat{a}'^{\dagger}(t) + f_l \frac{1}{\sqrt{N_c}} \sum_{k=0}^{N_c-1} \int_{t_{l+k}}^{t_{l+k+1}} dt \sqrt{\frac{N_c}{T_p}}\hat{b}'^{\dagger}(t)\right) \quad \text{(G.18)}$$

TABLE A1. Filter Coefficients With $q = k + l$

l	0	1	2	$\cdots$	N_c-1	N_c	N_c+1	
q	$\hat{a}'^{\dagger}_{\xi_0}$	$\hat{a}'^{\dagger}_{\xi_1}$	$\hat{a}'^{\dagger}_{\xi_2}$	$\cdots$	$\hat{a}'^{\dagger}_{\xi_{N_c-1}}$	$\hat{a}'^{\dagger}_{\xi_{N_c}}$	$\hat{a}'^{\dagger}_{\xi_{N_c+1}}$	
0	d_0	d_0	d_0	$\cdots$	d_0	0	0	$\sum_{l=0}^{\infty}\sum_{k=0}^{N_c-1} d_l \hat{a}'^{\dagger}_{\xi_{k+l}}$
1	0	d_1	d_1	$\cdots$	d_1	d_1	0	
2	0	0	d_2	$\cdots$	d_2	d_2	d_2	
			$\underbrace{\qquad\qquad}_{k:\,0\to N_c-1}$					
$\vdots$	0	0	0	$\ddots$			$\ddots$	
	$\sum_{q=0}^{\infty}\sum_{l=\max(0,q-N_c+1)}^{q} d_l \hat{a}'^{\dagger}_{\xi_q}$							

$$= \sum_{l=0}^{\infty}\left(\frac{1}{\sqrt{N_c}} d_l \sum_{k=0}^{N_c-1} \hat{a}'^{\dagger}_{\xi_{k+l}} + \frac{1}{\sqrt{N_c}} f_l \sum_{k=0}^{N_c-1} \hat{b}'^{\dagger}_{\xi_{k+l}}\right). \tag{G.19}$$

To further simplify the aforementioned relation, let $q = k + l$ (see Table 1). Note that the coefficient of $\hat{a}'^{\dagger}_{\xi_q}$ is

$$\sum_{\substack{l=0 \\ \text{s.t. } l\le q\le l+N_c-1}}^{\infty} \frac{1}{\sqrt{N_c}} d_l = \sum_{l=\max(0,q-N_c+1)}^{q} \frac{1}{\sqrt{N_c}} d_l \tag{G.20}$$

$$= \sum_{l=0}^{\min(q,N_c-1)} \frac{1}{\sqrt{N_c}} d_{q-l}. \tag{G.21}$$

Hence

$$\hat{\mathrm{H}}\hat{a}^{\dagger}_{\xi}\hat{\mathrm{H}}^{\dagger} = \sum_{q=0}^{\infty}\Bigg[\underbrace{\left(\sum_{l=\max(0,q-N_c+1)}^{q} \frac{1}{\sqrt{N_c}} d_l\right)}_{D_q} \hat{a}'^{\dagger}_{\xi_q} \tag{G.22}$$

$$+ \underbrace{\left(\sum_{l=\max(0,q-N_c+1)}^{q} \frac{1}{\sqrt{N_c}} f_l\right)}_{F_q} \hat{b}'^{\dagger}_{\xi_q}\Bigg]$$

$$= \sum_{q=0}^{\infty}(D_q \hat{a}'^{\dagger}_{\xi_q} + F_q \hat{b}'^{\dagger}_{\xi_q}). \tag{G.23}$$

Since the temporal encoding leaves the temporal width of the wavepacket intact, with a similar approach, we have

$$\hat{\mathrm{H}}\hat{a}^{\dagger}_{\xi^d}\hat{\mathrm{H}}^{\dagger} = \sum_{l=0}^{\infty}\left(d_l \int_{lT_c}^{T_p+lT_c} dt\xi^d(t - lT_c)\hat{a}'^{\dagger}(t)\right.$$

$$\left. + f_l \int_{lT_c}^{T_p+lT_c} dt\xi^d(t - lT_c)\hat{b}'^{\dagger}(t)\right) \tag{G.24}$$

$$= \sum_{l=0}^{\infty}\left(d_l \sum_{k=0}^{N_c-1} \int_{t_{l+k}}^{t_{l+k+1}} dt\xi^d(t - lT_c)\hat{a}'^{\dagger}(t)\right.$$

$$\left. + f_l \sum_{k=0}^{N_c-1} \int_{t_{l+k}}^{t_{l+k+1}} dt\xi^d(t - lT_c)\hat{b}'^{\dagger}(t)\right) \tag{G.25}$$

$$= \sum_{l=0}^{\infty}\left(d_l \sum_{k=0}^{N_c-1} \tilde{\lambda}_k\lambda_k \int_{t_{l+k}}^{t_{l+k+1}} dt\xi(t - lT_c)\hat{a}'^{\dagger}(t)\right.$$

$$\left. + f_l \sum_{k=0}^{N_c-1} \tilde{\lambda}_k\lambda_k \int_{t_{l+k}}^{t_{l+k+1}} dt\xi(t - lT_c)\hat{b}'^{\dagger}(t)\right) \tag{G.26}$$

$$= \sum_{l=0}^{\infty}\left(d_l \frac{1}{\sqrt{N_c}} \sum_{k=0}^{N_c-1} \tilde{\lambda}_k\lambda_k \int_{t_{l+k}}^{t_{l+k+1}} dt\sqrt{N_c}\xi(t - lT_c)\hat{a}'^{\dagger}(t)\right.$$

$$\left. + f_l \frac{1}{\sqrt{N_c}} \sum_{k=0}^{N_c-1} \tilde{\lambda}_k\lambda_k \int_{t_{l+k}}^{t_{l+k+1}} dt\sqrt{N_c}\xi(t - lT_c)\hat{b}'^{\dagger}(t)\right) \tag{G.27}$$

$$= \sum_{l=0}^{\infty}\left(\frac{1}{\sqrt{N_c}} d_l \sum_{k=0}^{N_c-1} \tilde{\lambda}_k\lambda_k \hat{a}'^{\dagger}_{\xi_{k+l}} + \frac{1}{\sqrt{N_c}} f_l \sum_{k=0}^{N_c-1} \tilde{\lambda}_k\lambda_k \hat{b}'^{\dagger}_{\xi_{k+l}}\right). \tag{G.28}$$

Letting $q = k + l$, we obtain

$$\hat{\mathrm{H}}\hat{a}^{\dagger}_{\xi^d}\hat{\mathrm{H}}^{\dagger} = \sum_{q=0}^{\infty}\Bigg[\underbrace{\left(\sum_{l=\max(0,q-N_c+1)}^{q} \frac{1}{\sqrt{N_c}} d_l\tilde{\lambda}_{q-l}\lambda_{q-l}\right)}_{\tilde{D}_q} \hat{a}'^{\dagger}_{\xi_q}$$

$$+ \underbrace{\left(\sum_{l=\max(0,q-N_c+1)}^{q} \frac{1}{\sqrt{N_c}} f_l\tilde{\lambda}_{q-l}\lambda_{q-l}\right)}_{\tilde{F}_q} \hat{b}'^{\dagger}_{\xi_k}\Bigg] \tag{G.29}$$

$$= \sum_{q=0}^{\infty}(\tilde{D}_q \hat{a}'^{\dagger}_{\xi_q} + \tilde{F}_q \hat{b}'^{\dagger}_{\xi_q}). \tag{G.30}$$

For the FIR filter

$$\hat{\mathrm{H}}\hat{a}^{\dagger}_{\xi^d}\hat{\mathrm{H}}^{\dagger} = \sum_{q=0}^{L+N_c-1}\left[\left(\sum_{l=\max(0,q-N_c+1)}^{\min(q,L)} \frac{1}{\sqrt{N_c}} d_l\tilde{\lambda}_{q-l}\lambda_{q-l}\right)\hat{a}'^{\dagger}_{\xi_q}\right.$$

$$\left. + \left(\sum_{l=\max(0,q-N_c+1)}^{\min(q,L)} \frac{1}{\sqrt{N_c}} f_l\tilde{\lambda}_{q-l}\lambda_{q-l}\right)\hat{b}'^{\dagger}_{\xi_q}\right] \tag{G.31}$$

$$= \sum_{q=0}^{L+N_c-1} (\tilde{D}_q \hat{a}'^{\dagger}_{\xi_q} + \tilde{F}_q \hat{b}'^{\dagger}_{\xi_q}) \tag{G.32}$$

where L is the number of FIR filter coefficients.

A. ASYMPTOTIC BEHAVIOR

It would be interesting to investigate the asymptotic behavior of the filter to give further insight into the operation of the quantum spread-spectrum communication systems. We use numerical simulations to qualitatively describe the behavior of the filter.

First, we assume that the transmission filter's bandwidth (see Fig. 8) is high enough to pass the correctly decoded signal with very low loss. With this choice of filter, the signal wavepacket $\xi(t)$ almost entirely transmits through the filter H_{T}. Thus, in case $\tilde{\Lambda} = \Lambda$, the transmitted wavepacket is almost equal to the signal wavepacket, i.e., $\left\langle \xi(t) | \xi_{\mathrm{T}}(t - T_{\mathrm{delay}}) \right\rangle \approx 1$, where $T_{\mathrm{delay}} = k_{\mathrm{delay}} \times T_c$ is the delay imposed by the causal filter and k_{delay} is the number of chip times corresponding to T_{delay}. Fig. 10 illustrates the absolute value of coefficients D_q and F_q corresponding to the correct decoding of the quantum spread-spectrum signal. As can be seen from this figure, with a sufficiently good filter $|D_q| \approx \frac{1}{\sqrt{N_c}}$, $q_{\mathrm{delay}} \leq q < q_{\mathrm{delay}} + N_c$ and $|F_q| \approx 0$.

The other assumption required to obtain the ideal behavior corresponds to the rejection of the incorrectly decoded signals. The asymptotic behavior can be observed by assuming a high value of processing gain N_c, or equivalently $T_c \ll T$. This assumption implies that applying the code spreads the quantum signal in a way that a very small portion of the undesired quantum signals passes through the transmission filter, H_{T}. Therefore, when the two (approximately) orthogonal random codes $\tilde{\Lambda}$ and Λ do not match, $\langle \xi | \xi_{\mathrm{T}} \rangle \approx 0$. The transmission and reflection coefficients in case of incorrect decoding, $\tilde{D}_q$ and $\tilde{F}_q$, are shown in Fig. 10 for a very high processing gain. According to this figure, we asymptotically have $|\tilde{F}_q| \approx \frac{1}{\sqrt{N_c}}$, $q_{\mathrm{delay}} \leq q < q_{\mathrm{delay}} + N_c$ and $|\tilde{D}_q| \approx 0$, which means that the incorrectly decoded signal is almost entirely reflected from the filter.

APPENDIX H
EFFECT OF FILTER

A. COHERENT STATES

Denote the output of the filter in both modes by superscript F. For encoded and then decoded coherent state, we may write

$$|\alpha_{\xi^F}\rangle = \hat{\mathrm{H}}|\alpha_{\xi^d}\rangle = \hat{\mathrm{H}} e^{-\frac{|\alpha|^2}{2}} e^{\alpha \hat{a}^{\dagger}_{\xi^d}} \hat{\mathrm{H}}^{\dagger}|0\rangle \tag{H.1}$$

$$= e^{-\frac{|\alpha|^2}{2}} e^{\alpha \hat{\mathrm{H}} \hat{a}^{\dagger}_{\xi^d} \hat{\mathrm{H}}^{\dagger}}|0\rangle \tag{H.2}$$

$$= e^{-\frac{|\alpha|^2}{2}} \exp\left(\sum_{q=0}^{\infty} \left(\tilde{D}_q \alpha \hat{a}^{'\dagger}_{\xi_q} + \tilde{F}_q \alpha \hat{b}^{'\dagger}_{\xi_q} \right) \right)|0\rangle \tag{H.3}$$

$$= e^{-\frac{|\alpha|^2}{2}} \prod_{q=0}^{\infty} \exp(\tilde{D}_q \alpha \hat{a}^{'\dagger}_{\xi_q}) \exp(\tilde{F}_q \alpha \hat{b}^{'\dagger}_{\xi_q})|0\rangle \tag{H.4}$$

$$= \prod_{q=0}^{\infty} \exp\left(-\frac{1}{2} |\tilde{D}_q \alpha|^2 \right) \exp(\tilde{D}_q \alpha \hat{a}^{'\dagger}_{\xi_q}) \times \exp\left(-\frac{1}{2} |\tilde{F}_q \alpha|^2 \right) \exp(\tilde{F}_q \alpha \hat{b}^{'\dagger}_{\xi_q})|0\rangle \tag{H.5}$$

$$= \prod_{q=0}^{\infty} |\tilde{D}_q \alpha_{\xi_q}\rangle |\tilde{F}_q \alpha_{\xi_q}\rangle. \tag{H.6}$$

Note that

$$\sum_{q=0}^{\infty} \left(|\tilde{D}_q|^2 + |\tilde{F}_q|^2 \right) = 1 \tag{H.7}$$

which is due to the unitary condition. (This relation can also be derived from Lemma 1 in Section IV-D).

Taking partial trace with respect to the reflected modes gives the following expression:

$$|\alpha_{\xi_{\mathrm{T}}}\rangle = \prod_{q=0}^{\infty} |\tilde{D}_q \alpha_{\xi_q}\rangle. \tag{H.8}$$

Each term in the tensor product results in a Poisson distribution for number of photons in that specific chip-time, i.e., n_{q,ξ_q}. Therefore, the output statistics can be obtained by noting that the sum of independent Poisson random variables is also a Poisson random variable

$$\mathbb{P}(n) = \sum_{n_0 + n_1 + \cdots = n} \left| \langle n_{0,\xi_0}, n_{1,\xi_1}, \ldots | \alpha_{\xi_{\mathrm{T}}} \rangle \right|^2 \tag{H.9}$$

$$= \mathrm{Poisson}\left(|\alpha|^2 \sum_{q=0}^{\infty} |\tilde{D}_q|^2 \right). \tag{H.10}$$

B. NUMBER STATES

For the number state, we have

$$|n_{\xi^F}\rangle = \hat{\mathrm{H}}|n_{\xi^d}\rangle = \frac{(\hat{\mathrm{H}} \hat{a}^{\dagger}_{\xi^d} \hat{\mathrm{H}}^{\dagger})^n}{\sqrt{n!}}|0\rangle \tag{H.11}$$

$$= \frac{1}{\sqrt{n!}} \left(\sum_{q=0}^{\infty} \left(\tilde{D}_q \hat{a}^{'\dagger}_{\xi_q} + \tilde{F}_q \hat{b}^{'\dagger}_{\xi_q} \right) \right)^n |0\rangle \tag{H.12}$$

$$= \sum_{\substack{n_{\mathrm{T},0}, n_{\mathrm{T},1}, \ldots, n_{\mathrm{R},0}, n_{\mathrm{R},1}, \ldots \geq 0 \\ \text{s.t. } \sum_{q=0}^{\infty} (n_{\mathrm{T},q} + n_{\mathrm{R},q}) = n}} \sqrt{\binom{n}{n_{\mathrm{T},0}, n_{\mathrm{T},1}, \ldots, n_{\mathrm{R},0}, n_{\mathrm{R},1}, \ldots}} \times \prod_{q=0}^{\infty} \left((\tilde{D}_q)^{n_{\mathrm{T},q}} (\tilde{F}_q)^{n_{\mathrm{R},q}} |n_{\mathrm{T},q,\xi_q}\rangle |n_{\mathrm{R},q,\xi_q}\rangle \right) \tag{H.13}$$

where $n_{\mathrm{T},q}$ and $n_{\mathrm{R},q}$ denotes the number of photons at chip time q at the transmission and reflection ports of the filter, respectively.

For single-photon states, the aforementioned equation reduces to

$$|1_{\xi^F}\rangle = \hat{\mathrm{H}}|1_{\xi^d}\rangle = \sum_{q=0}^{\infty} \left(\tilde{D}_q |1_{\mathrm{T},\xi_q}\rangle + \tilde{F}_q |1_{\mathrm{R},\xi_q}\rangle \right). \tag{H.14}$$

Taking the partial trace with respect to the reflected part gives the final state of the receiver

$$\rho^{\mathrm{T}} = \mathrm{Tr}_R(\rho^F) = \mathrm{Tr}_R(|1_{\xi^F}\rangle\langle 1_{\xi^F}|) \tag{H.15}$$

$$= \langle 0_R|\rho^F|0_R\rangle + \sum_{q=0}^{\infty} \langle 1_{R,\xi_q}|\rho^F|1_{R,\xi_q}\rangle \tag{H.16}$$

$$= \langle 0_R|1_{\xi^F}\rangle\langle 1_{\xi^F}|0_R\rangle + \sum_{q=0}^{\infty} \langle 1_{R,\xi_q}|1_{\xi^F}\rangle\langle 1_{\xi^F}|1_{R,\xi_q}\rangle \tag{H.17}$$

where

$$\langle 0_R|1_{\xi^F}\rangle = \sum_{q=0}^{\infty} (\tilde{D}_q)\,|1_{T,\xi_q}\rangle \tag{H.18}$$

$$= \left(\sqrt{\sum_{q=0}^{\infty} |\tilde{D}_q|^2}\right)|1_{\xi_T}\rangle$$

$$\langle 1_{R,\xi_q}|1_{\xi^F}\rangle = (\tilde{F}_q)\,|0_T\rangle \tag{H.19}$$

where

$$|1_{\xi_T}\rangle := \frac{1}{\sqrt{\sum_{q=0}^{\infty}|\tilde{D}_q|^2}} \sum_{q=0}^{\infty} \tilde{D}_q|1_{T,\xi_q}\rangle. \tag{H.20}$$

Hence

$$\rho^T = \left(\sum_{q=0}^{\infty} \tilde{D}_q|1_{T,\xi_q}\rangle\right)\left(\sum_{q=0}^{\infty} \tilde{D}_q^*\langle 1_{T,\xi_q}|\right) \tag{H.21}$$

$$+ \sum_{q=0}^{\infty} |\tilde{F}_q|^2\,|0_T\rangle\langle 0_T|$$

$$= \left(\sum_{q=0}^{\infty} |\tilde{F}_q|^2\right)|0\rangle\langle 0| + \left(\sum_{q=0}^{\infty} |\tilde{D}_q|^2\right)|1_{\xi_T}\rangle\langle 1_{\xi_T}|. \tag{H.22}$$

APPENDIX I
QUANTUM BROADCASTING CHANNEL

A. COHERENT STATES

For coherent state inputs, we have

$$|\Phi\rangle = \hat{B}|\Psi\rangle = \hat{B}\prod_{s=0}^{M-1}|\alpha_{s,\xi}\rangle \tag{I.1}$$

$$= \hat{B}\prod_{s=0}^{M-1}\prod_{k=0}^{N_c-1}\left|\frac{\alpha_{s,\xi_k}}{\sqrt{N_c}}\right\rangle \tag{I.2}$$

$$= \hat{B}\prod_{s=0}^{M-1}\prod_{k=0}^{N_c-1} D\left(\frac{\alpha_{s,\xi_k}}{\sqrt{N_c}}\right)|0\rangle \tag{I.3}$$

$$= \hat{B}\prod_{k=0}^{N_c-1}\prod_{s=0}^{M-1} D\left(\frac{\alpha_{s,\xi_k}}{\sqrt{N_c}}\right)\hat{B}^\dagger|0\rangle \tag{I.4}$$

$$= \hat{B}\left[\prod_{s=0}^{M-1} D\left(\frac{\alpha_{s,\xi_0}}{\sqrt{N_c}}\right)\right]\left[\prod_{s=0}^{M-1} D\left(\frac{\alpha_{s,\xi_1}}{\sqrt{N_c}}\right)\right]\cdots$$

$$\times\left[\prod_{s=0}^{M-1} D\left(\frac{\alpha_{s,\xi_{N_c-1}}}{\sqrt{N_c}}\right)\right]\hat{B}^\dagger|0\rangle \tag{I.5}$$

$$= \hat{B}\left[\prod_{s=0}^{M-1} D\left(\frac{\alpha_{s,\xi_0}}{\sqrt{N_c}}\right)\right]\hat{B}^\dagger\hat{B}\left[\prod_{s=0}^{M-1} D\left(\frac{\alpha_{s,\xi_1}}{\sqrt{N_c}}\right)\right]\hat{B}^\dagger\hat{B}$$

$$\cdots\hat{B}\left[\prod_{s=0}^{M-1} D\left(\frac{\alpha_{s,\xi_{N_c-1}}}{\sqrt{N_c}}\right)\right]\hat{B}^\dagger|0\rangle \tag{I.6}$$

$$= \prod_{k=0}^{N_c-1}\hat{B}\left[\prod_{s=0}^{M-1} D\left(\frac{\alpha_{s,\xi_k}}{\sqrt{N_c}}\right)\right]\hat{B}^\dagger|0\rangle \tag{I.7}$$

$$= \prod_{k=0}^{N_c-1}\hat{B}\left[\prod_{s=0}^{M-1} D\left(\frac{\alpha_{s,\xi_k}}{\sqrt{N_c}}\right)\right]|0\rangle \tag{I.8}$$

$$= \prod_{k=0}^{N_c-1}\hat{B}\prod_{s=0}^{M-1}\left|\frac{\alpha_{s,\xi_k}}{\sqrt{N_c}}\right\rangle. \tag{I.9}$$

The aforementioned equation shows that the effect of star coupler on the coherent state inputs is equivalent to the tensor product of the effect of star coupler on each chip of the decomposed states.

According to [16], we have

$$\hat{B}\prod_{s=0}^{M-1}\left|\frac{\alpha_{s,\xi_k}}{\sqrt{N_c}}\right\rangle = \prod_{r=0}^{M-1}\left|\sum_{s=0}^{M-1}\frac{B_{rs}}{\sqrt{N_c}}\alpha_{s,\xi_k}\right\rangle. \tag{I.10}$$

Therefore

$$|\Phi\rangle = \hat{B}|\Psi\rangle = \prod_{k=0}^{N_c-1}\prod_{r=0}^{M-1}\left|\sum_{s=0}^{M-1}\frac{B_{rs}}{\sqrt{N_c}}\alpha_{s,\xi_k}\right\rangle \tag{I.11}$$

$$= \prod_{r=0}^{M-1}\prod_{k=0}^{N_c-1}\left|\sum_{s=0}^{M-1}\frac{B_{rs}}{\sqrt{N_c}}\alpha_{s,\xi_k}\right\rangle \tag{I.12}$$

Now, assume that the input of the star-coupler broadcasting channel is the encoded spread-spectrum coherent states

$$|\Phi^e\rangle = \hat{B}|\Psi^e\rangle = \prod_{k=0}^{N_c-1}\prod_{r=0}^{M-1}\left|\sum_{s=0}^{M-1}\frac{B_{rs}}{\sqrt{N_c}}\alpha_{s,\xi_k^e}\right\rangle \tag{I.13}$$

$$= \prod_{r=0}^{M-1}\prod_{k=0}^{N_c-1}\left|\sum_{s=0}^{M-1}\frac{B_{rs}}{\sqrt{N_c}}\lambda_{s,k}\alpha_{s,\xi_k}\right\rangle \tag{I.14}$$

For coherent states, the received signal at receiver r is a pure state that can be obtained by $\rho_r^e = \mathrm{Tr}_{r'\neq r}(|\Phi^e\rangle\langle\Phi^e|) = |\phi_r^e\rangle\langle\phi_r^e|$.

Hence

$$|\phi_r^e\rangle = \prod_{k=0}^{N_c-1}\left|\sum_{s=0}^{M-1}\frac{B_{rs}}{\sqrt{N_c}}\lambda_{s,k}\alpha_{s,\xi_k}\right\rangle \tag{I.15}$$

Now, we apply the decoding operator on this state

$$|\phi_r^d\rangle = \hat{\mathrm{U}}^\dagger \left| \phi_r^e \right\rangle = \prod_{k=0}^{N_c-1} |\lambda_{r,k} \sum_{s=0}^{M-1} \frac{B_{rs}}{\sqrt{N_c}} \lambda_{s,k} \alpha_{s,\xi_k} \Big\rangle \tag{I.16}$$

$$= \prod_{k=0}^{N_c-1} \left| \lambda_{r,k} \sum_{s=0}^{M-1} \frac{B_{rs}}{\sqrt{N_c}} \lambda_{s,k} \alpha_{s,\xi_k} \right\rangle \tag{I.17}$$

$$= \prod_{k=0}^{N_c-1} \left| (\lambda_{r,k})^2 \frac{B_{rr}}{\sqrt{N_c}} \alpha_{s=r,\xi_k} + \sum_{s\neq r} \lambda_{r,k}\lambda_{s,k} \frac{B_{rs}}{\sqrt{N_c}} \alpha_{s,\xi_k} \right\rangle \tag{I.18}$$

$$= \prod_{k=0}^{N_c-1} \left| \frac{B_{rr}}{\sqrt{N_c}} \alpha_{s=r,\xi_k} + \frac{1}{\sqrt{N_c}} \sum_{s\neq r} \lambda_{r,k}\lambda_{s,k} B_{rs} \alpha_{s,\xi_k} \right\rangle \tag{I.19}$$

$$= \left| \sum_{k=0}^{N_c-1} \left(\frac{B_{rr}}{\sqrt{N_c}} \alpha_{s=r,\xi_k} + \frac{1}{\sqrt{N_c}} \sum_{s\neq r} \lambda_{r,k}\lambda_{s,k} B_{rs} \alpha_{s,\xi_k} \right) \right\rangle \tag{I.20}$$

$$= \left| B_{rr} \alpha_{s=r,\xi} + \sum_{s\neq r} B_{rs} \alpha_{s,\xi^e s d_r} \right\rangle. \tag{I.21}$$

Note that $(\lambda_{r,k})^2 = 1$.

B. NUMBER (FOCK) STATES

For encoded signals, we have

$$|\Psi^e\rangle = \prod_{s=0}^{M-1} |n_{s,\xi^e}\rangle \tag{I.22}$$

$$= \prod_{s=0}^{M-1} \frac{1}{\sqrt{n_s!}} (\hat{a}^\dagger_{s,\xi^e})^{n_s} |0\rangle \tag{I.23}$$

$$= \prod_{s=0}^{M-1} \frac{1}{\sqrt{n_s!}} \left(\frac{1}{\sqrt{N_c}} \sum_{k=0}^{N_c-1} \hat{a}^\dagger_{s,\xi^e_k} \right)^{n_s} |0\rangle \tag{I.24}$$

$$= \prod_{s=0}^{M-1} \frac{1}{\sqrt{n_s!}} \left(\frac{1}{\sqrt{N_c}} \sum_{k=0}^{N_c-1} \lambda_{s,k} \hat{a}^\dagger_{s,\xi_k} \right)^{n_s} |0\rangle. \tag{I.25}$$

After the quantum broadcasting channel, we have

$$|\Phi^e\rangle = \hat{\mathrm{B}} |\Psi^e\rangle \tag{I.26}$$

$$= \hat{\mathrm{B}} \prod_{s=0}^{M-1} \frac{1}{\sqrt{n_s!}} (\hat{a}^\dagger_{s,\xi^e})^{n_s} |0\rangle \tag{I.27}$$

$$= \prod_{s=0}^{M-1} \frac{1}{\sqrt{n_s!}} (\hat{\mathrm{B}} \hat{a}^\dagger_{s,\xi^e} \hat{\mathrm{B}}^\dagger)^{n_s} |0\rangle \tag{I.28}$$

$$= \prod_{s=0}^{M-1} \frac{1}{\sqrt{n_s!}} \left(\sum_{r=0}^{M-1} B_{rs} \hat{a}^\dagger_{r,\xi^e} \right)^{n_s} |0\rangle \tag{I.29}$$

$$= \prod_{s=0}^{M-1} \frac{1}{\sqrt{n_s!}} \left(\frac{1}{\sqrt{N_c}} \sum_{k=0}^{N_c-1} \sum_{r=0}^{M-1} B_{rs} \hat{a}^\dagger_{r,\xi^e_k} \right)^{n_s} |0\rangle \tag{I.30}$$

$$= \prod_{s=0}^{M-1} \frac{1}{\sqrt{n_s!}} \left(\frac{1}{\sqrt{N_c}} \sum_{k=0}^{N_c-1} \sum_{r=0}^{M-1} B_{rs} \lambda_{s,k} \hat{a}^\dagger_{r,\xi_k} \right)^{n_s} |0\rangle. \tag{I.31}$$

Assuming that receiver r intends to decode the quantum signal of transmitter $s = r$ by applying the appropriate decoding operator, we obtain

$$|\Phi^d\rangle = \hat{\mathrm{U}}^\dagger |\Phi^e\rangle \tag{I.32}$$

$$= \hat{\mathrm{U}}^\dagger \prod_{s=0}^{M-1} \frac{1}{\sqrt{n_s!}} \left(\sum_{r=0}^{M-1} B_{rs} \hat{a}^\dagger_{r,\xi^e} \right)^{n_s} |0\rangle \tag{I.33}$$

$$= \prod_{s=0}^{M-1} \frac{1}{\sqrt{n_s!}} \left(\sum_{r=0}^{M-1} B_{rs} \hat{\mathrm{U}}^\dagger \hat{a}^\dagger_{r,\xi^e} \hat{\mathrm{U}} \right)^{n_s} |0\rangle \tag{I.34}$$

$$= \prod_{s=0}^{M-1} \frac{1}{\sqrt{n_s!}} \left(\sum_{r=0}^{M-1} B_{rs} \hat{a}^\dagger_{r,\xi^e s d_r} \right)^{n_s} |0\rangle. \tag{I.35}$$

From the chip-time perspective, we have

$$|\Phi^d\rangle = \hat{\mathrm{U}}^\dagger |\Phi^e\rangle \tag{I.36}$$

$$= \hat{\mathrm{U}}^\dagger \prod_{s=0}^{M-1} \frac{1}{\sqrt{n_s!}} \left(\frac{1}{\sqrt{N_c}} \sum_{k=0}^{N_c-1} \sum_{r=0}^{M-1} B_{rs} \lambda_{s,k} \hat{a}^\dagger_{r,\xi_k} \right)^{n_s} |0\rangle \tag{I.37}$$

$$= \prod_{s=0}^{M-1} \frac{1}{\sqrt{n_s!}} \left(\frac{1}{\sqrt{N_c}} \sum_{k=0}^{N_c-1} \sum_{r=0}^{M-1} B_{rs} \lambda_{s,k} \hat{\mathrm{U}}^\dagger \hat{a}^\dagger_{r,\xi_k} \hat{\mathrm{U}} \right)^{n_s} |0\rangle \tag{I.38}$$

$$= \prod_{s=0}^{M-1} \frac{1}{\sqrt{n_s!}} \left(\frac{1}{\sqrt{N_c}} \sum_{k=0}^{N_c-1} \sum_{r=0}^{M-1} B_{rs} \lambda_{s,k} \lambda_{r,k} \hat{a}^\dagger_{r,\xi_k} \right)^{n_s} |0\rangle \tag{I.39}$$

$$= \prod_{s=0}^{M-1} \frac{1}{\sqrt{n_s!}} \left(\frac{1}{\sqrt{N_c}} \sum_{k=0}^{N_c-1} \left(B_{ss} \hat{a}^\dagger_{r=s,\xi_k} + \sum_{r\neq s} B_{rs} \lambda_{s,k} \lambda_{r,k} \hat{a}^\dagger_{r,\xi_k} \right) \right)^{n_s} |0\rangle$$

$$= \prod_{s=0}^{M-1} \frac{1}{\sqrt{n_s!}} \left(B_{ss} \hat{a}^\dagger_{r=s,\xi} + \sum_{r\neq s} B_{rs} \hat{a}^\dagger_{r,\xi^e s d_r} \right)^{n_s} |0\rangle. \tag{I.40}$$

We apply the effect of filter, using (G.29), to obtain

$$\hat{\mathrm{H}} \hat{a}^\dagger_{r,\xi^e s d_r} \hat{\mathrm{H}}^\dagger \tag{I.41}$$

$$= \sum_{q=0}^{\infty} \left[\left(\sum_{l=\max(0,q-N_c+1)}^{q} \frac{1}{\sqrt{N_c}} d_l \lambda_{s,q-l} \lambda_{r,q-l} \right) \hat{a}'^\dagger_{r,\xi_q} \right.$$

$$+\left(\sum_{l=\max(0,q-N_c+1)}^{q}\frac{1}{\sqrt{N_c}}f_l\lambda_{s,q-l}\lambda_{r,q-l}\right)\hat{b}'^{\dagger}_{r,\xi_q}\Bigg]$$

$$:=\sum_{q=0}^{\infty}\left(D_q^{s,r}\hat{a}'^{\dagger}_{r,\xi_q}+F_q^{s,r}\hat{b}'^{\dagger}_{r,\xi_q}\right) \tag{I.42}$$

where $D_q^{s,r}$ and $F_q^{s,r}$ are defined in (80) and (81), respectively.

Thus, we obtain the quantum signal after the filter as

$$|\Phi^F\rangle=\prod_{s=0}^{M-1}\frac{1}{\sqrt{n_s!}}\Bigg(\sum_{q=0}^{\infty}\sum_{r=0}^{M-1}(B_{rs}D_q^{s,r}\hat{a}'^{\dagger}_{r,\xi_q}+B_{rs}F_q^{s,r}\hat{b}'^{\dagger}_{r,\xi_q})\Bigg)^{n_s}|0\rangle. \tag{I.43}$$

APPENDIX J
INTENSITY OF THE RECEIVED QUANTUM SIGNAL

First, we prove Lemma 1 by calculating $[\hat{a}_{\xi^{e_s d_r}},\hat{a}^{\dagger}_{\xi^{e_{s'}d_r}}]$ by two methods and comparing the results. From [16, eqs. (A.32) and (B.55)], we obtain

$$\left[\hat{a}_{\xi^{e_s d_r}},\hat{a}^{\dagger}_{\xi^{e_{s'}d_r}}\right]=\left\langle\xi^{e_s d_r}|\xi^{e_{s'}d_r}\right\rangle=\left\langle\xi^{e_s}|\xi^{e_{s'}}\right\rangle \tag{J.1}$$

$$=\frac{1}{N_c}\sum_{k=0}^{N_c-1}\lambda_{s,k}\lambda_{s',k} \tag{J.2}$$

$$=\langle\Lambda_s|\Lambda_{s'}\rangle\,. \tag{J.3}$$

Using the chip-time interval decomposition and considering the effect of filter, we may write

$$\begin{aligned}\left[\hat{a}_{\xi^{e_s d_r}},\hat{a}^{\dagger}_{\xi^{e_{s'}d_r}}\right]&=\sum_{q=0}^{\infty}\sum_{q'=0}^{\infty}D_q^{s,r*}D_{q'}^{s',r}\left[\hat{a}'_{r,\xi_q},\hat{a}'^{\dagger}_{r,\xi_{q'}}\right]\\&\quad+\sum_{q=0}^{\infty}\sum_{q'=0}^{\infty}D_q^{s,r*}F_{q'}^{s',r}\left[\hat{a}'_{r,\xi_q},\hat{b}'^{\dagger}_{r,\xi_{q'}}\right]\\&\quad+\sum_{q=0}^{\infty}\sum_{q'=0}^{\infty}F_q^{s,r*}D_{q'}^{s',r}\left[\hat{b}'_{r,\xi_q},\hat{a}'^{\dagger}_{r,\xi_{q'}}\right]\\&\quad+\sum_{q=0}^{\infty}\sum_{q'=0}^{\infty}F_q^{s,r*}F_{q'}^{s',r}\left[\hat{b}'_{r,\xi_q},\hat{b}'^{\dagger}_{r,\xi_{q'}}\right]\\&=\sum_{q=0}^{\infty}\sum_{q'=0}^{\infty}D_q^{s,r*}D_{k'}^{s',r}\delta_{qq'}\\&\quad+\sum_{q=0}^{\infty}\sum_{q'=0}^{\infty}F_q^{s,r*}F_{k'}^{s',r}\delta_{qq'}\\&=\sum_{q=0}^{\infty}\left(D_q^{s,r*}D_q^{s',r}+F_q^{s,r*}F_q^{s',r}\right).\end{aligned} \tag{J.4}$$

Thus, from (J.2) and (J.4), we conclude that

$$\sum_{q=0}^{\infty}\left(D_q^{s,r*}D_q^{s',r}+F_q^{s,r*}F_q^{s',r}\right)=\frac{1}{N_c}\sum_{k=0}^{N_c-1}\lambda_{s,k}\lambda_{s',k} \tag{J.5}$$

which completes the proof of Lemma 1.

The intensity of the decoded quantum signal after the filter can be obtained according to the following equation:

$$I_{r_0}(t)=\langle\Phi^d|\hat{a}'^{\dagger}_{r_0}(t)\hat{a}'_{r_0}(t)|\Phi^d\rangle. \tag{J.6}$$

Since $\hat{a}'_r(t)|0\rangle=0$, we have $\hat{a}'_r(t)|\psi_\xi\rangle=[\hat{a}'_r(t),f(\hat{a}^{\dagger}_{\xi})]|0\rangle$. Thus, we find $\hat{a}'_{r_0}(t)|\Phi^F\rangle$ for number state inputs using (I.43) as follows:

$$\hat{a}'_{r_0}(t)|\Phi^F\rangle=\hat{a}'_{r_0}(t)\prod_{s=0}^{M-1}\frac{1}{\sqrt{n_s!}}\left(\sum_{q=0}^{\infty}\sum_{r=0}^{M-1}(B_{rs}D_q^{s,r}\hat{a}'^{\dagger}_{r,\xi_q}+B_{rs}F_q^{s,r}\hat{b}'^{\dagger}_{r,\xi_q})\right)^{n_s}|0\rangle \tag{J.7}$$

$$=\left[\hat{a}'_{r_0}(t),\prod_{s=0}^{M-1}\frac{1}{\sqrt{n_s!}}\left(\sum_{q=0}^{\infty}\sum_{r=0}^{M-1}(B_{rs}D_q^{s,r}\hat{a}'^{\dagger}_{r,\xi_q}+B_{rs}F_q^{s,r}\hat{b}'^{\dagger}_{r,\xi_q})\right)^{n_s}\right]|0\rangle. \tag{J.8}$$

Note that

$$\left[\hat{a}(t),f(\hat{a}_\xi)\right]=\xi(t)\frac{\partial}{\partial\hat{a}_\xi}f(\hat{a}_\xi). \tag{J.9}$$

Therefore

$$\left[\hat{a}'_r(t),f(\hat{a}'_{r,\xi_q})\right]=\xi_q(t)\frac{\partial}{\partial\hat{a}'_{r,\xi_q}}f(\hat{a}'_{r,\xi_q}) \tag{J.10}$$

$$=\begin{cases}\sqrt{\frac{N_c}{T_p}}\frac{\partial}{\partial\hat{a}'_{r,\xi_q}}f(\hat{a}'_{r,\xi_q}), & t\in[t_q,t_{q+1})\\ 0, & t\notin[t_q,t_{q+1}).\end{cases} \tag{J.11}$$

Thus, if $t\in[t_l,t_{l+1})$, and we want to decode at receiver r_0, then

$$\hat{a}'_{r_0}(t)|\Phi^d\rangle=\sqrt{\frac{N_c}{T_p}}\frac{\partial}{\partial\hat{a}'_{r_0,\xi_l}}\prod_{s=0}^{M-1}\frac{1}{\sqrt{n_s!}} \tag{J.12}$$

$$\times\left(\sum_{q=0}^{\infty}\sum_{r=0}^{M-1}(B_{rs}D_q^{s,r}\hat{a}'^{\dagger}_{r,\xi_q}+B_{rs}F_q^{s,r}\hat{b}'^{\dagger}_{r,\xi_q})\right)^{n_s}|0\rangle$$

$$=\sqrt{\frac{N_c}{T_p}}\sum_{s=0}^{M-1}\left(B_{r_0s}D_l^{s,r_0}\right)\frac{n_s}{\sqrt{n_s!}}$$

$$\times\left(\sum_{q=0}^{\infty}\sum_{r=0}^{M-1}(B_{rs}D_q^{s,r}\hat{a}'^{\dagger}_{r,\xi_q}+B_{rs}F_q^{s,r}\hat{b}'^{\dagger}_{r,\xi_q})\right)^{n_s-1}$$

$$\times\prod_{s'\neq s}\frac{1}{\sqrt{n_{s'}!}}\left(\sum_{q=0}^{\infty}\sum_{r=0}^{M-1}(B_{rs'}D_q^{s',r}\hat{a}'^{\dagger}_{r,\xi_q}\right.$$

$$+ B_{rs'} F_q^{s',r} \hat{b}_{r,\xi_q}^{'\dagger}) \Big)^{n_{s'}} |0\rangle. \tag{J.13}$$

Define the auxiliary operator $\hat{v}_s^\dagger$ as

$$\hat{v}_s^\dagger = \sum_{q=0}^{\infty} \sum_{r=0}^{M-1} B_{rs} D_q^{s,r} \hat{a}_{r,\xi_q}^{'\dagger} + B_{rs} F_q^{s,r} \hat{b}_{r,\xi_q}^{'\dagger}. \tag{J.14}$$

We have

$$\hat{a}'_{r_0}(t)|\Phi^d\rangle = \sqrt{\frac{N_c}{T_p}} \sum_{s=0}^{M-1} \left(B_{r_0 s} D_l^{s,r_0}\right) \frac{n_s}{\sqrt{n_s!}} (\hat{v}_s^\dagger)^{n_s-1} \times \prod_{s' \neq s} \frac{1}{\sqrt{n_{s'}!}} (\hat{v}_{s'}^\dagger)^{n_{s'}} |0\rangle. \tag{J.15}$$

We show that the defined auxiliary operator has the property of creation operators and thus can be considered as a virtual creation operator

$$\left[\hat{v}_s, \hat{v}_{s'}^\dagger\right] \tag{J.16}$$

$$= \sum_{q=0}^{\infty} \sum_{r=0}^{M-1} \sum_{q'=0}^{\infty} \sum_{r'=0}^{M-1} B_{rs}^* D_q^{s,r*} B_{r's'} D_{q'}^{s',r'} \left[\hat{a}'_{r,\xi_q}, \hat{a}_{r',\xi_{q'}}^{'\dagger}\right] + \sum_{q=0}^{\infty} \sum_{r=0}^{M-1} \sum_{q'=0}^{\infty} \sum_{r'=0}^{M-1} B_{rs}^* D_q^{s,r*} B_{r's'} F_{q'}^{s',r'} \left[\hat{a}'_{r,\xi_q}, \hat{b}_{r',\xi_{q'}}^{'\dagger}\right] + \sum_{q=0}^{\infty} \sum_{r=0}^{M-1} \sum_{q'=0}^{\infty} \sum_{r'=0}^{M-1} B_{rs}^* F_q^{s,r*} B_{r's'} D_{q'}^{s',r'} \left[\hat{b}'_{r,\xi_q}, \hat{a}_{r',\xi_{q'}}^{'\dagger}\right] + \sum_{q=0}^{\infty} \sum_{r=0}^{M-1} \sum_{q'=0}^{\infty} \sum_{r'=0}^{M-1} B_{rs}^* F_q^{s,r*} B_{r's'} F_{q'}^{s',r'} \left[\hat{b}'_{r,\xi_q}, \hat{b}_{r',\xi_{q'}}^{'\dagger}\right]$$

$$= \sum_{q=0}^{\infty} \sum_{r=0}^{M-1} \sum_{q'=0}^{\infty} \sum_{r'=0}^{M-1} B_{rs}^* D_q^{s,r*} B_{r's'} D_{q'}^{s',r'} \delta_{rr'} \delta_{qq'} + \sum_{q=0}^{\infty} \sum_{r=0}^{M-1} \sum_{q'=0}^{\infty} \sum_{r'=0}^{M-1} B_{rs}^* F_q^{s,r*} B_{r's'} F_{q'}^{s',r'} \delta_{rr'} \delta_{qq'} \tag{J.17}$$

$$= \sum_{q=0}^{\infty} \sum_{r=0}^{M-1} B_{rs}^* D_q^{s,r*} B_{rs'} D_q^{s',r} + \sum_{q=0}^{\infty} \sum_{r=0}^{M-1} B_{rs}^* F_q^{s,r*} B_{rs'} F_q^{s',r} \tag{J.18}$$

$$= \sum_{r=0}^{M-1} B_{rs}^* B_{rs'} \left(\sum_{q=0}^{\infty} (D_q^{s,r*} D_q^{s',r} + F_q^{s,r*} F_q^{s',r}) \right) \tag{J.19}$$

$$= \left(\frac{1}{N_c} \sum_{k=0}^{N_c-1} \lambda_{s,k} \lambda_{s',k} \right) \sum_{r=0}^{M-1} B_{rs}^* B_{rs'} \tag{J.20}$$

$$= \delta_{ss'}. \tag{J.21}$$

Since the commutation relation $[\hat{v}_s, \hat{v}_{s'}^\dagger] = \delta_{ss'}$ holds, the corresponding number states of these auxiliary field creation operators form orthogonal modes; hence, we define

$$|n_s\rangle_{v_s} = \frac{1}{\sqrt{n_{s'}!}} (\hat{v}_{s'}^\dagger)^{n_{s'}} |0\rangle \tag{J.22}$$

which denotes a quantum state with n_s photons in mode v_s.

Therefore

$$\hat{a}'_{r_0}(t)|\Phi^d\rangle = \sqrt{\frac{N_c}{T_p}} \sum_{s=0}^{M-1} \sqrt{n_s} \left(B_{r_0 s} D_l^{s,r_0}\right) \times |n_0\rangle_{v_0} |n_1\rangle_{v_1} \cdots |n_s - 1\rangle_{v_s} \cdots |n_{M-1}\rangle_{v_{M-1}}. \tag{J.23}$$

Thus, the intensity at time $t \in [t_q, t_{q+1})$ is obtained as

$$I_{r_0}(t) = \langle \Phi^d | \hat{a}_{r_0}^{'\dagger}(t) \hat{a}'_{r_0}(t) | \Phi^d \rangle \tag{J.24}$$

$$= \frac{N_c}{T_p} \sum_{s=0}^{M-1} n_s |B_{r_0 s} D_q^{s,r_0}|^2 \tag{J.25}$$

$$= \frac{N_c}{T_p} n_{r_0} |B_{r_0 r_0} D_q|^2 + \frac{N_c}{T_p} \sum_{s \neq r_0} n_s |B_{r_0 s} D_q^{s,r_0}|^2 \tag{J.26}$$

where

$$D_q^{s,r_0} = \sum_{l=\max(0,q-N_c+1)}^{q} \frac{1}{\sqrt{N_c}} d_l \lambda_{s,q-l} \lambda_{r_0,q-l} \tag{J.27}$$

$$D_q^{s=r_0,r_0} = D_q = \sum_{l=\max(0,q-N_c+1)}^{q} \frac{1}{\sqrt{N_c}} d_l. \tag{J.28}$$

Next, we pursue the same procedure for coherent states using Proposition 14. If $t \in [t_l, t_{l+1})$, and receiver r_0 decodes the data of sender $s_0 = r_0$, then

$$|\alpha_{\xi_T}\rangle = \prod_{q=0}^{\infty} \left| B_{r_0 r_0} D_q \alpha_{s_0=r_0,\xi_k} + \sum_{s \neq r_0} B_{r_0 s} D_q^{s,r_0} \alpha_{s,\xi_k} \right\rangle \tag{J.29}$$

$$= \prod_{q=0}^{\infty} \exp\left(-\frac{1}{2} \left| \sum_{s=0}^{M-1} B_{r_0 s} D_q^{s,r_0} \alpha_s \right|^2 \right) \times \exp\left(\sum_{s=0}^{M-1} B_{r_0 s} D_q^{s,r_0} \alpha_s \hat{a}_{r,\xi_k}^{'\dagger} \right) |0\rangle. \tag{J.30}$$

Based on the aforementioned equation, we may write

$$\hat{a}'_{r_0}(t)|\alpha_{r_0,\xi_T}\rangle = \sqrt{\frac{N_c}{T_p}} \frac{\partial}{\partial \hat{a}'_{r_0,\xi_l}} \left[\prod_{q=0}^{\infty} \exp\left(-\frac{1}{2} \left| \sum_{s=0}^{M-1} B_{r_0 s} D_q^{s,r_0} \alpha_s \right|^2 \right) \times \exp\left(\sum_{s=0}^{M-1} B_{r_0 s} D_q^{s,r_0} \alpha_s \hat{a}_{r,\xi_q}^{'\dagger} \right) \right] |0\rangle$$

$$= \sqrt{\frac{N_c}{T_p}} \left(\sum_{s=0}^{M-1} B_{r_0 s} D_l^{s,r_0} \alpha_s \right) \times \prod_{q=0}^{\infty} \exp\left(-\frac{1}{2} \left| \sum_{s=0}^{M-1} B_{r_0 s} D_q^{s,r_0} \alpha_s \right|^2 \right) \times \exp\left(\sum_{s=0}^{M-1} B_{r_0 s} D_q^{s,r_0} \alpha_s \hat{a}_{r,\xi_q}^{'\dagger} \right) |0\rangle$$

$$= \sqrt{\frac{N_c}{T_p}} \left(\sum_{s=0}^{M-1} B_{r_0 s} D_l^{s,r_0} \alpha_s \right) |\alpha_{r_0,\xi_T}\rangle. \tag{J.31}$$

Then, for $t \in [t_q, t_{q+1})$, we obtain

$$I_{r_0}(t) = \langle \Phi^d | \hat{a}_{r_0}^{'\dagger}(t) \hat{a}_{r_0}'(t) | \Phi^d \rangle = \frac{N_c}{T_p} \left| \sum_{s=0}^{M-1} B_{r_0 s} D_q^{s,r_0} \alpha_s \right|^2. \tag{J.32}$$

APPENDIX K
TWO-USER QUANTUM SPREAD-SPECTRUM INTERFERENCE

As an example, we study a two-user multiple-access communication system utilizing OOK modulation for the transmission of one bit. Assume that the receiver with index 0 is decoding the signal from transmitter 0. We consider a balanced star coupler, i.e.,

$$\begin{pmatrix} B_{00} & B_{01} \\ B_{10} & B_{11} \end{pmatrix} = \frac{1}{\sqrt{2}} \begin{pmatrix} 1 & 1 \\ -1 & 1 \end{pmatrix}. \tag{K.1}$$

A. COHERENT INPUT QUANTUM SIGNALS

The output of a two-user coherent quantum spread-spectrum CDMA communication system at receiver $r = 0$ is a pure state given by Proposition 14 as

$$\rho_0^{\mathrm{T}} = |\alpha_{0,\xi_T}\rangle\langle\alpha_{0,\xi_T}| \tag{K.2}$$

where

$$|\alpha_{0,\xi_T}\rangle = \prod_{q=0}^{\infty} \left| \frac{1}{\sqrt{2}} D_q \alpha_{0,\xi_q} + \frac{1}{\sqrt{2}} D_q^{1,0} \alpha_{1,\xi_q} \right\rangle. \tag{K.3}$$

The average intensity of the received signal is given by Proposition 16 as

$$I_0(t) = \frac{1}{2} \frac{N_c}{T_p} \left| D_q \alpha_0 + D_q^{1,0} \alpha_1 \right|^2 \quad t \in [t_q, t_{q+1}). \tag{K.4}$$

Let $n_{0,q}$ be the number of photons in time interval q. Since the quantum signal is a coherent state at each chip time, the chip-time photon statistics, $\mathbb{P}(n_{0,q})$, has a Poisson distribution

$$n_{0,q} \sim \text{Poisson}\left(\frac{1}{2} \left| D_q \alpha_0 + D_q^{1,0} \alpha_1 \right|^2 \right) \tag{K.5}$$

which gives the overall photon statistics as follows:

$$n_0 \sim \text{Poisson}\left(\frac{1}{2} \left| \sum_q (D_q \alpha_0 + D_q^{1,0} \alpha_1) \right|^2 \right) \tag{K.6}$$

where n_0 is the number of photons at the receiver after the filter.

B. SINGLE-PHOTON INPUT QUANTUM SIGNALS

In this section, we consider the output of a two-user single-photon quantum spread-spectrum CDMA communication system at receiver $r = 0$. The details are given in Appendix L. In this case, due to superposition of single photons, the received quantum signal at each receiver appears as a mixed states.

1) ONE USER IS TRANSMITTING

If transmitter $s = 1$ is turned OFF, i.e., it is in vacuum state $|0\rangle$, the received signal of receiver $r = 0$ after decoder is

$$\rho_0^d = \frac{1}{2}|0_0\rangle\langle 0_0| + \frac{1}{2}|1_{0,\xi}\rangle\langle 1_{0,\xi}|. \tag{K.7}$$

Applying the filter gives

$$\rho_0^{\mathrm{T}} = \frac{1}{2}\left(1 + \sum_{q=0}^{\infty} |F_q|^2\right)|0_{0,\mathrm{T}}\rangle\langle 0_{0,\mathrm{T}}| + \frac{1}{2}\left(\sum_{q=0}^{\infty} |D_q|^2\right)|1_{0,\xi_T}\rangle\langle 1_{0,\xi_T}| \tag{K.8}$$

where $|1_{0,\xi_T}\rangle$ is the desired signal after the filter defined as

$$|1_{0,\xi_T}\rangle := \frac{1}{\sqrt{\sum_{q=0}^{\infty} |D_q|^2}} \sum_{q=0}^{\infty} D_q |1_{0,\mathrm{T},\xi_q}\rangle. \tag{K.9}$$

The signal intensity is obtained using Proposition 16

$$I_0(t) = \frac{1}{2}\frac{N_c}{T_p}|D_q|^2, \quad t \in [t_q, t_{q+1}). \tag{K.10}$$

2) BOTH USERS ARE TRANSMITTING

If the second transmitter is also transmitting single photons, we obtain

$$|\Phi^d\rangle\Big|_{M=2,\text{balanced}} = \frac{1}{2N_c}\left(\sum_{k_0=0}^{N_c-1} |1_{0,\xi_{k_0}}\rangle\right)\left(\sum_{k_1=0}^{N_c-1} \lambda_{0,k_1}\lambda_{1,k_1}|1_{0,\xi_{k_1}}\rangle\right) - \frac{1}{2N_c}\left(\sum_{k_1=0}^{N_c-1} |1_{1,\xi_{k_1}}\rangle\right)\left(\sum_{k_0=0}^{N_c-1} \lambda_{1,k_0}\lambda_{1,k_0}|1_{1,\xi_{k_0}}\rangle\right)$$

$$+\frac{1}{2N_c}\left(\sum_{k_0=0}^{N_c-1}\sum_{k_1=0}^{N_c-1}(1-\lambda_{0,k_0}\lambda_{1,k_0}\lambda_{0,k_1}\lambda_{1,k_1})\right.$$
$$\left.\times\,|1_{0,\xi_{k_0}}\rangle|1_{1,\xi_{k_1}}\rangle\right). \tag{K.11}$$

The last term in summation is zero for $k_0 = k_1$ regardless of the encoding sequences, which gives the spread spectrum version of the Hong–Ou–Mandel effect [37] as follows.

Corollary 3 (Spread-Spectrum Hong–Ou–Mandel Effect): The state $|1_{0,\xi_k}\rangle|1_{1,\xi_k}\rangle$ never appears in the output of the balanced two-user quantum broadcasting channel for spread-spectrum single-photon inputs when two users are simultaneously transmitting information.

For identical codes $\Lambda_1 = \Lambda_0$, (K.11) reduces to the following NOON state,[5] which corresponds to the normal Hong–Ou–Mandel effect

$$|\Phi^d\rangle\Big|_{M=2,\text{balanced}} = \frac{1}{\sqrt{2}}\left(|2_{0,\xi}\rangle|0_1\rangle - |0_0\rangle|2_{1,\xi}\rangle\right). \tag{K.12}$$

The overall received quantum signal after decoder of receiver $r = 0$ is obtained, in terms of the normalized correlation $\langle\Lambda_0|\Lambda_1\rangle$, by taking partial trace of $|\Phi^d\rangle\langle\Phi^d|$ with respect to $r = 1$, which gives

$$\rho_0^d = \frac{1}{4}\left(1+|\langle\Lambda_0|\Lambda_1\rangle|^2\right)|(1+1)_{0,e_1d_0}\rangle\langle(1+1)_{0,e_1d_0}|$$
$$+\frac{1}{4}\left(1+|\langle\Lambda_0|\Lambda_1\rangle|^2\right)|0_0\rangle\langle 0_0|$$
$$+\frac{1}{2N_c}\sum_{k=0}^{N_c-1}\left(1-\lambda_{0,k}\lambda_{1,k}\,\langle\Lambda_0|\Lambda_1\rangle\right)$$
$$\times\,|1_{0,e_1d_0,k}\rangle\langle 1_{0,e_1d_0,k}|. \tag{K.13}$$

For random (approximately orthogonal) codes with $\langle\Lambda_0|\Lambda_1\rangle \approx 0$, (K.13) reduces to

$$\rho_0^d \approx \frac{1}{4}|(1+1)_{0,e_1d_0}\rangle\langle(1+1)_{0,e_1d_0}| + \frac{1}{4}|0_0\rangle\langle 0_0|$$
$$+\frac{1}{2N_c}\sum_{k=0}^{N_c-1}|1_{0,e_1d_0,k}\rangle\langle 1_{0,e_1d_0,k}| \tag{K.14}$$

where state $|(1+1)_{0,e_1d_0}\rangle \propto |1_{0,\xi}\rangle|1_{0,\xi^{e_1d_0}}\rangle$ is defined in (L.39) and is associated with the product of the desired quantum signal with interference from transmitter $s = 1$. On the other hand, $|1_{0,e_1d_0,k}\rangle$ given by

$$|1_{0,e_1d_0,k}\rangle = \frac{|1_{0,\xi}\rangle - \lambda_{0,k}\lambda_{1,k}|1_{0,\xi^{e_1d_0}}\rangle}{\sqrt{2(1-\lambda_{0,k}\lambda_{1,k}\,\langle\Lambda_0|\Lambda_1\rangle)}} \tag{K.15}$$

contains the desired signal in superposition with the multiple access interference signal.

[5]NOON states belong to the class of Schrodinger cat states and have emerging applications in quantum communications, protocol design [38], and quantum error correction [39].

After applying the filter and taking the partial trace, we obtain the mixed received quantum signal at the output of receiver $r = 0$

$$\rho_0^{\mathrm{T}} = \mathcal{C}_{DD}|(1+1)_{0,\mathrm{T},e_1d_0}\rangle\langle(1+1)_{0,\mathrm{T},e_1d_0}|$$
$$+\sum_{q=0}^{\infty}\mathcal{C}_{F_qD}|1_{0,\mathrm{T},e_1d_0,F_q}\rangle\langle 1_{0,\mathrm{T},e_1d_0,F_q}|$$
$$+\sum_{k=0}^{N_c-1}\mathcal{C}_{D,1_k}|1_{0,\mathrm{T},e_1d_0,k}\rangle\langle 1_{0,\mathrm{T},e_1d_0,k}|$$
$$+\mathcal{C}\mathcal{C}_0|0_{0,\mathrm{T}}\rangle\langle 0_{0,\mathrm{T}}|. \tag{K.16}$$

In the aforementioned expression, $|(1+1)_{0,\mathrm{T},e_1d_0}\rangle$ corresponds to the case where two photons from the two transmitters have arrived at receiver $r = 0$ and both have passed through the filter. Quantum signals of the form $|1_{0,\mathrm{T},e_1d_0,F_q}\rangle$ correspond to the cases where two photons from the two transmitters have arrived at receiver $r = 0$; one of them have passed through the filter and the reflected one corresponds to time interval q. State $|1_{0,\mathrm{T},e_1d_0,k}\rangle$ corresponds to the case where one photon has arrived at receiver $r = 0$ and it is also transmitted through the filter. The expressions for these states along with the corresponding multiplying factors are defined and calculated in Appendix L.

According to Proposition 16, the signal intensity is

$$I_0(t) = \frac{1}{2}\frac{N_c}{T_p}\left(|D_q|^2 + |D_q^{1,0}|^2\right), \quad t \in [tq, tq+1). \tag{K.17}$$

One can also use a rough approximation to gain insight into the photon statistics of the received quantum signal independently of the reflection coefficients, as follows.

Proposition 17: Consider a two-user spread-spectrum QCDMA communication system utilizing single photons with random spreading sequences and a balanced broadcasting channel. Denote the set of active transmitters by $\mathcal{S}$. The photon statistics at receiver $r = 0$ that utilizes the code Λ_0 to decode the quantum signal can be approximated as follows.

1) $\mathcal{S} = \{0\}$

$$\mathbb{P}(n_0) \approx \left(1-\frac{1}{2}\mathfrak{D}\right)\delta_{n_0,0} + \frac{1}{2}\mathfrak{D}\times\delta_{n_0,1}. \tag{K.18}$$

2) $\mathcal{S} = \{1\}$

$$\mathbb{P}(n_0) \approx \left(1-\frac{1}{2}\mathfrak{D}^{0,1}\right)\delta_{n_0,0} + \frac{1}{2}\mathfrak{D}^{0,1}\times\delta_{n_0,1}. \tag{K.19}$$

3) $\mathcal{S} = \{0, 1\}$

$$\mathbb{P}(n_0) \approx \left(1-\frac{1}{2}(\mathfrak{D}+\mathfrak{D}^{0,1})+\frac{1}{4}\mathfrak{D}\mathfrak{D}^{0,1}\right)\delta_{n_0,0}$$
$$+\left(\frac{1}{2}(\mathfrak{D}+\mathfrak{D}^{0,1})-\frac{1}{2}\mathfrak{D}\mathfrak{D}^{0,1}\right)\delta_{n_0,1}$$

IEEE Transactions on Quantum Engineering

$$+\frac{1}{4}\mathfrak{D}\mathfrak{D}^{0,1}\times\delta_{n_0,2}. \tag{K.20}$$

Here, the signal and interference overall transmission coefficients are, respectively, denoted by

$$\mathfrak{D}:=\sum_{q=0}^{\infty}|D_q|^2 \tag{K.21}$$

$$\mathfrak{D}^{0,1}:=\sum_{q=0}^{\infty}|D_q^{0,1}|^2. \tag{K.22}$$

Proposition 17 shows that the output photon statistics is approximately dominated by the transmission coefficients of the filter. As shown in Fig. 10 and discussed in Appendix G-A, we asymptotically have $\mathfrak{D}\approx 1$ and $\mathfrak{D}^{0,1}\approx 0$.

APPENDIX L
DETAILED DERIVATIONS OF TWO-USER SPREAD-SPECTRUM SYSTEM WITH SINGLE PHOTONS

In this section, we consider the case of $M=2$ users with single-photon transmitters and OOK modulation scheme over a balanced star coupler.

A. ONE USER IS TRANSMITTING

Assume that only transmitter $s=0$ is transmitting single-photon quantum signal and the other source is turned OFF and thus is in vacuum state. From (I.39), the receiver's decoded state is

$$|\Phi^d\rangle=\left(\frac{1}{\sqrt{N_c}}\sum_{k=0}^{N_c-1}\sum_{r=0}^{1}B_{r0}\lambda_{0,k}\lambda_{r,k}\hat{a}^{\dagger}_{r,\xi_k}\right)|0\rangle \tag{L.1}$$

$$=\frac{1}{\sqrt{N_c}}\Bigg(\sum_{k=0}^{N_c-1}B_{00}\hat{a}^{\dagger}_{0,\xi_k}+\sum_{k=0}^{N_c-1}B_{10}\lambda_{0,k}\lambda_{1,k}\hat{a}^{\dagger}_{1,\xi_k}\Bigg)|0\rangle. \tag{L.2}$$

The first term means that the single photon has arrived at receiver 0, while in the second term stands for the case that single photon has arrived at the other receiver.

The overall density matrix is

$$\rho_d=|\Phi^d\rangle\langle\Phi^d|. \tag{L.3}$$

In order to calculate the received state at the receiver $r=0$, we need to calculate the partial trace of ρ_d with respect to $r\neq 0$. Basis vectors of the Hilbert space of $r\neq 0$, with nonzero contribution to the partial trace, are of the form $\{|0_1\rangle,|1_{1,\xi_k}\rangle\}$. $|0_1\rangle$ is the state where receiver $r=1$ is in the vacuum state, and $|1_{1,\xi_k}\rangle$ are the cases where 1 photon has arrived at receivers $r=1$ at chip time k

$$\rho_0^d:=\mathrm{Tr}_{r\neq 0}(\rho_d)=\mathrm{Tr}_{r\neq 0}(|\Phi^d\rangle\langle\Phi^d|)$$

$$=\langle 0_1|\Phi^d\rangle\langle\Phi^d|0_1\rangle+\sum_{k=0}^{N_c-1}\langle 1_{1,\xi_k}|\Phi^d\rangle\langle\Phi^d|1_{1,\xi_k}\rangle. \tag{L.4}$$

The projection of $|\Phi^d\rangle$ with respect to $|0_1\rangle$ is

$$\langle 0_1|\Phi^d\rangle=\frac{1}{\sqrt{N_c}}\sum_{k=0}^{N_c-1}B_{00}\lambda_{0,k}\lambda_{0,k}\hat{a}^{\dagger}_{0,\xi_k}|0_0\rangle$$

$$=B_{00}\frac{1}{\sqrt{N_c}}\sum_{k=0}^{N_c-1}\lambda_{0,k}\lambda_{0,k}|1_{0,\xi_k}\rangle$$

$$=B_{00}|1_{0,\xi}\rangle \tag{L.5}$$

and the projection with respect to $|1_{1,\xi_k}\rangle$ is

$$\langle 1_{1,\xi_k}|\Phi^d\rangle=\frac{1}{\sqrt{N_c}}B_{10}\lambda_{0,k}\lambda_{1,k}|0_0\rangle. \tag{L.6}$$

Therefore

$$\rho_0^d=|B_{00}|^2|1_{0,\xi}\rangle\langle 1_{0,\xi}|+\sum_{k=0}^{N_c-1}\frac{1}{N_c}|B_{10}|^2|0_0\rangle\langle 0_0|$$

$$=|B_{10}|^2|0_0\rangle\langle 0_0|+|B_{00}|^2|1_{0,\xi}\rangle\langle 1_{0,\xi}| \tag{L.7}$$

where $|\psi_0\rangle=|1_{0,\xi}\rangle$ is the transmitted quantum signal by sender $s=0$. The term $|1_{0,\xi}\rangle\langle 1_{0,\xi}|$ in the aforementioned statistical mixture denotes that the single-photon quantum signal of transmitter $s=0$ is correctly recovered. In contrast, the term $|0_0\rangle\langle 0_0|$ stands for the inevitable loss induced by the broadcasting channel.

Since the evolution of the filter is represented by operator $\hat{\mathrm{H}}$, we may obtain the effect of filter using the following relation:

$$\rho_0^F=\hat{\mathrm{H}}\rho_0^d\hat{\mathrm{H}}^{\dagger}. \tag{L.8}$$

The transmitted signal through the filter can be obtained by taking the partial trace with respect to the filter's reflection. The basis for partial trace (with nonzero projection value) is $\{|0_{0,\mathrm{R}}\rangle,|1_{0,\mathrm{R},\xi_q}\rangle\}$. The two types of states $|0_{0,\mathrm{R}}\rangle$ and $|1_{0,\mathrm{R},\xi_q}\rangle$ denote the vacuum state and the single-photon state at time interval q in the reflected output port of the filter, respectively.

In order to obtain the state after the filter, we need to calculate the following partial trace:

$$\rho_0^{\mathrm{T}}=\mathrm{Tr}_{\mathrm{R}}(\rho_0^F) \tag{L.9}$$

$$=\langle 0_{0,\mathrm{R}}|\rho_0^F|0_{0,\mathrm{R}}\rangle+\sum_{q=0}^{\infty}\langle 1_{0,\mathrm{R},\xi_q}|\rho_0^F|1_{0,\mathrm{R},\xi_q}\rangle$$

$$=|B_{10}|^2\langle 0_{0,\mathrm{R}}|0_0\rangle\langle 0_0|0_{0,\mathrm{R}}\rangle \tag{L.10}$$

$$+|B_{00}|^2\langle 0_{0,\mathrm{R}}|\hat{\mathrm{H}}|1_{0,\xi}\rangle\langle 1_{0,\xi}|\hat{\mathrm{H}}^{\dagger}|0_{0,\mathrm{R}}\rangle \tag{L.11}$$

$$+\sum_{q=0}^{\infty}|B_{10}|^2\langle 1_{0,\mathrm{R},\xi_q}|0_0\rangle\langle 0_0|1_{0,\mathrm{R},\xi_q}\rangle \tag{L.12}$$

$$+\sum_{q=0}^{\infty}|B_{00}|^2\langle 1_{0,\mathrm{R},\xi_q}|\hat{\mathrm{H}}|1_{0,\xi}\rangle\langle 1_{0,\xi}|\hat{\mathrm{H}}^{\dagger}|1_{0,\mathrm{R},\xi_q}\rangle. \tag{L.13}$$

The projections of $|0\rangle$ with respect to the basis functions are

$$\langle 1_{0,\mathrm{R},\xi_q}|0\rangle = 0 \tag{L.14}$$

$$\langle 0_{0,\mathrm{R}}|0\rangle = |0_{0,\mathrm{T}}\rangle. \tag{L.15}$$

From Theorem 4, the correctly decoded single-photon quantum signal after the filter is

$$|1_{0,\xi^F}\rangle = \hat{\mathrm{H}}|1_{0,\xi}\rangle = \sum_{q=0}^{\infty}\left(D_q|1_{0,\mathrm{T},\xi_q}\rangle + F_q|1_{0,\mathrm{R},\xi_q}\rangle\right). \tag{L.16}$$

The projections of this quantum signal with respect to the basis functions are obtained as follows:

$$\langle 1_{0,\mathrm{R},\xi_k}|\hat{\mathrm{H}}|1_{0,\xi}\rangle = F_q|0_{0,\mathrm{T}}\rangle \tag{L.17}$$

$$\langle 0_{0,\mathrm{R}}|\hat{\mathrm{H}}|1_{0,\xi}\rangle = \sum_{q=0}^{\infty} D_q|1_{0,\mathrm{T},\xi_q}\rangle. \tag{L.18}$$

The transmitted state after the filter in case where the single photon has passed the filter is

$$|1_{0,\xi_\mathrm{T}}\rangle := \frac{1}{\sqrt{\sum_{q=0}^{\infty}|D_q|^2}}\sum_{q=0}^{\infty} D_q|1_{0,\mathrm{T},\xi_q}\rangle \tag{L.19}$$

which gives the following state at the receiver end:

$$\rho_0^{\mathrm{T}} = \left(|B_{10}|^2 + |B_{00}|^2\sum_{q=0}^{\infty}|F_q|^2\right)|0_{0,\mathrm{T}}\rangle\langle 0_{0,\mathrm{T}}| + |B_{00}|^2\left(\sum_{q=0}^{\infty}|D_q|^2\right)|1_{0,\xi_\mathrm{T}}\rangle\langle 1_{0,\xi_\mathrm{T}}|. \tag{L.20}$$

For a balanced star coupler, the chip-time photon statistics can be easily calculated

$$\mathbb{P}(n=0) = \frac{1}{2}\left(1 + \sum_{q=0}^{\infty}|F_q|^2\right) \tag{L.21}$$

$$\mathbb{P}(n_k=1) = \frac{1}{2}|D_q|^2 \tag{L.22}$$

which gives the overall photon statistics

$$\mathbb{P}(n=0) = \frac{1}{2}\left(1 + \sum_{q=0}^{\infty}|F_q|^2\right) = 1 - \frac{1}{2}\mathfrak{D} \tag{L.23}$$

$$\mathbb{P}(n=1) = \frac{1}{2}\sum_{k}|D_q|^2 = \frac{1}{2}\mathfrak{D}. \tag{L.24}$$

Similarly, when $s=1$ is transmitting single photons and $s=0$ is turned OFF, the following mixed state is obtained at the receiver of user $s=0$:

$$\rho_0^{\mathrm{T}} = \left(|B_{10}|^2 + |B_{00}|^2\sum_{q=0}^{\infty}|F_q^{0,1}|^2\right)|0_{0,\mathrm{T}}\rangle\langle 0_{0,\mathrm{T}}| + |B_{00}|^2\left(\sum_{q=0}^{\infty}|D_q^{0,1}|^2\right)|1_{0,\xi_\mathrm{T}}\rangle\langle 1_{0,\xi_\mathrm{T}}| \tag{L.25}$$

where

$$|1_{0,\xi_\mathrm{T}}\rangle = \frac{1}{\sqrt{\sum_{q=0}^{\infty}|D_q^{0,1}|^2}}\sum_{q=0}^{\infty} D_q^{0,1}|1_{0,\mathrm{T},\xi_q}\rangle \tag{L.26}$$

Also

$$\mathbb{P}(n_0=0) = 1 - \frac{1}{2}\mathfrak{D}^{0,1} \tag{L.27}$$

$$\mathbb{P}(n_0=1) = \frac{1}{2}\mathfrak{D}^{0,1} \tag{L.28}$$

where $\mathfrak{D}^{0,1} = \sum_{q=0}^{\infty}|D_q^{0,1}|^2$.

B. TWO USERS

Assume that transmitters $\mathcal{S}=\{0,1\}$ are transmitting single photons simultaneously. Using Proposition 15, we have

$$|\Phi^d\rangle = \prod_{s=0}^{1}\left(\frac{1}{\sqrt{N_c}}\sum_{k=0}^{N_c-1}\sum_{r=0}^{1}B_{rs}\lambda_{s,k}\lambda_{r,k}\hat{a}_{r,\xi_k}^{\dagger}\right)|0\rangle. \tag{L.29}$$

The state $|\Phi^d\rangle$ can be expressed in terms of the chip-time number states as follows:

$$\begin{aligned}|\Phi^d\rangle &= \frac{1}{N_c}\left(\sum_{k_0=0}^{N_c-1}B_{00}|1_{0,\xi_{k_0}}\rangle\right)\left(\sum_{k_1=0}^{N_c-1}B_{01}\lambda_{0,k_1}\lambda_{1,k_1}|1_{0,\xi_{k_1}}\rangle\right)\\ &+ \frac{1}{N_c}\left(\sum_{k_1=0}^{N_c-1}B_{11}|1_{1,\xi_{k_1}}\rangle\right)\left(\sum_{k_0=0}^{N_c-1}B_{10}\lambda_{1,k_0}\lambda_{0,k_0}|1_{1,\xi_{k_0}}\rangle\right)\\ &+ \frac{1}{N_c}\left(\sum_{k_0=0}^{N_c-1}\sum_{k_1=0}^{N_c-1}\left(B_{00}B_{11}|1_{0,\xi_{k_0}}\rangle|1_{1,\xi_{k_1}}\rangle\right.\right.\\ &\left.\left.+ B_{01}B_{10}\lambda_{0,k_1}\lambda_{1,k_1}\lambda_{0,k_0}\lambda_{1,k_0}|1_{0,\xi_{k_0}}\rangle|1_{1,\xi_{k_1}}\rangle\right)\right).\end{aligned} \tag{L.30}$$

For a balanced star coupler, we have

$$\begin{aligned}|\Phi^d\rangle\Big|_{M=2,\text{balanced}} &= \frac{1}{2N_c}\left(\sum_{k_0=0}^{N_c-1}|1_{0,\xi_{k_0}}\rangle\right)\left(\sum_{k_1=0}^{N_c-1}\lambda_{0,k_1}\lambda_{1,k_1}|1_{0,\xi_{k_1}}\rangle\right)\\ &- \frac{1}{2N_c}\left(\sum_{k_1=0}^{N_c-1}|1_{1,\xi_{k_1}}\rangle\right)\left(\sum_{k_0=0}^{N_c-1}\lambda_{1,k_0}\lambda_{0,k_0}|1_{1,\xi_{k_0}}\rangle\right)\\ &+ \frac{1}{2N_c}\left(\sum_{k_0=0}^{N_c-1}\sum_{k_1=0}^{N_c-1}\left((1-\lambda_{0,k_0}\lambda_{1,k_0}\lambda_{0,k_1}\lambda_{1,k_1})\right.\right.\\ &\left.\left.\times\ |1_{0,\xi_{k_0}}\rangle|1_{1,\xi_{k_1}}\rangle\right)\right).\end{aligned} \tag{L.31}$$

The last term in summation is zero for $k_0 = k_1$, which gives the spread-spectrum Hong–Ou–Mandel effect. That is, the state $|1_{0,\xi_k}\rangle|1_{1,\xi_k}\rangle$ never appears in the output of the balanced star coupler for spread-spectrum single-photon inputs when two users are simultaneously transmitting information.

The overall density matrix is

$$\rho_d = |\Phi^d\rangle\langle\Phi^d|. \tag{L.32}$$

Basis vectors for the Hilbert space of $r \neq 0$ are of the form $\{|0_1\rangle, |1_{1,\xi_k}\rangle, |2_{1,\xi_k}\rangle, |1_{1,\xi_{k_0}}\rangle|1_{1,\xi_{k_1}}\rangle (k_0 < k_1)\}$. Then, we calculate the partial projections with respect to the basis vectors. The projection of Φ^d with respect to $|0_1\rangle$ is

$$\langle 0_1|\Phi^d\rangle\langle\Phi^d|0_1\rangle = \frac{1}{4}|1_{0,\xi}\rangle|1_{0,\xi^{e_1d_0}}\rangle\langle 1_{0,\xi^{e_1d_0}}|\langle 1_{0,\xi}|. \tag{L.33}$$

The product form of $|1_{0,\xi}\rangle|1_{0,\xi^{e_1d_0}}\rangle$ is not normalized. Therefore, we need to obtain the normalization factor. First, we express the chip-time interval decomposition of this quantum signal

$$\begin{aligned}|1_{0,\xi}\rangle|1_{0,\xi^{e_1d_0}}\rangle &:= \left(\frac{1}{\sqrt{N_c}}\sum_{k_0=0}^{N_c-1}|1_{0,\xi_{k_0}}\rangle\right) \\ &\quad\times\left(\frac{1}{\sqrt{N_c}}\sum_{k_1=0}^{N_c-1}\lambda_{1,k_1}\lambda_{0,k_1}|1_{0,\xi_{k_1}}\rangle\right) \qquad \text{(L.34)}\\ &= \frac{1}{N_c}\left(\sum_{\substack{k_0=0\\ \text{s.t.}k_0\neq k_1}}^{N_c-1}\sum_{k_1=0}^{N_c-1}\lambda_{1,k_1}\lambda_{0,k_1}|1_{0,\xi_{k_0}}\rangle|1_{0,\xi_{k_1}}\rangle\right) \\ &\quad+\frac{1}{N_c}\sum_{k=0}^{N_c-1}\lambda_{1,k}\lambda_{0,k}\sqrt{2}|2_{0,\xi_k}\rangle \qquad \text{(L.35)}\\ &= \frac{1}{N_c}\left(\sum_{\substack{k_0=0\\ \text{s.t.}k_0<k_1}}^{N_c-1}\sum_{k_1=0}^{N_c-1}(\lambda_{1,k_0}\lambda_{0,k_0}+\lambda_{1,k_1}\lambda_{0,k_1})|1_{0,\xi_{k_0}}\rangle|1_{0,\xi_{k_1}}\rangle\right) \\ &\quad+\frac{1}{N_c}\sum_{k=0}^{N_c-1}\lambda_{1,k}\lambda_{0,k}\sqrt{2}|2_{0,\xi_k}\rangle. \qquad \text{(L.36)}\end{aligned}$$

Therefore

$$\begin{aligned}\mathcal{C}_{(1+1)} &:= \|\frac{1}{2}|1_{0,\xi}\rangle|1_{0,\xi^{e_1d_0}}\rangle\|^2 \qquad \text{(L.37)}\\ &= \frac{1}{4N_c^2}\left(\sum_{\substack{k_0=0\\ \text{s.t.}k_0<k_1}}^{N_c-1}\sum_{k_1=0}^{N_c-1}(\lambda_{1,k_0}\lambda_{0,k_0}+\lambda_{1,k_1}\lambda_{0,k_1})^2\right) \\ &\quad+\frac{1}{4N_c^2}\sum_{k=0}^{N_c-1}(\lambda_{1,k}\lambda_{0,k}\sqrt{2})^2 \\ &= \frac{1}{4N_c^2}\left(\sum_{\substack{k_0=0\\ \text{s.t.}k_0<k_1}}^{N_c-1}\sum_{k_1=0}^{N_c-1}(2+2\lambda_{1,k_0}\lambda_{0,k_0}\lambda_{1,k_1}\lambda_{0,k_1})\right) \\ &\quad+\frac{1}{4N_c^2}2N_c \\ &= \frac{1}{4N_c^2}2\frac{N_c(N_c-1)}{2}+\frac{1}{2N_c^2}N_c \\ &\quad+\frac{1}{4N_c^2}\sum_{\substack{k_0=0\\ \text{s.t.}k_0\neq k_1}}^{N_c-1}\sum_{k_1=0}^{N_c-1}(\lambda_{1,k_0}\lambda_{0,k_0}\lambda_{1,k_1}\lambda_{0,k_1}) \\ &\quad+\frac{1}{4N_c^2}\underbrace{\sum_{k=0}^{N_c-1}(\lambda_{1,k}\lambda_{0,k}\lambda_{1,k}\lambda_{0,k})}_{N_c}-\frac{1}{4N_c^2}N_c \\ &= \frac{1}{4N_c^2}2\frac{N_c(N_c-1)}{2}+\frac{1}{2N_c^2}N_c-\frac{1}{4N_c^2}N_c \\ &\quad+\frac{1}{4N_c^2}\sum_{k_0=0}^{N_c-1}\sum_{k_1=0}^{N_c-1}(\lambda_{1,k_0}\lambda_{0,k_0}\lambda_{1,k_1}\lambda_{0,k_1}) \\ &= \frac{1}{4}\left(1+\left(\frac{1}{N_c}\sum_{k_0=0}^{N_c-1}\lambda_{1,k_0}\lambda_{0,k_0}\right)\left(\frac{1}{N_c}\sum_{k_1=0}^{N_c-1}\lambda_{1,k_1}\lambda_{0,k_1}\right)\right) \\ &= \frac{1}{4}\left(1+|\langle\Lambda_0|\Lambda_1\rangle|^2\right). \qquad \text{(L.38)}\end{aligned}$$

We may define the normalized state corresponding to $\frac{1}{2}|1_{0,\xi}\rangle|1_{0,\xi^{e_1d_0}}\rangle$ as

$$\begin{aligned}|(1+1)_{0,e_1d_0}\rangle &:= \frac{1}{2}(\mathcal{C}_{(1+1)})^{-\frac{1}{2}}\hat{a}^\dagger_{\xi}\hat{a}^\dagger_{\xi^{e_1d_0}}|0\rangle \qquad \text{(L.39)}\\ &= \frac{1}{2}(\mathcal{C}_{(1+1)})^{-\frac{1}{2}}|1_{0,\xi}\rangle|1_{0,\xi^{e_1d_0}}\rangle. \qquad \text{(L.40)}\end{aligned}$$

Therefore, the projection of Φ^d with respect to $|0_1\rangle$ is further simplified as

$$\langle 0_1|\Phi^d\rangle\langle\Phi^d|0_1\rangle = \mathcal{C}_{(1+1)}|(1+1)_{0,e_1d_0}\rangle\langle(1+1)_{0,e_1d_0}|. \tag{L.41}$$

This part of the received mixed quantum signal corresponds to the case where both transmitted photons arrive at receiver 0 (with probability $|B_{00}B_{01}|^2 = \frac{1}{4}$).

The projection of Φ^d on $|1_{1,\xi_k}\rangle$ is calculated as follows:

$$\begin{aligned}\langle 1_{1,\xi_k}|\Phi^d\rangle &= \frac{1}{2N_c}\langle 1_{1,\xi_k}|\left(\sum_{k_0=0}^{N_c-1}\sum_{k_1=0}^{N_c-1}\right. \qquad \text{(L.42)}\\ &\qquad\left.\left((1-\lambda_{0,k_0}\lambda_{1,k_0}\lambda_{0,k_1}\lambda_{1,k_1})|1_{0,\xi_{k_0}}\rangle|1_{1,\xi_{k_1}}\rangle\right)\right) \\ &= \frac{1}{2N_c}\langle 1_{1,\xi_k}|\left(\sum_{k_0=0}^{N_c-1}(1-\lambda_{0,k_0}\lambda_{1,k_0}\lambda_{0,k}\lambda_{1,k})|1_{0,\xi_{k_0}}\rangle|1_{1,\xi_k}\rangle\right. \\ &\qquad\text{(L.43)}\end{aligned}$$

$$+\sum_{\substack{k_0=0\\k_1\neq k}}^{N_c-1}\sum_{k_1=0}^{N_c-1}\left((1-\lambda_{0,k_0}\lambda_{1,k_0}\lambda_{0,k_1}\lambda_{1,k_1})|1_{0,\xi_{k_0}}\rangle|1_{1,\xi_{k_1}}\rangle\right)\Bigg)$$

$$=\frac{1}{2N_c}\left(\sum_{k_0=0}^{N_c-1}(1-\lambda_{0,k_0}\lambda_{1,k_0}\lambda_{0,k}\lambda_{1,k})|1_{0,\xi_{k_0}}\rangle\underbrace{\langle 1_{1,\xi_k}|1_{1,\xi_k}\rangle}_{1}\right. \tag{L.44}$$

$$\left.+\sum_{\substack{k_0=0\\k_1\neq k}}^{N_c-1}\sum_{k_1=0}^{N_c-1}\left((1-\lambda_{0,k_0}\lambda_{1,k_0}\lambda_{0,k_1}\lambda_{1,k_1})|1_{0,\xi_{k_0}}\rangle\underbrace{\langle 1_{1,\xi_k}|1_{1,\xi_{k_1}}\rangle}_{0}\right)\right)$$

$$=\frac{1}{2N_c}\sum_{k_0=0}^{N_c-1}(1-\lambda_{0,k_0}\lambda_{1,k_0}\lambda_{0,k}\lambda_{1,k})|1_{0,\xi_{k_0}}\rangle. \tag{L.45}$$

Again, the norm of the aforementioned equation is not one, and we should find the normalization factor

$$\begin{aligned}\mathcal{C}_{1_k}&:=\|\langle 1_{1,\xi_k}|\Phi^d\rangle\|^2\\&=\frac{1}{4N_c^2}\sum_{k_0=0}^{N_c-1}|1-\lambda_{0,k_0}\lambda_{1,k_0}\lambda_{0,k}\lambda_{1,k}|^2\\&=\frac{1}{4N_c^2}\sum_{k_0=0}^{N_c-1}\left(2-2\lambda_{0,k_0}\lambda_{1,k_0}\lambda_{0,k}\lambda_{1,k}\right)\\&=\frac{1}{2N_c}\left(1-\frac{\lambda_{0,k}\lambda_{1,k}}{N_c}\sum_{k_0=0}^{N_c-1}\lambda_{0,k_0}\lambda_{1,k_0}\right)\\&=\frac{1}{2N_c}\left(1-\lambda_{0,k}\lambda_{1,k}\langle\Lambda_0|\Lambda_1\rangle\right).\end{aligned} \tag{L.46}$$

Next, we define the normalized state as

$$\begin{aligned}|1_{0,e_1d_0,k}\rangle&:=\frac{(\mathcal{C}_{1_k})^{-\frac{1}{2}}}{2N_c}\sum_{k_0=0}^{N_c-1}(1-\lambda_{0,k_0}\lambda_{1,k_0}\lambda_{0,k}\lambda_{1,k})|1_{0,\xi_{k_0}}\rangle\\&=\frac{(\mathcal{C}_{1_k})^{-\frac{1}{2}}}{2\sqrt{N_c}}\frac{1}{\sqrt{N_c}}\sum_{k_0=0}^{N_c-1}|1_{0,\xi_{k_0}}\rangle \qquad \text{(L.47)}\\&\quad-\frac{(\mathcal{C}_{1_k})^{-\frac{1}{2}}}{2\sqrt{N_c}}\lambda_{0,k}\lambda_{1,k}\frac{1}{\sqrt{N_c}}\sum_{k_0=0}^{N_c-1}\lambda_{0,k_0}\lambda_{1,k_0}|1_{0,\xi_{k_0}}\rangle\\&=\frac{(\mathcal{C}_{1_k})^{-\frac{1}{2}}}{2\sqrt{N_c}}\left(|1_{0,\xi}\rangle-\lambda_{0,k}\lambda_{1,k}|1_{0,\xi^{e_1d_0}}\rangle\right) \qquad \text{(L.48)}\\&=\frac{|1_{0,\xi}\rangle-\lambda_{0,k}\lambda_{1,k}|1_{0,\xi^{e_1d_0}}\rangle}{\sqrt{2(1-\lambda_{0,k}\lambda_{1,k}\langle\Lambda_0|\Lambda_1\rangle)}} \qquad \text{(L.49)}\end{aligned}$$

which is the superposition of the original signal and the multiple access interference signal.

The projection of Φ^d on $|1_{1,\xi_{k_0}}\rangle|1_{1,\xi_{k_1}}\rangle$ with $k_0<k_1$ is calculated as follows:

$$\begin{aligned}&(\langle 1_{1,\xi_{k_1}}|\langle 1_{1,\xi_{k_0}}|)|\Phi^d\rangle\\&=(\langle 1_{1,\xi_{k_1}}|\langle 1_{1,\xi_{k_0}}|)-\frac{1}{2N_c}\left(\sum_{k_1'=0}^{N_c-1}|1_{1,\xi_{k_1'}}\rangle\right)\\&\quad\times\left(\sum_{k_0'=0}^{N_c-1}\lambda_{1,k_0'}\lambda_{0,k_0'}|1_{1,\xi_{k_0'}}\rangle\right)\\&=-\frac{1}{2N_c}(\langle 1_{1,\xi_{k_1}}|\langle 1_{1,\xi_{k_0}}|)\\&\quad\times\left(|1_{1,\xi_{k_0}}\rangle+|1_{1,\xi_{k_1}}\rangle+\sum_{\substack{k_1'=0\\\text{s.t.}k_1'\neq k_0,k_1}}^{N_c-1}|1_{1,\xi_{k_1'}}\rangle\right)\\&\quad\times\left(\lambda_{1,k_0}\lambda_{0,k_0}|1_{1,\xi_{k_0}}\rangle+\lambda_{1,k_1}\lambda_{0,k_1}|1_{1,\xi_{k_1}}\rangle\right.\\&\quad\left.+\sum_{\substack{k_0'=0\\\text{s.t.}k_0'\neq k_0,k_1}}^{N_c-1}\lambda_{1,k_0'}\lambda_{0,k_0'}|1_{1,\xi_{k_0'}}\rangle\right)\\&=-\frac{1}{2N_c}(\lambda_{0,k_0}\lambda_{1,k_0}+\lambda_{0,k_1}\lambda_{1,k_1})|0_0\rangle.\end{aligned} \tag{L.50}$$

Therefore

$$\begin{aligned}&(\langle 1_{1,\xi_{k_1}}|\langle 1_{1,\xi_{k_0}}|)|\Phi^d\rangle\langle\Phi^d|(|1_{1,\xi_{k_0}}\rangle|1_{1,\xi_{k_1}}\rangle)\\&=\frac{1}{4N_c^2}\left|\lambda_{0,k_0}\lambda_{1,k_0}+\lambda_{0,k_1}\lambda_{1,k_1}\right|^2|0_0\rangle\langle 0_0|\\&=\frac{1}{2N_c^2}\left(1+\lambda_{0,k_0}\lambda_{1,k_0}\lambda_{0,k_1}\lambda_{1,k_1}\right)|0_0\rangle\langle 0_0|.\end{aligned} \tag{L.51}$$

The projection of Φ^d on $|2_{1,\xi_k}\rangle$ is

$$\begin{aligned}&\langle 2_{1,\xi_k}|\Phi^d\rangle\\&=-\frac{1}{2N_c}\langle 2_{1,\xi_k}|\left(\sum_{k_1'=0}^{N_c-1}|1_{1,\xi_{k_1'}}\rangle\right)\\&\quad\times\left(\sum_{k_0'=0}^{N_c-1}\lambda_{1,k_0'}\lambda_{0,k_0'}|1_{1,\xi_{k_0'}}\rangle\right)\\&=-\frac{1}{2N_c}\langle 2_{1,\xi_k}|\left(|1_{1,\xi_k}\rangle+\sum_{\substack{k_1'=0\\\text{s.t.}k_1'\neq k}}^{N_c-1}|1_{1,\xi_{k_1'}}\rangle\right)\\&\quad\times\left(\lambda_{1,k}\lambda_{0,k}|1_{1,\xi_k}\rangle+\sum_{\substack{k_1'=0\\\text{s.t.}k_1'\neq k}}^{N_c-1}\lambda_{1,k_1'}\lambda_{0,k_1'}|1_{1,\xi_{k_1'}}\rangle\right)\end{aligned}$$

$$= -\frac{1}{2N_c}\lambda_{1,k}\lambda_{0,k}\sqrt{2}\left|2_{1,\xi_k}\right|\rangle$$
$$= -\frac{1}{2N_c}\lambda_{1,k}\lambda_{0,k}\sqrt{2}|0_0\rangle. \tag{L.52}$$

Therefore

$$\left\langle 2_{1,\xi_k}|\Phi^d\right\rangle\left\langle\Phi^d|2_{1,\xi_k}\right\rangle = \frac{1}{2N_c^2}|0_0\rangle\langle 0_0| \tag{L.53}$$

From (L.51) and (L.53), the coefficient of $|0_0\rangle\langle 0_0|$ is

$$\begin{aligned}\mathcal{C}_0 :=& \frac{1}{2N_c^2}\sum_{\substack{k_0=0\\ \text{s.t.}k_0<k_1}}^{N_c-1}\sum_{k_1=0}^{N_c-1}(1+\lambda_{0,k_0}\lambda_{1,k_0}\lambda_{0,k_1}\lambda_{1,k_1})\\ &+\sum_{k=0}^{N_c-1}\frac{1}{2N_c^2}\\ =& \frac{1}{4N_c^2}\sum_{\substack{k_0=0\\ \text{s.t.}k_0\neq k_1}}^{N_c-1}\sum_{k_1=0}^{N_c-1}(1+\lambda_{0,k_0}\lambda_{1,k_0}\lambda_{0,k_1}\lambda_{1,k_1})\\ &+\frac{1}{4N_c^2}\underbrace{\sum_{k=0}^{N_c-1}(\lambda_{1,k}\lambda_{0,k}\lambda_{1,k}\lambda_{0,k})}_{N_c}-\frac{1}{4N_c}+\frac{1}{2N_c}\\ =& \frac{1}{4N_c^2}N_c(N_c-1)+\frac{1}{4N_c}+\frac{1}{4}\left|\langle\Lambda_0|\Lambda_1\rangle\right|^2\\ =& \frac{1}{4}+\frac{1}{4}\left|\langle\Lambda_0|\Lambda_1\rangle\right|^2\\ =& \frac{1}{4}\left(1+\left|\langle\Lambda_0|\Lambda_1\rangle\right|^2\right) \qquad \text{(L.54)}\\ =& \mathcal{C}_{(1+1)}. \qquad \text{(L.55)}\end{aligned}$$

The overall received quantum signal is

$$\begin{aligned}\rho_0^d =& \mathcal{C}_{(1+1)}|(1+1)_{0,e_1d_0}\rangle\langle(1+1)_{0,e_1d_0}| \qquad \text{(L.56)}\\ &+\sum_{k=0}^{N_c-1}\mathcal{C}_{1_k}|1_{0,e_1d_0,k}\rangle\langle 1_{0,e_1d_0,k}|+\mathcal{C}_0|0_0\rangle\langle 0_0|\\ =& \frac{1}{4}\left(1+\left|\langle\Lambda_0|\Lambda_1\rangle\right|^2\right)|(1+1)_{0,e_1d_0}\rangle\langle(1+1)_{0,e_1d_0}|\\ &+\frac{1}{4}\left(1+\left|\langle\Lambda_0|\Lambda_1\rangle\right|^2\right)|0_0\rangle\langle 0_0|\\ &+\frac{1}{2N_c}\sum_{k=0}^{N_c-1}\left(1-\lambda_{0,k}\lambda_{1,k}\left\langle\Lambda_0|\Lambda_1\right\rangle\right)|1_{0,e_1d_0,k}\rangle\langle 1_{0,e_1d_0,k}|. \qquad \text{(L.57)}\end{aligned}$$

For random (approximately orthogonal) codes, $\langle\Lambda_0|\Lambda_1\rangle \approx 0$; therefore, $\mathcal{C}_{(1+1)} = \mathcal{C}_0 \approx \frac{1}{4}$ and $\mathcal{C}_{1_k} \approx \frac{1}{2N_c}$. Consequently

$$\begin{aligned}\rho_0^d \approx& \frac{1}{4}|(1+1)_{0,e_1d_0}\rangle\langle(1+1)_{0,e_1d_0}|+\frac{1}{4}|0_0\rangle\langle 0_0|\\ &+\frac{1}{2N_c}\sum_{k=0}^{N_c-1}|1_{0,e_1d_0,k}\rangle\langle 1_{0,e_1d_0,k}|. \qquad \text{(L.58)}\end{aligned}$$

For similar codes $\Lambda_0 = \Lambda_1$, $\mathcal{C}_{(1+1)} = \mathcal{C}_0 = \frac{1}{2}$, $\mathcal{C}_{1_k} = 0$, and $|(1+1)_{0,e_1d_0}\rangle = |2_0\rangle$. Therefore, the density matrix (L.56), due to the Hong–Ou–Mandel interference, reduces to

$$\rho_0^d = \frac{1}{2}|2_0\rangle\langle 2_0|+\frac{1}{2}|0_0\rangle\langle 0_0|. \tag{L.59}$$

Next, we apply the filter to ρ^d, and then, we take the trace with respect to the reflected signals. The states $|1_{0,e_1d_0,k}\rangle$ correspond to the case when only a single photon arrives at the receiver; therefore, the derivation is similar to the single-photon transmitter in (L.20). Therefore, utilizing Theorem 4 and Proposition 9 for (L.48), we may write

$$\begin{aligned}&\hat{\mathrm{H}}|1_{0,e_1d_0,k}\rangle\\ &= \frac{(\mathcal{C}_{1_k})^{-\frac{1}{2}}}{2\sqrt{N_c}}\left(\hat{\mathrm{H}}|1_{0,\xi}\rangle-\lambda_{0,k}\lambda_{1,k}\hat{\mathrm{H}}|1_{0,\xi^{e_1d_0}}\rangle\right)\\ &= \frac{(\mathcal{C}_{1_k})^{-\frac{1}{2}}}{2\sqrt{N_c}}\Bigg(\sum_{q=0}^{\infty}\left(D_q|1_{0,\mathrm{T},\xi_q}\rangle+F_q|1_{0,\mathrm{R},\xi_q}\rangle\right)\\ &\quad-\lambda_{0,k}\lambda_{1,k}\sum_{q=0}^{\infty}\left(D_q^{0,1}|1_{0,\mathrm{T},\xi_q}\rangle+F_q^{0,1}|1_{0,\mathrm{R},\xi_q}\rangle\right)\Bigg).\end{aligned}$$

The projection with respect to $|0_{0,\mathrm{R}}\rangle$ is

$$\begin{aligned}&(\mathcal{C}_{1_k})^{\frac{1}{2}}\langle 0_{0,\mathrm{R}}|\hat{\mathrm{H}}|1_{0,e_1d_0,k}\rangle\\ &= \frac{1}{2\sqrt{N_c}}\left(\sum_{q=0}^{\infty}D_q|1_{0,\mathrm{T},\xi_q}\rangle-\lambda_{0,k}\lambda_{1,k}\sum_{q=0}^{\infty}D_q^{0,1}|1_{0,\mathrm{T},\xi_q}\rangle\right).\end{aligned} \tag{L.60}$$

We define the normalized state as

$$\begin{aligned}&|1_{0,\mathrm{T},e_1d_0,k}\rangle\\ &:= \left(\mathcal{C}_{D,1_k}\right)^{-\frac{1}{2}}\times\Bigg(\sum_{q=0}^{\infty}D_q|1_{0,\mathrm{T},\xi_q}\rangle\\ &\quad-\lambda_{0,k}\lambda_{1,k}\sum_{q=0}^{\infty}D_q^{0,1}|1_{0,\mathrm{T},\xi_q}\rangle\Bigg) \qquad \text{(L.61)}\\ &= \left(\mathcal{C}_{D,1_k}\right)^{-\frac{1}{2}}\times\Bigg[\left(\sum_{q=0}^{\infty}|D_q|^2\right)^{\frac{1}{2}}|1_{0,\xi_{\mathrm{T}}}\rangle\\ &\quad-\lambda_{0,k}\lambda_{1,k}\left(\sum_{q=0}^{\infty}|D_q^{0,1}|^2\right)^{\frac{1}{2}}|1_{0,\xi_{\mathrm{T}}^{e_1d_0}}\rangle\Bigg] \qquad \text{(L.62)}\end{aligned}$$

where the corresponding normalization coefficient is

$$\mathcal{C}_{D,1_k} := \frac{1}{4N_c}\sum_{q=0}^{\infty}|D_q-\lambda_{0,k}\lambda_{1,k}D_q^{0,1}|^2. \tag{L.63}$$

The projection with respect to $|1_{0,\mathrm{R},\xi_q}\rangle$ is

$$(\mathcal{C}_{1_k})^{\frac{1}{2}}\langle 1_{0,\mathrm{R},\xi_q}|\hat{\mathrm{H}}|1_{0,e_1d_0,k}\rangle = \frac{1}{2\sqrt{N_c}}(F_q - \lambda_{0,k}\lambda_{1,k}F_q^{0,1})|0_{0,\mathrm{T}}\rangle. \tag{L.64}$$

We define the following coefficient to simplify the terms involving $|0_{0,\mathrm{T}}\rangle\langle 0_{0,\mathrm{T}}|$:

$$\mathcal{C}_{F,0_k} := \frac{1}{4N_c}\sum_{q=0}^{\infty}|F_q - \lambda_{0,k}\lambda_{1,k}F_q^{0,1}|^2. \tag{L.65}$$

Therefore

$$\begin{aligned}&\mathrm{Tr}_{\mathrm{R}}(\mathcal{C}_{1_k}\hat{\mathrm{H}}|1_{0,e_1d_0,k}\rangle\langle 1_{0,e_1d_0,k}|\hat{\mathrm{H}}^\dagger)\\ &= \mathcal{C}_{1_k}\langle 0_{0,\mathrm{R}}|\hat{\mathrm{H}}|1_{0,e_1d_0,k}\rangle\langle 1_{0,e_1d_0,k}|\hat{\mathrm{H}}^\dagger|0_{0,\mathrm{R}}\rangle\\ &\quad + \mathcal{C}_{1_k}\sum_{q=0}^{\infty}\langle 1_{0,\mathrm{R},\xi_q}|\hat{\mathrm{H}}|1_{0,e_1d_0,k}\rangle\langle 1_{0,e_1d_0,k}|\hat{\mathrm{H}}^\dagger|1_{0,\mathrm{R},\xi_q}\rangle\\ &= \mathcal{C}_{F,0_k}|0_{0,\mathrm{T}}\rangle\langle 0_{0,\mathrm{T}}| + \mathcal{C}_{D,1_k}|1_{0,\mathrm{T},e_1d_0,k}\rangle\langle 1_{0,\mathrm{T},e_1d_0,k}|.\end{aligned} \tag{L.66}$$

Using Theorem 4 and Proposition 9, the effect of filter on the two-photon state of (L.40) is obtained as

$$\begin{aligned}&(\mathcal{C}_{(1+1)})^{\frac{1}{2}}\hat{\mathrm{H}}|(1+1)_{0,e_1d_0}\rangle\\ &= \frac{1}{2}\left(\sum_{q_0=0}^{\infty}(D_{q_0}|1_{0,\mathrm{T},\xi_{q_0}}\rangle + F_{q_0}|1_{0,\mathrm{R},\xi_{q_0}}\rangle)\right)\\ &\quad\times\left(\sum_{q_1=0}^{\infty}(D_{q_1}^{0,1}|1_{0,\mathrm{T},\xi_{q_1}}\rangle + F_{q_1}^{0,1}|1_{0,\mathrm{R},\xi_{q_1}}\rangle)\right).\end{aligned} \tag{L.67}$$

When we have two photons at the receiver, the basis for partial trace (with nonzero projection value) is $\{|0_{0,\mathrm{R}}\rangle, |1_{0,\mathrm{R},\xi_q}\rangle, |2_{0,\mathrm{R},\xi_q}\rangle, |1_{0,\mathrm{R},\xi_{q_0}}\rangle|1_{0,\mathrm{R},\xi_{q_1}}\rangle(q_0 < q_1)\}$.

In order to obtain the quantum signal corresponding to $\hat{\mathrm{H}}|(1+1)_{0,e_1d_0}\rangle$ after the filter, we need to compute $\mathrm{Tr}_{\mathrm{R}}(\hat{\mathrm{H}}|(1+1)_{0,e_1d_0}\rangle\langle(1+1)_{0,e_1d_0}|\hat{\mathrm{H}}^\dagger)$. The projection of $\hat{\mathrm{H}}|(1+1)_{0,e_1d_0}\rangle$ with respect to $|0_{0,\mathrm{R}}\rangle$ is

$$\begin{aligned}&(\mathcal{C}_{(1+1)})^{\frac{1}{2}}\langle 0_{0,\mathrm{R}}|\hat{\mathrm{H}}|(1+1)_{0,e_1d_0}\rangle =\\ &= \frac{1}{2}\left(\sum_{q_0=0}^{\infty}D_{q_0}|1_{0,\mathrm{T},\xi_{q_0}}\rangle\right)\left(\sum_{q_1=0}^{\infty}D_{q_1}^{0,1}|1_{0,\mathrm{T},\xi_{q_1}}\rangle\right)\\ &= \frac{1}{2}\sum_{\substack{q_1=0\\ \text{s.t. } q_1>q_0}}^{\infty}\sum_{q_0=0}^{\infty}(D_{q_0}^{0,1}D_{q_1} + D_{q_0}D_{q_1}^{0,1})|1_{0,\mathrm{T},\xi_{q_0}}\rangle|1_{0,\mathrm{T},\xi_{q_1}}\rangle\\ &\quad + \frac{1}{2}\sum_{q=0}^{\infty}\sqrt{2}D_qD_q^{0,1}|2_{0,\mathrm{T},\xi_q}\rangle\end{aligned} \tag{L.68, L.69}$$

which corresponds to the case where two photons have arrived at receiver $r = 0$ and both have passed through the filter. The norm of the aforementioned expression is

$$\begin{aligned}\mathcal{C}_{DD} &:= \frac{1}{4}\sum_{\substack{q_1=0\\ \text{s.t. } q_1>q_0}}^{\infty}\sum_{q_0=0}^{\infty}|D_{q_0}^{0,1}D_{q_1} + D_{q_0}D_{q_1}^{0,1}|^2\\ &\quad + \frac{1}{4}2\sum_{q_0=0}^{\infty}|D_{q_0}D_{q_0}^{0,1}|^2.\end{aligned} \tag{L.70}$$

We obtain the normalized transmitted two-photon state as

$$\begin{aligned}&|(1+1)_{0,\mathrm{T},e_1d_0}\rangle\\ &:= \frac{1}{2}(\mathcal{C}_{DD})^{-\frac{1}{2}}\\ &\quad\times\left(\sum_{q_0=0}^{\infty}D_{q_0}|1_{0,\mathrm{T},\xi_{q_0}}\rangle\right)\left(\sum_{q_1=0}^{\infty}D_{q_1}^{0,1}|1_{0,\mathrm{T},\xi_{q_1}}\rangle\right)\end{aligned} \tag{L.71}$$

$$\begin{aligned}&= (\mathcal{C}_{DD})^{-\frac{1}{2}}\left(\sum_{q_0=0}^{\infty}|D_{q_0}|^2\right)^{\frac{1}{2}}\left(\sum_{q_0=0}^{\infty}|D_{q_0}^{0,1}|^2\right)^{\frac{1}{2}}\\ &\quad\times|1_{0,\xi_{\mathrm{T}}}\rangle|1_{0,\xi_{\mathrm{T}}^{e_1d_0}}\rangle.\end{aligned} \tag{L.72}$$

Hence

$$(\mathcal{C}_{(1+1)})^{\frac{1}{2}}\langle 0_{0,\mathrm{R}}|\hat{\mathrm{H}}|(1+1)_{0,e_1d_0}\rangle = (\mathcal{C}_{DD})^{\frac{1}{2}}|(1+1)_{0,\mathrm{T},e_1d_0}\rangle. \tag{L.73}$$

Another term in the expression of the partial trace is the projection of (L.67) with respect to $|1_{0,\mathrm{R},\xi_q}\rangle$

$$\begin{aligned}&(\mathcal{C}_{(1+1)})^{\frac{1}{2}}\langle *|1_{0,\mathrm{R},\xi_q}\hat{\mathrm{H}}|(1+1)_{0,e_1d_0}\rangle\\ &= \frac{1}{2}F_q^{0,1}\sum_{q_0=0}^{\infty}D_{q_0}|1_{0,\mathrm{T},\xi_{q_0}}\rangle + \frac{1}{2}F_q\sum_{q_1=0}^{\infty}D_{q_1}^{0,1}|1_{0,\mathrm{T},\xi_{q_1}}\rangle\\ &= \frac{1}{2}\sum_{q_0=0}^{\infty}(F_q^{0,1}D_{q_0} + F_qD_{q_0}^{0,1})|1_{0,\mathrm{T},\xi_{q_0}}\rangle\end{aligned} \tag{L.74}$$

which corresponds to the case where two photons have arrived at receiver $r = 0$ and only one has passed through the filter. The norm of the aforementioned expression is obtained as

$$\mathcal{C}_{F_qD} := \frac{1}{4}\sum_{q_0=0}^{\infty}|F_q^{0,1}D_{q_0} + F_qD_{q_0}^{0,1}|^2. \tag{L.75}$$

Therefore, the normalized state corresponding to $\langle 1_{0,\mathrm{R},\xi_k}|(1+1)_{0,\mathrm{T},e_1d_0}\rangle$ can be defined as

$$|1_{0,\mathrm{T},e_1d_0,F_q}\rangle := \frac{1}{2}\left(\mathcal{C}_{F_qD}\right)^{-\frac{1}{2}}\sum_{q_0=0}^{\infty}(F_q^{0,1}D_{q_0} + F_qD_{q_0}^{0,1})|1_{0,\mathrm{T},\xi_{q_0}}\rangle \tag{L.76}$$

$$= \frac{1}{2}\left(\mathcal{C}_{F_qD}\right)^{-\frac{1}{2}}\left[F_q^{0,1}\left(\sum_{q_0=0}^{\infty}|D_{q_0}|^2\right)^{\frac{1}{2}}|1_{0,\xi_T}\rangle + F_q\left(\sum_{q_0=0}^{\infty}|D_{q_0}^{0,1}|^2\right)^{\frac{1}{2}}|1_{0,\xi_T^{e_1d_0}}\rangle\right]. \quad \text{(L.77)}$$

Hence, we may write

$$(\mathcal{C}_{(1+1)})^{\frac{1}{2}}\langle 1_{0,\mathrm{R},\xi_q}|\hat{\mathrm{H}}|(1+1)_{0,e_1d_0}\rangle = \mathcal{C}_{F_qD}|1_{0,\mathrm{T},e_1d_0,F_q}\rangle\langle 1_{0,\mathrm{T},e_1d_0,F_q}|. \quad \text{(L.78)}$$

The final term in the partial trace corresponds to zero photons at the intended receiver due to the loss induced by the filter's frequency mismatch obtained from (L.67) as

$$(\mathcal{C}_{(1+1)})^{\frac{1}{2}}(\langle 1_{0,\mathrm{R},\xi_{q_1}}|\langle 1_{0,\mathrm{R},\xi_{q_0}}|)\hat{\mathrm{H}}|(1+1)_{0,e_1d_0}\rangle = \frac{1}{2}(F_{q_0}^{0,1}F_{q_1} + F_{q_0}F_{q_1}^{0,1})|0_{0,\mathrm{T}}\rangle \quad \text{(L.79)}$$

and

$$\langle 2_{0,\mathrm{R},\xi_q}|\hat{\mathrm{H}}|(1+1)_{0,e_1d_0}\rangle = \frac{1}{2}\sqrt{2}F_q^{0,1}F_q|0_{0,\mathrm{T}}\rangle \quad \text{(L.80)}$$

which corresponds to the case where two photons have arrived at receiver $r = 0$ and none of them has passed through the filter. For this case, we define the following coefficient, for summation of coefficients of $|0_{0,\mathrm{T}}\rangle\langle 0_{0,\mathrm{T}}|$, to simplify the final result:

$$\mathcal{C}_{FF} := \frac{1}{4}\sum_{\substack{q_1=0\\ \text{s.t. } q_1>q_0}}^{\infty}\sum_{q_0=0}^{\infty}|F_{q_0}^{0,1}F_{q_1} + F_{q_0}F_{q_1}^{0,1}|^2 + \frac{1}{4}2\sum_{q_0=0}^{\infty}|F_{q_0}F_{q_0}^{0,1}|^2. \quad \text{(L.81)}$$

Also, based on (L.63), (L.65), and (L.75), we define

$$\mathcal{C}_F := \sum_{k=0}^{N_c-1}\mathcal{C}_{F,0_k} = \frac{1}{4N_c}\sum_{k=0}^{N_c-1}\sum_{q=0}^{\infty}|F_q - \lambda_{0,k}\lambda_{1,k}F_q^{0,1}|^2 \quad \text{(L.82)}$$

$$\mathcal{C}_D := \sum_{k=0}^{N_c-1}\mathcal{C}_{D,1_k} = \frac{1}{4N_c}\sum_{k=0}^{N_c-1}\sum_{q=0}^{\infty}|D_q - \lambda_{0,k}\lambda_{1,k}D_q^{0,1}|^2 \quad \text{(L.83)}$$

$$\mathcal{C}_{FD} := \sum_{q=0}^{\infty}\mathcal{C}_{F_qD} = \frac{1}{4}\sum_{q=0}^{\infty}\sum_{q_0=0}^{\infty}|F_q^{0,1}D_{q_0} + F_qD_{q_0}^{0,1}|^2. \quad \text{(L.84)}$$

Using the density matrix in (L.56), and the projections in (L.66), (L.73), (L.74), (L.79), and (L.80), the transmitted quantum signal after the filter can be described as

$$\rho_0^{\mathrm{T}} = \mathrm{Tr}_{\mathrm{R}}(\hat{\mathrm{H}}\rho_0^d\hat{\mathrm{H}}^\dagger) \quad \text{(L.85)}$$

$$\begin{aligned}
&= \langle 0_{0,\mathrm{R}}|\hat{\mathrm{H}}\rho_0^d\hat{\mathrm{H}}^\dagger|0_{0,\mathrm{R}}\rangle + \sum_{q=0}^{\infty}\langle 1_{0,\mathrm{R},\xi_q}|\hat{\mathrm{H}}\rho_0^d\hat{\mathrm{H}}^\dagger|1_{0,\mathrm{R},\xi_q}\rangle \\
&\quad + \sum_{q=0}^{\infty}\langle 2_{0,\mathrm{R},\xi_q}|\hat{\mathrm{H}}\rho_0^d\hat{\mathrm{H}}^\dagger|2_{0,\mathrm{R},\xi_q}\rangle \\
&\quad + \sum_{q_0=0}^{\infty}\sum_{q_1=0}^{\infty}\langle 1_{0,\mathrm{R},\xi_{q_1}}|\langle 1_{0,\mathrm{R},\xi_{q_0}}|\hat{\mathrm{H}}\rho_0^d\hat{\mathrm{H}}^\dagger|1_{0,\mathrm{R},\xi_{q_0}}\rangle|1_{0,\mathrm{R},\xi_{q_1}}\rangle \\
&= \mathcal{C}_{DD}|(1+1)_{0,\mathrm{T},e_1d_0}\rangle\langle(1+1)_{0,\mathrm{T},e_1d_0}| \\
&\quad + \sum_{q=0}^{\infty}\mathcal{C}_{F_qD}|1_{0,\mathrm{T},e_1d_0,F_q}\rangle\langle 1_{0,\mathrm{T},e_1d_0,F_q}| \\
&\quad + \sum_{k=0}^{N_c-1}\mathcal{C}_{D,1_k}|1_{0,\mathrm{T},e_1d_0,k}\rangle\langle 1_{0,\mathrm{T},e_1d_0,k}| \\
&\quad + \mathcal{CC}_0|0_{0,\mathrm{T}}\rangle\langle 0_{0,\mathrm{T}}| \qquad \text{(L.86)}
\end{aligned}$$

where

$$\mathcal{CC}_0 := \mathcal{C}_0 + \mathcal{C}_{FF} + \mathcal{C}_F. \quad \text{(L.87)}$$

Therefore, the photon statistics of the output of receiver $r = 0$, i.e., n_0, are calculated as follows:

$$\begin{aligned}
\mathbb{P}(n_0 = 0) &= \mathcal{C}_0 + \mathcal{C}_{FF} + \mathcal{C}_F \\
\mathbb{P}(n_0 = 1) &= \mathcal{C}_{FD} + \mathcal{C}_D \\
\mathbb{P}(n_0 = 2) &= \mathcal{C}_{DD}. \qquad \text{(L.88)}
\end{aligned}$$

Let us further simplify the aforementioned expressions in terms of the signal and interference amplitudes defined by

$$\mathfrak{D} := \sum_{q=0}^{\infty}|D_q|^2 \quad \text{(L.89)}$$

$$\mathfrak{D}^{0,1} := \sum_{q=0}^{\infty}|D_q^{0,1}|^2. \quad \text{(L.90)}$$

We use the narrowband filter approximation and the approximate orthogonality of the spreading sequences, i.e., $\frac{1}{N_c}\sum_{k=0}^{N_c-1}\lambda_{0,k}\lambda_{1,k} \approx 0$, $\sum_{q=0}^{\infty}F_q^{0,1}F_q \approx 0$, and $\sum_{q=0}^{\infty}D_q^{0,1}D_q \approx 0$ (due to the random phase of the coefficients), to simplify the results.

Note that from (L.81)

$$\mathcal{C}_{FF} = \frac{1}{4}\left(\sum_{q_0=0}^{\infty}|F_{q_0}^{0,1}|^2\right)\left(\sum_{q_1=0}^{\infty}|F_{q_1}|^2\right) + \frac{1}{4}\left|\sum_{q=0}^{\infty}F_q^{0,1}F_q\right|^2 \quad \text{(L.91)}$$

$$= \frac{1}{4}(1-\mathfrak{D})(1-\mathfrak{D}^{0,1}) + \frac{1}{4}\left|\sum_{q=0}^{\infty}F_q^{0,1}F_q\right|^2 \quad \text{(L.92)}$$

$$\approx \frac{1}{4}(1-\mathfrak{D})(1-\mathfrak{D}^{0,1}). \quad \text{(L.93)}$$

Similarly, from (L.70), we have

$$\mathcal{C}_{DD} = \frac{1}{4}\left(\sum_{q_0=0}^{\infty}|D_{q_0}^{0,1}|^2\right)\left(\sum_{q_1=0}^{\infty}|D_{q_1}|^2\right) + \frac{1}{4}\left|\sum_{q=0}^{\infty}D_q^{0,1}D_q\right|^2 \tag{L.94}$$

$$= \frac{1}{4}\mathfrak{D}\mathfrak{D}^{0,1} + \frac{1}{4}\left|\sum_{q=0}^{\infty}D_q^{0,1}D_q\right|^2 \tag{L.95}$$

$$\approx \frac{1}{4}\mathfrak{D}\mathfrak{D}^{0,1}. \tag{L.96}$$

Furthermore, from (L.82), we have

$$\begin{aligned}\mathcal{C}_F &= \frac{1}{4N_c}\sum_{k=0}^{N_c-1}\sum_{q=0}^{\infty}|F_q - \lambda_{0,k}\lambda_{1,k}F_q^{0,1}|^2\\ &= \frac{1}{4N_c}\sum_{k=0}^{N_c-1}\sum_{q=0}^{\infty}(|F_q^{0,1}|^2 + |F_q|^2 - 2\lambda_{0,k}\lambda_{1,k}\mathrm{Re}\{F_qF_q^{0,1}\})\\ &= \frac{1}{4N_c}\sum_{k=0}^{N_c-1}\left(2 - \sum_{q=0}^{\infty}(|D_q^{0,1}|^2 + |D_q|^2)\right)\\ &\quad - \frac{1}{2N_c}\left(\sum_{k=0}^{N_c-1}\lambda_{0,k}\lambda_{1,k}\right)\mathrm{Re}\left\{\sum_{q=0}^{\infty}F_qF_q^{0,1}\right\} \qquad \text{(L.97)}\\ &\approx \frac{1}{2} - \frac{1}{4}\sum_{q=0}^{\infty}(|D_q^{0,1}|^2 + |D_q|^2)\\ &= \frac{1}{2} - \frac{1}{4}(\mathfrak{D} + \mathfrak{D}^{0,1}). \qquad \text{(L.98)}\end{aligned}$$

Similarly, from (L.83), we have

$$\begin{aligned}\mathcal{C}_D &= \frac{1}{4N_c}\sum_{k=0}^{N_c-1}\sum_{q=0}^{\infty}|D_q - \lambda_{0,k}\lambda_{1,k}D_q^{0,1}|^2\\ &= \frac{1}{4N_c}\sum_{k=0}^{N_c-1}\sum_{q=0}^{\infty}(|D_q^{0,1}|^2 + |D_q|^2 - 2\lambda_{0,k}\lambda_{1,k}\mathrm{Re}\{D_qD_q^{0,1}\})\\ &\approx \frac{1}{4}\sum_{q=0}^{\infty}(|D_q^{0,1}|^2 + |D_q|^2) = \frac{1}{4}(\mathfrak{D}^{0,1} + \mathfrak{D}). \qquad \text{(L.99)}\end{aligned}$$

Also, from (L.84), we have

$$\begin{aligned}\mathcal{C}_{FD} &= \frac{1}{4}\sum_{q_0=0}^{\infty}\sum_{q_1=0}^{\infty}|F_{q_0}^{0,1}D_{q_1} + F_{q_0}D_{q_1}^{0,1}|^2\\ &= \frac{1}{4}\left(\sum_{q_1=0}^{\infty}|D_{q_1}|^2\right)\left(\sum_{q_0=0}^{\infty}|F_{q_0}^{0,1}|^2\right)\\ &\quad + \frac{1}{4}\left(\sum_{q_0=0}^{\infty}|F_{q_0}|^2\right)\left(\sum_{q_1=0}^{\infty}|D_{q_1}^{0,1}|^2\right)\\ &\quad + \frac{1}{2}\mathrm{Re}\left\{\left(\sum_{q_0=0}^{\infty}F_{q_0}F_{q_0}^{0,1}\right)\left(\sum_{q_1=0}^{\infty}D_{q_1}D_{q_1}^{0,1}\right)\right\}\\ &\approx \frac{1}{4}\left(\sum_{q_1=0}^{\infty}|D_{q_1}|^2\right)\left(1 - \sum_{q_1=0}^{\infty}|D_{q_1}^{0,1}|^2\right)\\ &\quad + \frac{1}{4}\left(1 - \sum_{q_1=0}^{\infty}|D_{q_1}|^2\right)\left(\sum_{q_1=0}^{\infty}|D_{q_1}^{0,1}|^2\right)\\ &= \frac{1}{4}\left(\mathfrak{D}(1-\mathfrak{D}^{0,1}) + \mathfrak{D}^{0,1}(1-\mathfrak{D})\right)\\ &= \frac{1}{4}(\mathfrak{D}^{0,1} + \mathfrak{D} - 2\mathfrak{D}\mathfrak{D}^{0,1}). \qquad \text{(L.100)}\end{aligned}$$

Substituting approximate values of the coefficients into (L.88) gives

$$\begin{aligned}\mathbb{P}(n_0=0) &\approx \frac{1}{4} + \frac{1}{2} - \frac{1}{4}(\mathfrak{D} + \mathfrak{D}^{0,1}) + \frac{1}{4}(1-\mathfrak{D})(1-\mathfrak{D}^{0,1})\\ &= 1 - \frac{1}{2}(\mathfrak{D} + \mathfrak{D}^{0,1}) + \frac{1}{4}\mathfrak{D}^{0,1}\mathfrak{D} \qquad \text{(L.101)}\\ \mathbb{P}(n_0=1) &\approx \frac{1}{4}(\mathfrak{D}^{0,1} + \mathfrak{D} - 2\mathfrak{D}\mathfrak{D}^{0,1}) + \frac{1}{4}(\mathfrak{D}^{0,1} + \mathfrak{D})\\ &= \frac{1}{2}(\mathfrak{D}^{0,1} + \mathfrak{D}) - \frac{1}{2}\mathfrak{D}\mathfrak{D}^{0,1} \qquad \text{(L.102)}\\ \mathbb{P}(n_0=2) &\approx \frac{1}{4}\mathfrak{D}\mathfrak{D}^{0,1}. \qquad \text{(L.103)}\end{aligned}$$

APPENDIX M
TENSOR PRODUCT NOTATION

We use the symbol $\prod$ for both the tensor product of quantum states and ordinary product of operators. Since some authors use the symbol $\otimes$, it is beneficial to discuss this notation. For complex numbers, the symbol $\prod$ denotes the ordinary product. For example

$$\prod_{k=0}^{N_c-1}\lambda_k = \lambda_0\lambda_1\cdots\lambda_{N_c-1}.$$

For quantum states, the tensor product of vectors $|\psi_{\xi_k}\rangle \in \mathcal{H}_k$, i.e.,

$$\otimes_{k=0}^{N_c-1}|\psi_{\xi_k}\rangle = \prod_{k=0}^{N_c-1}|\psi_{\xi_k}\rangle$$

results in a vector in the Hilbert space $\mathcal{H}$ with higher dimensions. Also note that, as a convention, vacuum states are often not shown in the tensor product state [40]. This convention, for example, implies that

$$\begin{aligned}|1_{\xi_k}\rangle &:= |0_{\xi_0}\rangle|0_{\xi_1}\rangle\cdots|1_{\xi_k}\rangle\cdots|0_{\xi_{N_c-1}}\rangle\\ &= |1_{\xi_k}\rangle\prod_{l\neq k}|0_{\xi_l}\rangle.\end{aligned}$$

For quantum operators, the tensor product is utilized to bring an operator that acts on states inside a chip-time Hilbert

IEEE Transactions on Quantum Engineering

space $\mathcal{H}_k$ into the larger Hilbert space $\mathcal{H}$. As an example of quantum operators, note that the chip-time interval spreading operator $\hat{\mathrm{U}}_k$ is defined in $\mathcal{H}$, but its action only affects quantum signals with components inside $\mathcal{H}_k$ and corresponds to unity for other chip times. Then, we have

$$\hat{\mathrm{U}}_k = \underbrace{I \otimes I \otimes \cdots \otimes I \otimes}_{k} \hat{\mathrm{U}}'_k \underbrace{\otimes I \otimes I \otimes \cdots \otimes I}_{N_c-k-1}$$

where $\hat{\mathrm{U}}'_k$ is represented in the chip-time Hilbert space $\mathcal{H}_k$, and we have

$$\prod_{k=0}^{N_c-1} \hat{\mathrm{U}}_k = \prod_{k=0}^{N_c-1} \underbrace{I \otimes I \otimes \cdots \otimes I \otimes}_{k} \hat{\mathrm{U}}'_k \underbrace{\otimes I \otimes I \otimes \cdots \otimes I}_{N_c-k-1}$$
$$= \hat{\mathrm{U}}'_0 \otimes \hat{\mathrm{U}}'_1 \otimes \cdots \hat{\mathrm{U}}'_k \otimes \cdots \hat{\mathrm{U}}'_{N_c-1}.$$

REFERENCES

[1] M. A. Dastgheib, J. A. Salehi, and M. Rezai, "Quantum spread-spectrum CDMA communication systems," in *Proc. IEEE Middle East Conf. Commun. Netw.*, 2024, pp. 140–144, doi: 10.1109/MECOM61498.2024.10881055.

[2] M. M. Wilde, *Quantum Information Theory*. Cambridge, U.K.: Cambridge Univ. Press, 2013, doi: 10.1017/CBO9781139525343.

[3] G. Cariolaro, *Quantum Communications*. Berlin, Germany: Springer, 2015, doi: 10.1007/978-3-319-15600-2.

[4] M. Razavi, *An Introduction to Quantum Communications Networks*. San Rafael, CA, USA: Morgan & Claypool, 2018, [Online]. Available: https://iopscience.iop.org/book/mono/978-1-6817-4653-1

[5] M. Bathaee, M. Rezai, and J. A. Salehi, "Quantum wavelength-division multiplexing and multiple-access communication systems and networks: Global and unified approach," *Phys. Rev. A*, vol. 107, no. 1, 2023, Art. no. 012613, doi: 10.1103/PhysRevA.107.012613.

[6] H. K. Lo, "Classical-communication cost in distributed quantum-information processing: A generalization of quantum-communication complexity," *Phys. Rev. A*, vol. 62, no. 1, 2000, Art. no. 012313, doi: 10.1103/PhysRevA.62.012313.

[7] M. Rezai and J. A. Salehi, "Fundamentals of quantum Fourier optics," *IEEE Trans. Quantum Eng.*, vol. 4, 2023, Art. no. 2100122, doi: 10.1109/TQE.2022.3224799.

[8] Y. A. Chen et al., "An integrated space-to-ground quantum communication network over 4,600 kilometres," *Nature*, vol. 589, no. 7841, pp. 214–219, 2021, doi: 10.1038/s41586-020-03093-8.

[9] E. E. Moghaddam, H. Beyranvand, and J. A. Salehi, "Resource allocation in space division multiplexed elastic optical networks secured with quantum key distribution," *IEEE J. Sel. Areas Commun.*, vol. 39, no. 9, pp. 2688–2700, Sep. 2021, doi: 10.1109/JSAC.2021.3064641.

[10] M. Keller, B. Lange, K. Hayasaka, W. Lange, and H. Walther, "Continuous generation of single photons with controlled waveform in an ion-trap cavity system," *Nature*, vol. 431, no. 7012, pp. 1075–1078, 2004, doi: 10.1038/nature02961.

[11] H. P. Specht et al., "Phase shaping of single-photon wave packets," *Nat. Photon.*, vol. 3, no. 8, pp. 469–472, 2009, doi: 10.1038/nphoton.2009.115.

[12] M. Kues et al., "Quantum optical microcombs," *Nat. Photon.*, vol. 13, no. 3, pp. 170–179, 2019, doi: 10.1038/s41566-019-0363-0.

[13] M. Simon, J. Omura, R. Scholtz, and B. Levitt, *Spread Spectrum Communications Handbook*. New York, NY, USA: McGraw-Hill Educ., 2002, [Online]. Available: https://www.accessengineeringlibrary.com/content/book/9780071382151

[14] C. Belthangady, C. S. Chuu, A. Y. Ite, G. Yin, J. Kahn, and S. Harris, "Hiding single photons with spread spectrum technology," *Phys. Rev. Lett.*, vol. 104, no. 22, 2010, Art. no. 223601, doi: 10.1103/PhysRevLett.104.223601.

[15] J. C. Garcia-Escartin and P. Chamorro-Posada, "Quantum spread spectrum multiple access," *IEEE J. Sel. Top. Quantum Electron.*, vol. 21, no. 3, pp. 30–36, May/Jun. 2014, doi: 10.1109/JSTQE.2014.2360366.

[16] M. Rezai and J. A. Salehi, "Quantum CDMA communication systems," *IEEE Trans. Inf. Theory*, vol. 67, no. 8, pp. 5526–5547, Aug. 2021, doi: 10.1109/TIT.2021.3087959.

[17] J. A. Salehi, A. M. Weiner, and J. P. Heritage, "Coherent ultrashort light pulse code-division multiple access communication systems," *J. Lightw. Technol.*, vol. 8, no. 3, pp. 478–491, Mar. 1990, doi: 10.1109/50.50743.

[18] P. Kolchin, C. Belthangady, S. Du, G. Yin, and S. E. Harris, "Electro-optic modulation of single photons," *Phys. Rev. Lett.*, vol. 101, no. 10, 2008, Art. no. 103601, doi: 10.1103/PhysRevLett.101.103601.

[19] M. Xu and X. Cai, "Advances in integrated ultra-wideband electro-optic modulators," *Opt. Exp.*, vol. 30, no. 5, pp. 7253–7274, 2022, doi: 10.1364/OE.449022.

[20] Y. Zhang et al., "High-speed electro-optic modulation in topological interface states of a one-dimensional lattice," *Light: Sci. Appl.*, vol. 12, no. 1, 2023, Art. no. 206, doi: 10.1038/s41377-023-01251-x.

[21] J. Liu et al., "Lithium niobate thin film electro-optic modulator," *Nanophotonics*, vol. 13, no. 8, pp. 1503–1508, 2024, doi: 10.1515/nanoph-2023-0865.

[22] K. Powell et al., "Integrated silicon carbide electro-optic modulator," *Nat. Commun.*, vol. 13, no. 1, 2022, Art. no. 1851, doi: 10.1038/s41467-022-29448-5.

[23] M. Karpiński, A. O. Davis, F. Sośnicki, V. Thiel, and B. J. Smith, "Control and measurement of quantum light pulses for quantum information science and technology," *Adv. Quantum Technol.*, vol. 4, no. 9, 2021, Art. no. 2000150, doi: 10.1002/qute.202000150.

[24] P. L. Hagelstein, S. D. Senturia, and T. P. Orlando, *Introductory Applied Quantum and Statistical Mechanics*. Hoboken, NJ, USA: Wiley, 2004, [Online]. Available: https://www.wiley.com/en-us/Introductory+Applied+bQuantum+and+Statistical+Mechanics-p-9780471202769

[25] R. Loudon, *The Quantum Theory of Light*. Oxford, U.K.: Oxford Univ. Press, 2000, doi: 10.1093/oso/9780198501770.001.0001.

[26] A. Hayat, X. Xing, A. Feizpour, and A. M. Steinberg, "Multi-dimensional quantum information based on single-photon temporal wavepackets," *Opt. Exp.*, vol. 20, no. 28, pp. 29174–29184, 2012, doi: 10.1364/OE.20.029174.

[27] J. W. Negele and H. Orland, *Quantum Many-Particle Systems*. Boulder, CO, USA: Westview Press, 1998, doi: 10.1201/9780429497926.

[28] B. Moslehi, J. W. Goodman, M. Tur, and H. J. Shaw, "Fiber-optic lattice signal processing," *Proc. IEEE*, vol. 72, no. 7, pp. 909–930, 1984, doi: 10.1109/PROC.1984.12948.

[29] J. A. Salehi, R. C. Menendez, and C. A. Brackett, "A low-pass digital optical filter for optical fiber communications," *J. Lightw. Technol.*, vol. 6, no. 12, pp. 1841–1847, Dec. 1988, doi: 10.1109/50.9253.

[30] M. Razavi and J. A. Salehi, "Performance of optical bit rate limiters with pre- or post-optical amplification," *J. Lightw. Technol.*, vol. 20, no. 10, pp. 1797–1804, Oct. 2002, doi: 10.1109/JLT.2002.804033.

[31] S. J. van Enk, "Time-dependent spectrum of a single photon and its positive-operator-valued measure," *Phys. Rev. A*, vol. 96, no. 3, 2017, Art. no. 033834, doi: 10.1103/PhysRevA.96.033834.

[32] S. M. Barnett, J. Jeffers, A. Gatti, and R. Loudon, "Quantum optics of lossy beam splitters," *Phys. Rev. A*, vol. 57, no. 3, 1998, Art. no. 2134, doi: 10.1103/PhysRevA.57.2134.

[33] C. K. Madsen and J. H. Zhao, *Optical Filter Design and Analysis: A Signal Processing Approach*. New York, NY, USA: Wiley, 1999, doi: doi: 10.1002/0471213756.

[34] A. V. Oppenheim, A. S. Willsky, and S. H. Nawab, *Signals and Systems*. Englewood Cliffs, NJ, USA: Prentice-Hall, 1997.

[35] A. V. Oppenheim and R. W. Schafer, *Discrete-Time Signal Processing*. London, U.K.: Pearson, 2009, [Online]. Available: https://www.pearson.com/en-us/subject-catalog/p/discrete-time-signal-processing/P200000003226/9780137549771

[36] W. Huggins, P. Patil, B. Mitchell, K. B. Whaley, and E. M. Stoudenmire, "Towards quantum machine learning with tensor networks," *Quantum Sci. Technol.*, vol. 4, no. 2, 2019, Art. no. 024001, doi: 10.1088/2058-9565/aaea94.

[37] C. K. Hong, Z. Y. Ou, and L. Mandel, "Measurement of subpicosecond time intervals between two photons by interference," *Phys. Rev. Lett.*, vol. 59, no. 18, 1987, Art. no. 2044, doi: 10.1103/PhysRevLett.59.2044.

[38] D. S. Grün, K. Wittmann W., L. H. Ymai, J. Links, and A. Foerster, "Protocol designs for NOON states," *Commun. Phys.*, vol. 5, no. 1, 2022, Art. no. 36, doi: 10.1038/s42005-022-00812-7.

[39] M. Bergmann and P. van Loock, "Quantum error correction against photon loss using NOON states," *Phys. Rev. A*, vol. 94, no. 1, 2016, Art. no. 012311, doi: 10.1103/PhysRevA.94.012311.

[40] M. Beck, *Quantum Mechanics: Theory and Experiment*. Oxford, U.K.: Oxford Univ. Press, 2012, [Online]. Available: https://global.oup.com/academic/product/quantum-mechanics-9780199798124

Mohammad Amir Dastgheib was born in Shiraz, Iran, in 1994. He received the B.Sc. degree from Shiraz University, Shiraz, in 2016, and the M.Sc. and Ph.D. degrees from the Sharif University of Technology (SUT), Tehran, Iran, in 2018 and 2023, respectively, all in electrical engineering, with honors and as an outstanding student.

Since 2016, he has been a Member of the Optical Networks Research Lab, SUT, where he has been a Postdoctoral Researcher with the Sharif Quantum Center and a Member of the Technical Staff of the Advanced Quantum Communications Lab since 2021. His current research interests include quantum data communication networks, quantum communication signals and systems, optical wireless communications, statistical learning, and machine learning applications in communication networks.

Dr. Dastgheib received the National Khwarizmi Youth Award in mathematics in 2011, the Award of Research Endeavors among the electrical engineering department's M.Sc. students from the Sharif University of Technology in 2018, and the Outstanding M.Sc. Thesis Award from the IEEE Iran Section in 2020.

Jawad A. Salehi (Fellow, IEEE) was born in Kazemain, Iraq, in 1956. He received the B.Sc. degree from the University of California, Irvine, CA, USA, in 1979, and the M.Sc. and Ph.D. degrees from the University of Southern California, Los Angeles, CA, in 1980 and 1984, respectively, all in electrical engineering.

From 1984 to 1993, he was a Member of the Technical Staff of the Applied Research Area, Bell Communications Research (Bellcore), Morristown, NJ, USA. In 1990, he was with the Laboratory of Information and Decision Systems, Massachusetts Institute of Technology, Cambridge, MA, USA, as a Visiting Research Scientist conducting research on optical multiple access networks. From 1997 to 2003, he was an Associate Professor with the Department of Electrical Engineering, Sharif University of Technology (SUT), Tehran, Iran, where he is currently a Distinguished Professor. From 2003 to 2006, he was the Director of the National Center of Excellence in Communications Science at the Department of Electrical Engineering, SUT. In 2003, he founded and directed the Optical Networks Research Laboratory for advanced theoretical and experimental research in futuristic all-optical networks. He is currently the Head of the Sharif Quantum Center and the quantum group of the Institute for Convergence Science and Technology, SUT, emphasizing in advancing quantum communication systems, quantum optical signal processing, and quantum information science. He holds 15 U.S. patents on optical code division multiple access (CDMA). His current research interests include quantum optics, quantum communication signals and systems, quantum multiple access networks, quantum Fourier optics, and optical wireless communication (indoors and underwater).

Dr. Salehi was named as among the 250 preeminent and most influential researchers worldwide by the Institute for Scientific Information Highly Cited in the Computer-Science Category, 2003. He was a recipient of the Bellcore's Award of Excellence, the Outstanding Research Award of the Department of Electrical Engineering, SUT, in 2002 and 2003, the Nationwide Outstanding Research Award in 2003, and the Nation's Highly Cited Researcher Award in 2004. From 2001 to 2012, he was an Associate Editor for Optical CDMA of the IEEE TRANSACTIONS ON COMMUNICATIONS. In 2024, he was elected as an OPTICA Fellow for contributions to the invention and fundamental principles of optical code-division multiple-access communication systems and of optical orthogonal codes. He is a member of the Iran Academy of Science and a Fellow of the Islamic World Academy of Science, Amman, Jordan.

Mohammad Rezai was born in Firoozabad, Iran in 1983. He received the B.S. degree in physics from the University of Sistan and Baluchestan, Zahedan, Iran, in 2006, the M.S. degree in physics from the Sharif University of Technology, Tehran, Iran, in 2009, and the Ph.D. degree in physics from the University of Stuttgart, Stuttgart, Germany, in 2018.

From 2010 to 2013, he was a Member of the International Max Planck Research School for Advanced Materials, Düsseldorf, Germany, and a Member of Research Staff in the field of condensed matter physics with the Institute for Theoretical Physics III, University of Stuttgart. In 2013, he joined the 3rd Physikalisches Institut, University of Stuttgart, where he was involved in optical quantum information processing experiments. From 2019 to 2022, he was a Postdoctoral Researcher with the Sharif Quantum Center and the Department of Electrical Engineering, Sharif University of Technology. Since 2022, he has been the Head of the Research Planning Department of the Sharif Quantum Center and a faculty member of the Institute for Convergence Science and Technology, Sharif University of Technology. His current research interests include quantum holography, quantum Fourier optics, quantum multiple access communication systems, and quantum coherence in photosynthetic systems.

Dr. Rezai was a recipient of the Max Planck Scholarship in 2010. He was elected to the Iran National Elite Foundation in 2019.